Vol. 203 No. 1, December 1, 1987 ISSN 0003-2670

ANALYTICA CHIMICA ACTA

International journal devoted to all branches of analytical chemistry

ELSEVIER

ANALYTICA CHIMICA ACTA

International journal devoted to all branches of analytical chemistry
Revue internationale consacrée à tous les domaines de la chimie analytique
Internationale Zeitschrift für alle Gebiete der analytischen Chemie

PUBLICATION SCHEDULE FOR 1988

	J	F	M	A	M	J	J	A	S	O	N	D
Analytica Chimica Acta	204	205	206	207	208	209	210/1 210/2	211	212	213	214	215

Scope. *Analytica Chimica Acta* publishes original papers, short communications, and reviews dealing with every aspect of modern chemical analysis both fundamental and applied.
Submission of Papers. Manuscripts (three copies) should be submitted as designated below for rapid and efficient handling:
Papers from the Americas to: Professor Harry L. Pardue, Department of Chemistry, Purdue University, West Lafayette, IN 47907, U.S.A.
Papers from all other countries to: Dr. A.M.G. Macdonald, Department of Chemistry, The University, P.O. Box 363, Birmingham B15 2TT, England. Papers dealing particularly with computer techniques to: Professor J.T. Clerc, Universität Bern, Pharmazeutisches Institut, Baltzerstrasse 5, CH-3012 Bern, Switzerland.
Submission of an article is understood to imply that the article is original and unpublished and is not being considered for publication elsewhere. Papers in English, French and German are published. There are no page charges. Manuscripts should conform in layout and style to the papers published in this Volume. See inside back cover for "Information for Authors".
Reprints. Fifty reprints will be supplied free of charge. Additional reprints (minimum 100) can be ordered. An order form containing price quotations will be sent to the authors together with the proofs of their article.
Publication. *Analytica Chimica Acta appears* in 12 volumes in 1988. The subscription for 1988 (Vols. 204-215) is Dfl. 2820.00 plus Dfl. 312.00 (p.p.h.) (total approx, US $1566.00). All earlier volumes (Vols. 1-203) except Vols. 23 and 28 are available at Dfl. 243.00 (US $121.50), plus Dfl. 18.00 (US $9.00) p.p.h., per volume.
Our p.p.h. (postage, packing and handling) charge includes surface delivery of all issues, except to subscribers in the U.S.A., Canada, Australia, New Zealand, P.R. China, India, Israel, South Africa, Malaysia, Thailand, Singapore, South Korea, Taiwan, Pakistan, Hong Kong, Brazil, Argentina and Mexico, who receive all issues by air delivery (S.A.L.–Surface Air Lifted) at no extra cost. For Japan, air delivery requires 50% additional charge; for all other countries airmail and S.A.L. charges are available upon request.
Subscription. Subscription should be sent to: Elsevier Science Publishers B.V., Journals Department, P.O. Box 211, 1000 AE Amsterdam, The Netherlands. Tel: 5803 911, Telex: 18582, to which requests for sample copies can also be sent. Claims for issues not received should be made within three months of publication of the issues. If not they cannot be honoured free of charge. Readers in the U.S.A. and Canada can contact the following address: Elsevier Science Publishing Co. Inc., Journal Information Center, 52 Vanderbilt Avenue, New York, NY 10017, U.S.A., Tel: (212) 916-1250, for further information, or a free sample copy of this or any other Elsevier Science Publishers journal.
Advertisements. Advertisement rates are available from the publisher on request.

0003-2670/87/$03.50

PRINTED IN THE NETHERLANDS

ANALYTICA CHIMICA ACTA

International journal devoted to all branches of analytical chemistry

(Abstracted, Indexed in: Anal. Abstr.; Biol. Abstr.; Chem. Abstr.; Curr. Contents Phys. Chem. Earth Sci.; Life Sci.; Index Med.; Mass Spectrom. Bull.; Sci. Citation Index; Excerpta Med.)

VOL. 203 CONTENTS DECEMBER 1, 1987

ANALYTICA CHIMICA ACTA
VOL. 203 (1987)

ANALYTICA CHIMICA ACTA

International journal devoted to all branches of analytical chemistry

Anal. Chim. Acta, Vol. 203 (1987)

ELSEVIER, Amsterdam – Oxford – New York – Tokyo

0003-2670/87/$03.50

PRINTED IN THE NETHERLANDS

Analytica Chimica Acta, 203 (1987) 1-10
Elsevier Science Publishers B.V., Amsterdam — Printed in The Netherlands

A WALL-JET CONDUCTOMETRIC DETECTOR FOR DETERMINATION OF SULPHUR DIOXIDE IN AIR AFTER PRECONCENTRATION IN WATER IN AN AERODISPERSION UNIT

FRANTIŠEK OPEKAR* and ANTONÍN TROJÁNEK

The UNESCO Laboratory of Environmental Electrochemistry, J. Heyrovský Institute of Physical Chemistry and Electrochemistry, Czechoslovak Academy of Sciences, Jilská 16, 110 00 Prague 1 (Czechoslovakia)

(Received 28th May 1987)

SUMMARY

Sulphur dioxide is preconcentrated from air into a polydispersed aerosol of water. The aerosol condenses on impact on the detector, on the surface of which a film of the condensate is maintained. The conductance of the liquid film is measured with a pair of platinum electrodes. The calibration dependence is nonlinear but corresponds to the theoretical model. The concentration range 0.05-2.2 mg SO_2 m^{-3} was studied. The detection limit was 2×10^{-3} mg m^{-3}; the relative standard deviation for 0.38 mg m^{-3} was 2.4%. A steady-state response to a change in SO_2 concentration was attained within ca. 70 s. Ammonia is the only interferent.

A device for preconcentration of gaseous pollutants from a large volume of gaseous phase into a small volume of liquid phase has been described [1]. The device involves absorption of the gaseous component into a polydispersed aerosol of a liquid, formed in a nebulizer and condensing on impact on a solid wall. Depending on the ratio of the volume flow rates of the test gas and the absorbing liquid passing through the nebulizer, a high degree of preconcentration (commonly around 10^4) can be achieved if the distribution coefficient of the test substance between the gaseous and the liquid phase is favourable.

So far, the test component has been determined in the condensate in a separate apparatus, after the condensate in the preconcentration unit has been sampled. In this way, phenols have been determined by liquid chromatography after absorption in water, and toluene by gas chromatography after absorption in n-decane [1]; sulphur dioxide has been determined pneumatoamperometrically after absorption in water [2] or spectrophotometrically after absorption in a formaldehyde solution [3].

In the present paper, a conductometric wall-jet detector placed directly inside the preconcentration unit is described. It can be used to detect ionic substances or substances altering the conductance of the absorption liquid by a

0003-2670/87/$03.50

suitable reaction with it. The detector is tested for the determination of sulphur dioxide preconcentrated from air into water. The detection takes place in a film of the enriched water which is continuously renewed by condensation of the aerosol impinging on the detector surface from the nebulizer. The determination is thus very rapid and the results obtained virtually correspond to the instantaneous concentration of sulphur dioxide in the test air.

THEORY

From the theory of absorption of a gaseous substance in a liquid in an aerodispersion unit [1], a relationship can be derived for the amount of analyte preconcentrated in the liquid phase, Q_l, under conditions characterized by the values of the distribution coefficient K, the volume flow rates of the gaseous and liquid phases, v_g and v_l, respectively, and the amount of the analyte in the gaseous phase, Q_g^0, entering the preconcentration unit:

$$Q_l = (Q_g^0 K v_l / v_g)/(1 + K v_l / v_g) \tag{1}$$

The distribution coefficient of sulphur(IV) compounds for absorption in water is

$$K = [\mathrm{S(IV)}]_l / [\mathrm{S(IV)}]_g = ([\mathrm{SO_2 \cdot H_2O}]_l + [\mathrm{HSO_3^-}]_l + [\mathrm{SO_3^{2-}}]_l)/[\mathrm{SO_2}]_g = K_H + K_1 K_H/[\mathrm{H^+}] + K_1 K_2 K_H/[H^+]^2 \tag{2a}$$

where K_H, K_1 and K_2 are the respective constants for the equilibria in the SO_2/H_2O) system,

$$(\mathrm{SO_2})_g + \mathrm{H_2O} \overset{K_H}{\rightleftharpoons} (\mathrm{SO_2 \cdot H_2O})_l$$

$$(\mathrm{SO_2 \cdot H_2O})_l \overset{K_1}{\rightleftharpoons} \mathrm{H^+} + \mathrm{HSO_3^-}$$

$$\mathrm{HSO_3^-} \overset{K_2}{\rightleftharpoons} \mathrm{H^+} + \mathrm{SO_3^{2-}}$$

Conductometric detection does not respond to $(SO_2 \cdot H_2O)_l$ and, as the aqueous solution is acidic, the contribution of SO_3^{2-} can be neglected. Thus the distribution coefficient can be expressed in terms of the simple relationship

$$K = [\mathrm{HSO_3^-}]/[\mathrm{SO_2}]_g = K_1 K_H/[\mathrm{H^+}] \tag{2b}$$

When Eqn. 1 is multiplied by the ratio v_l/v_g, a relationship is obtained for the analyte concentration in the liquid phase as a function of the analyte concentration in the gaseous phase entering the preconcentration unit:

$$c_l = c_g^0 K/(1 + K v_l / v_g) = c_g^0 D \tag{3}$$

where $c_l = [\mathrm{HSO_3^-}] = [\mathrm{H^+}]$ and $c_g^0 = [\mathrm{SO_2}]_g^0$ are the respective molar concen-

trations and D is the degree of preconcentration of the analyte in the aqueous phase.

It is possible to substitute for c_l in the relationship for the specific conductance (G) from Eqn. 3

$$G = 10^{-3} c_g^0 D \Lambda_{H_2SO_3} \quad (4)$$

and thus obtain an expression for the dependence of the specific conductance of the aqueous phase ($S\ cm^{-1}$) on the concentration of sulphur dioxide in the test air, X($mg\ m^{-3}$),

$$G = AX/[(BX)^{1/2} + C] \quad (5)$$

where $A = 10^{-9} \Lambda_{H_2SO_3}/M_{SO_2}$ (where M_{SO_2} is the molar mass of SO_2), $B = 10^{-6}/K_1 K_H M_{SO_2}$ and $C = v_l/v_g$.

EXPERIMENTAL

The conductometric detector

A schematic diagram of the apparatus for testing the conductometric detector is given in Fig. 1. The preconcentration unit with the conductometric de-

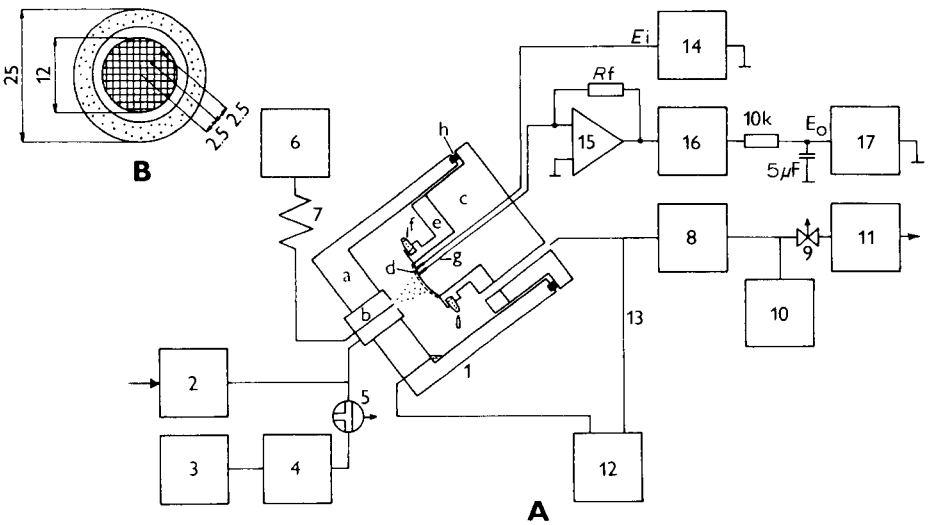

Fig. 1. (A) Schematic diagram of the apparatus: (1) preconcentration unit with detector (a, body; b, nebulizer; c, lid with detector and inlet for vacuum pump; d, polyethylene gauze; e, ring for fixing the gauze; f, polyurethane foam ring; g, conductometric electrodes; h, seal); (2) inlet filter; (3) nitrogen pressure cylinder; (4) SO_2 source; (5) valve; (6) water reservoir (Marriotte bottle); (7) throttling capillary; (8) flow meter; (9) valve; (10) mercury manometer; (11) vacuum pump; (12) waste vessel; (13) tube for spontaneous outflow of the condensate; (14) sine-wave generator; (15) measuring amplifier (LF 356); (16) converter to the absolute value; (17) line recorder. (B) Frontal view of the detector (with dimensions in mm).

tector (1) is made of plexiglas. Into the body (a) are screwed the nebulizer (b) and the lid with the detector (c). The aerosol from the nebulizer impinges on the detector, the front of which forms the condensation wall. The distance of the orifice of the nebulizer jet from the detector surface is 10 mm. The detector surface is covered with polyethylene gauze (d; 0.1 mm thick and with a mesh size of 0.15×0.15 mm) which prevents removal of the liquid from the detector surface by the stream of the air and permits the formation of a liquid film of a defined thickness on the front of the detector. The gauze is held on the detector surface by a plexiglas ring (e). The ring contains a groove filled with polyurethane foam (f), which ensures removal of the condensate without interfering pulsations of the liquid film. The liquid drops to the bottom of the preconcentration unit and flows to waste.

The conductometric electrodes (g) are made of two platinum wires (0.5 mm diameter) cemented into the plexiglas detector body, and ground and polished flush with the front surface, thus obtaining two disks 0.5 mm in diameter. The geometric arrangement of the electrodes can be seen in Fig. 1B.

General procedure for testing

The air is aspirated into the apparatus by a vacuum pump (11), through a dust filter and a chemical filter containing granulated manganese dioxide (2) to remove atmospheric SO_2. A known amount of SO_2 is introduced into the pure air from a permeation generator (4) [4]. It was found that the production of SO_2 in this type of generator varies somewhat on passage of air, because of the reaction of atmospheric oxygen with the hydrogensulphite solution in the generator. Therefore, SO_2 was introduced into the pure air in a stream of nitrogen (ca. 2 ml s^{-1}) from a pressure cylinder (3). The SO_2 production was monitored spectrophotometrically [5]. Valve 5 makes it possible to introduce either pure air or air with SO_2 into the preconcentration unit.

The total volume of the air aspirated into the preconcentration unit per time unit depends on the nebulizer jet diameter and on the underpressure in the preconcentration unit. The measurements were made at a pressure of 40 kPa, which was adjusted by valve 9 and measured by the mercury manometer (10). Under these conditions, the air flow rate was $v_g = 76.5$ ml s^{-1}, for the given nebulizer design [1].

The flow rate of the liquid entering the nebulizer from the reservoir (6) was adjusted by a throttling capillary (7) and was measured at the preconcentration unit outlet in a calibrated cylinder (12); most measurements were made at a flow rate $v_l = 2.76 \times 10^{-3}$ ml s^{-1}. Redistilled water containing the equilibrium concentration of carbon dioxide at the given atmospheric pressure was used as the absorption liquid. Tube 13 permits spontaneous flow of the condensate from the preconcentration unit (by creating a small underpressure in the waste vessel compared with the pressure in the preconcentration unit).

Measuring circuit

Sine-wave voltage E_i was applied to the electrodes from generator 14, with an amplitude of 1.0 V and a frequency of 100 Hz. The conductometric cell formed the input resistance, R_{el}, of the measuring amplifier (15). The amplified output signal was fed, through a converter (16) and an RC filter, to the line recorder (17). The value of output voltage E_o, which is inversely proportional to resistance R_{el}, was adjusted by the magnitude of the feed-back resistance R_f (the value used was $2 \times 10^5 \Omega$). The conductance is then obtained from the measured E_o by using the relationship

$$1/R_{el} = E_o/E_i R_f \qquad (6)$$

RESULTS AND DISCUSSION

Figure 2 shows the detector responses to three different SO_2 concentrations in the air. The time constant of the response, obtained from the exponential response to a step change from 0 to 0.61 mg m^{-3} SO_2, was 3 s under the given experimental conditions.

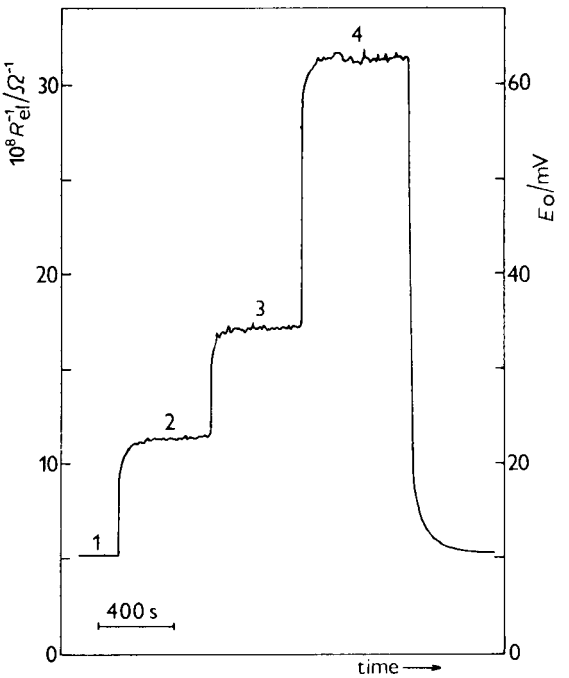

Fig. 2. Detector response to various SO_2 concentrations in the air. Concentrations (in mg m^{-3}): (1) 0; (2) 0.32; (3) 0.61; (4) 1.93. For experimental conditions, see text.

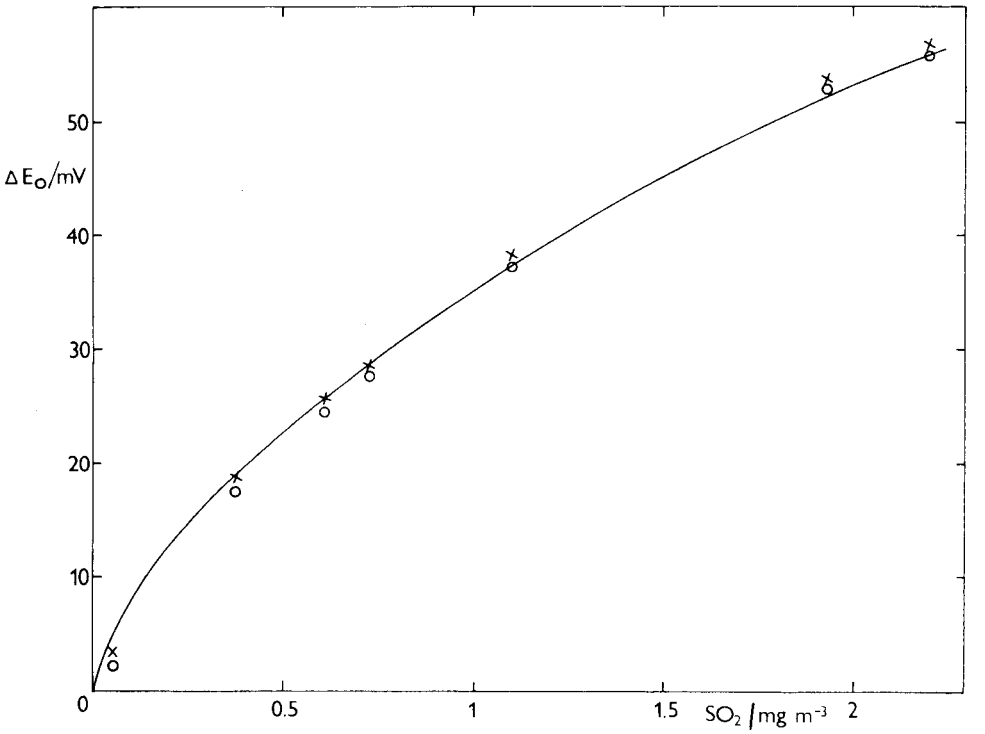

Fig. 3. Calibration curve: (-) theoretical dependence according to Eqn. 8; (O) measured values; (x) values after the correction for the loss in HCO_3^-. For experimental conditions, see text.

Comparison of the theoretical and experimental results

The values of the specific conductance , G_{theor}, calculated from Eqn. 5 for SO_2 concentrations from 0.05 to 2.2 mg m^{-3}, were compared with the experimental values

$$G_{exp} = \theta / R_{el} \qquad (7)$$

for which $1/R_{el}$ was evaluated from Eqn. 6. For E_o, the difference of the detector responses to the air with and without SO_2 was used, i.e., $\Delta E_o = E_o(H_2O + SO_2) - E_o(H_2O)$. The conductometric cell constant, θ, was evaluated by measuring the conductances of aqueous 1.26×10^{-4} and 1.26×10^{-5} M KCl, introduced into the preconcentration unit instead of redistilled water. The value obtained was $\theta = 1.78 \times 10^2$ cm^{-1}.

Because of evaporation of the water in the preconcentration unit, the ratio of the flow rates of water at the inlet and outlet was 1.26 under the given conditions. From the values for saturated water vapour at the actual temperature within the preconcentration unit and for the given air flow rate, a value of 1.4 was obtained, which is in reasonable agreement. Another consequence of evap-

oration of the water is that the temperature inside the preconcentration unit is several degrees lower than that outside. The temperature measured with a thermistor placed inside the preconcentration unit under the given measuring conditions was $15 \pm 1\,^{\circ}C$ compared to a temperature of $23 \pm 1\,^{\circ}C$ for the entering air and water. Therefore, to calculate G_{theor} and θ, the values of the constants corresponding to 15°C [6] were used, i.e., $K_H = 39.02$ and $K_1 = 2.12 \times 10^{-2}$ mol dm^{-3}. The equivalent conductance values, $\Lambda^{15}(H_2SO_3) = 350$ and $\Lambda^{15}(KCl) = 124$, were obtained from the relationship, $\Lambda^t = \Lambda^{25}\,[1 + 0.017(t-25)]$.

The calculated values of the distribution coefficient K, the degree of preconcentration D and the specific conductance G_{theor} are given in Table 1, together with the experimental values G_{exp}. It is evident that the experimental results obtained with the proposed detector are in reasonable accord with the theoretical model for preconcentration of SO_2 from air into water, followed by conductometric detection of the ions formed.

The deviation observed at the lowest concentrations studied can be explained by displacement of hydrogencarbonate (leading to a decrease in the conductance of the water used, i.e., of the background) which is caused by the decrease in the pH occurring during the SO_2 reaction with water. The hydrogencarbonate ions are virtually completely removed even at the lowest SO_2 concentration studied, because the condensate pH is decreased by more than one unit. Hence the decrease in the specific conductance roughly equals the conductance of water that is in equilibrium with the atmospheric carbon dioxide (i.e., ca. 10^{-6} S cm^{-1}). It can be seen from the values in Table 1 (and from Fig. 3) that, except for the lowest concentrations, the effect of displacement of the hydrogencarbonate is of little significance and thus deionized water need not be used in practical applications.

TABLE 1

Theoretical and experimental results of the SO_2 determination with the conductometric detector in the aerodispersion concentration unit. ($v_l/v_g = 3.61 \times 10^{-5}$, $T = 15\,^{\circ}C$)

SO_2 conc. (mg m^{-3})	K (10^3)	D (10^3)	G (10^{-5} S cm^{-1})		G_{exp}/G_{theor}
			Theor.	Exp.	
0.055	31.04	14.64	0.44	0.20	0.45 (0.68)[a]
0.38	11.81	8.28	1.72	1.56	0.91 (0.96)
0.61	9.32	6.97	2.32	2.17	0.93 (0.98)
0.73	8.52	6.52	2.60	2.46	0.95 (0.98)
1.10	6.94	5.55	3.34	3.32	0.99 (1.02)
1.93	5.24	4.41	4.65	4.70	1.01 (1.03)
2.20	4.91	4.17	5.01	4.98	0.99 (1.01)

[a]The values in parentheses were obtained after correction for the decrease in conductance caused by displacement of hydrogencarbonate.

Calibration curve

Because of the dependence of K on the hydrogen ion concentration, the calibration plot of the detector response, ΔE_o, to the SO_2 concentration in the air is nonlinear (see Fig. 3) and can be described by the relationship derived from Eqns. 5–7:

$$\Delta E_o = (E_i R_f A X/\theta)/[(BX)^{1/2} + C] \quad (8)$$

From the triple peak-to-peak noise on passage of pure air into the preconcentration unit (3×0.1 mV), a theoretical detection limit of 2.1×10^{-3} mg m^{-3} SO_2 can be obtained from Eqn. 8, if it can be assumed that the theoretical model is valid even for these low concentrations.

The long-term stability of the response was followed for 2 h at SO_2 concentrations of 0.05 and 0.38 mg m^{-3}; the response fluctuations did not exceed $\pm 2\%$.

The relative standard deviation was 2.4% ($n = 10$) for 0.38 mg m^{-3} sulphur dioxide. The critical factor governing the reproducibility of measurements was found to be the stability of the water flow rate, which can fluctuate in dependence of the hydrodynamic conditions in the throttling capillary (7 in Fig. 1A). The capillary material must be such that air bubbles do not adhere to the walls; glass capillaries used for the preparation of gas chromatographic capillary columns yielded good results, whereas plastic capillaries were totally unsuitable. With a glass capillary, flow-rate (v_l) fluctuations of $(2.76 \pm 0.17) \times 10^{-3}$ ml s^{-1} were obtained, causing ΔE_o fluctuations of ca. 1.6%.

Interfering gases

Although conductometric detection is inherently inselective, the determination of sulphur dioxide in the atmosphere is not significantly affected by the presence of common gaseous pollutants [7, 8] because they are mostly present as the undissociated molecules, except for ammonia, in aqueous solutions at pH < 5.7 (the pH of water in equilibrium with atmospheric carbon dioxide, i.e., ca. 5×10^2 mg m^{-3}). Table 2 lists the ratios of the distribution coefficients, K_i/K_{SO_2}, for potential interferents I_i and SO_2 at the same molar concentrations, $[I_i]_g^\circ = [SO_2]_g^\circ$, at 25°C. As the equivalent conductances of these gases are comparable, it is obvious that the only serious interferent would be ammonia.

As follows from the discussion above, the effect of real changes in the carbon dioxide concentration on the detector response is insignificant. The H_2S concentration in the air is generally several orders of magnitude lower than that of SO_2 and the decrease in the pH of the condensate in the presence of SO_2 shifts the ionization equilibrium in favour of the nonionic form, H_2S. Nitric oxide is poorly soluble in water and is nonionic. Surprisingly, nitrogen dioxide also does not interfere; this was verified experimentally. The detector response to 2.2 mg m^{-3} nitrogen dioxide was similar to that corresponding to the detection limit for sulphur dioxide ($\Delta E_o \approx 0.2$ mV). A small interference from nitro-

TABLE 2

Ratios of the distribution coefficients K_i/K_{SO_2} for some potential interferents[a]

Gas	K_H	K_1 (mol dm^{-3})	K_i/K_{SO_2}
SO_2	29.34	1.29×10^{-2}	1
CO_2	0.83	4.45×10^{-7}	9.87×10^{-4}
H_2S	2.44	1.26×10^{-7}	9.01×10^{-4}
NH_3	1342	1.75×10^{-5}	2.94×10^{-1}

[a]The K_H and K_1 values are taken from [8].

gen oxides has been noted [7] and explained by small absorption of the oxides in aqueous solutions.

Conclusions

The conductometric detector developed is suitable for continuous determination of SO_2 in the air after its absorption in water in the aerodispersion preconcentration unit. The detector is an integral part of the preconcentration unit and thus the information on the SO_2 concentration is available in real time (a stationary response was attained ca. 70 s after a change in the concentration). The consumption of redistilled water as the absorption medium was 0.3 l per 24 h under the given experimental conditions.

The determination is sensitive and thus the detector with the preconcentration unit is especially well suited for monitoring short-time changes of low concentrations of sulphur dioxide in the atmosphere.

The calibration dependence is nonlinear, but the dependence of the detector response on the SO_2 concentration in air satisfies the theoretical model and can be described by a mathematical equation which can be solved by an on-line computer during the measurement. The determination is sufficiently selective and the only serious interferent is ammonia.

As the detector is in contact with continuously renewed, dilute aqueous solution and the measuring reproducibility is determined virtually only by the reproducibility and stability of the flow rates of the air and water, which can be affected by the design of the apparatus, it can be expected that the detector properties will be stable over long time periods.

The authors are grateful to Dr. Z. Večeřa of the Institute of Analytical Chemistry, Czechoslovak Academy of Sciences, Brno, Czechoslovakia for his kindness in lending the nebulizer for the construction of the preconcentration unit.

REFERENCES

1 Z. Večeřa and J. Janák, Anal. Chem., 59 (1987) 1494.
2 F. Opekar, Z. Večeřa and J. Janák, Int. J. Environ. Anal. Chem., 27 (1986) 123.
3 F. Opekar and A. Trojánek, Chem. Listy, 81 (1987) 649.
4 J. Langmaier and F. Opekar, Anal. Chim. Acta, 166 (1984) 305.
5 P.K. Dasgupta, K. DeCesare and J.C. Ulrey, Anal. Chem., 52 (1980) 1912.
6 C.J. Walcek and H.R. Pruppacher, J. Atmos. Chem., 1 (1984) 269.
7 E.R. Kuczynski, Environ. Sci. Technol., 1 (1967) 68.
8 J.S. Symanski and S. Bruckenstein, Anal. Chem., 58 (1986) 1771.

Analytica Chimica Acta, 203 (1987) 11-21
Elsevier Science Publishers B.V., Amsterdam — Printed in The Netherlands

ION-CHROMATOGRAPHIC MEASUREMENTS OF AMMONIUM, FLUORIDE, ACETATE, FORMATE AND METHANESULPHONATE IONS AT VERY LOW LEVELS IN ANTARCTIC ICE

C. SAIGNE*, S. KIRCHNER and M. LEGRAND

Laboratoire de Glaciologie et Géophysique de l'Environnement, B.P. 96, 38402 St. Martin d'Heres Cedex (France)

(Received 18th March 1987)

SUMMARY

Ion chromatography is used to determine the concentrations of organic (formate, acetate and methanesulphonate) and inorganic (fluoride and ammonium) ions present in Antarctic ice at less than 10^{-9} g g^{-1} levels. With suitable columns, the simultaneous measurement of these ions requires only 6 min. A sample volume of 5 ml is sufficient to reach the 10^{-10} g g^{-1} level. The determination of such low concentrations requires stringent contamination-free techniques. For formate and acetate, the samples should never come into contact with plastics. Except for methanesulphonate, all the ions studied can be produced by dissolution of the various gaseous compounds present in a polluted atmosphere. Therefore a glass device with pure nitrogen circulation was designed for air-free melting of samples. To prevent possible biological activity on organic matter, samples were analysed immediately after melting. Measurements of ammonium ion in these Antarctic ice samples demonstrate that the problem of contamination by surrounding ammonia was not completely eliminated in previous studies. The serious contamination problems encountered, particularly for carboxylic acids, cast doubt on some earlier results for remote areas.

Because of its remoteness from polluted areas, the Antarctic continent would appear to be well suited to studies of precipitation chemistry. On the basis of similarities between atmospheric and snow contents, such glaciochemical data can provide information of global interest on atmospheric chemistry. Over the last five years, inorganic species (mainly Na^+, H^+, chloride, nitrate and sulphate) have been shown to represent the major ions in recent Antarctic precipitation [1,2]. Such comprehensive studies of Antarctic ice impurities have demonstrated the important role played by biogenic cycles (N and S) on the atmospheric background aerosol [3–6]. At present, organic compounds are arousing increasing interest. First, some carboxylic acids (mainly formic acid and, to a lesser degree, acetic acid) are thought to contribute significantly to

0003-2670/87/$03.50

the natural acidity of precipitation [7] and their atmospheric precursors (alkanes, alkenes and aldehydes) are thought to play an important role in the conversion of nitrogen and sulphur oxides to nitric and sulphuric acids [8]. Secondly, recent studies on marine aerosols [9] have indicated that methanesulphonic acid may be of interest in considerations of the sulphur cycle.

Besides the increasing geochemical interest of these anions, the possible role played by ammonia emissions in the natural background acidity remains poorly quantified. Indeed, previous studies of ammonium contents in Antarctic ice have demonstrated a crucial contamination problem in the measurement of this ion. Although an upper limit of a few ng g^{-1} was proposed by Legrand et al. [10], it seems that the problem of determination of ammonium ion in precipitation has not yet been solved completely.

In this paper, measurements of minor anions (fluoride, acetate, formate and methanesulphonate) and ammonium ion at the 10^{-10} g g^{-1} level are reported. For this, the chromatographic system (stationary phase and mobile phase) was optimized. The determination of such low concentrations requires stringent precautions in ice-core processing. Suitable analytical conditions have previously been established for major ions [6]. However, for minor anions and ammonium ion, some serious difficulties were encountered with such a procedure. All the ions (except methanesulphonate) studied here have a common property: the chemical compounds from which they can be derived are present as trace gases in polluted atmospheres. Accordingly, when the meltwater samples were in contact with air, these trace gases were dissolved and large contamination levels were observed. Moreover, the plastic vials previously used to store melt-water samples are a further source of contamination, especially for carboxylic acids. Such phenomena are quantified below and an alternative installation is described.

Contamination levels of up to several hundred ng g^{-1} exist for these ions on the outside of the cores but measured concentrations decrease abruptly from the outside to the centre of the core. The washing technique used in the final installation to remove outer contamination gave internal values around 10^{-10} g g^{-1} for acetate, formate, fluoride and ammonium ions and 10^{-9} g g^{-1} for methanesulphonate.

EXPERIMENTAL

Optimum conditions for ion chromatography

All ions measured in this work were quantified by using a Dionex model 2010i ion chromatograph. For Na^+, NH_4^+, K^+, Cl^-, nitrate and sulphate, the working conditions for ion chromatography previously used by Legrand et al. [10] were significantly modified. Analytical performance (especially a marked reduction in working time) was improved by using anion and cation hollow-fiber suppressor columns (AFS and CFS) [6,11]. More recently, cation mea-

TABLE 1

Working conditions for the Dionex 2010i chromatograph

Ions	Na^+, NH_4^+, K^+	Cl^-, NO_3^-, SO_4^{2-}	F^-, CH_3COO^-, $HCOO^-$, $CH_3SO_3^-$
Separator column	CS_2 (4×250 mm)	AS_4 (4×250 mm)	AS_4 (4×250 mm)
Eluent[a]	2.5×10^{-2} M HCl	2.5×10^{-3} M $NaHCO_3$/ 4×10^{-3} M Na_2CO_3	6.5×10^{-4} M $NaHCO_3$
Suppressor column	CMMS	AFS	AFS
Regenerating solution	7×10^{-2} M TMAOH[b]	1.4×10^{-2} M H_2SO_4	1.4×10^{-2} M H_2SO_4
Concentrator column	CG_1 (4×50 mm)	AG_4 (4×50 mm)	AG_4 (4×50 mm)

[a]At a flow rate of 2.0 ml min^{-1} in all cases. [b]Tetramethylammonium hydroxide.

surements were improved by using a micromembrane suppressor column (CMMS). Moreover, both the sensitivity and accuracy of the measurements improved when the newer HPIC separator columns supplied by Dionex were used. New working conditions for the above-mentioned ions are given in Table 1.

Minor anions (fluoride, acetate, formate and methanesulphonate) were measured with the same column used for common anions (chloride, nitrate and sulphate), but a weaker eluent (6.5×10^{-4} M sodium hydrogencarbonate, see Table 1) is required to detect these ions after the so-called water-dip (see Fig. 1). The eluent flow rate was selected with regard to the following two phenomena: (1) when the flow rate is too high, the fluoride peak starts in the water-dip, and good separation of fluoride and acetate peaks becomes difficult; (2) when the flow rate is too low, the retention time of methanesulphonate increases, causing reduced sensitivity for this ion. A good compromise between these two effects was obtained by using a 2 ml min^{-1} flow rate. Compared to previous measurements of methanesulphonate by Saltzman et al. [9], these working conditions for ion chromatography significantly reduce the time needed (6 instead of 15 min). Linear recorder plots of a typical chromatogram for the four minor anions are shown in Fig. 1, and for the three main cations in Fig. 2.

Calibration plots

Standard solutions (22.6 M hydrofluoric acid, 17.5 M acetic acid, 26 M formic acid, 15.1 M methanesulphonic acid and 0.1 M ammonium thiocyanate) were used to prepare stock solutions of 0.51 mg l^{-1} fluoride, 1.36 mg l^{-1} acetate, 1.39 mg l^{-1} formate, 1.19 mg l^{-1} methanesulphonate and 0.12 mg l^{-1} ammonium ion. Because of the observed decrease in the formic and acetic acid con-

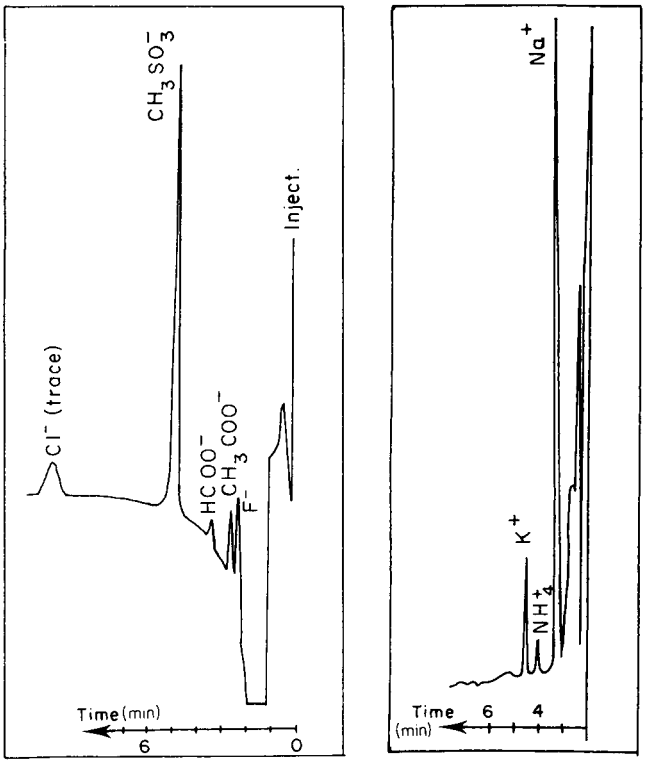

Fig. 1. Typical anion chromatogram: fluoride (0.14 ng g^{-1}), acetate (0.72 ng g^{-1}), formate (0.25 ng g^{-1}) and methanesulphonate (4.86 ng g^{-1}). Sample volume, 5 ml; meter setting, 1 μS; expansion 4.

Fig. 2. Typical cation chromatogram: sodium (3.55 ng g^{-1}), ammonium (0.65 ng g^{-1}) and potassium (1.68 ng g^{-1}). Sample volume, 5 ml; meter setting 10 μS; expansion 4.

tents in these stock solutions with time (see below), it was necessary to make new solutions for these compounds at regular intervals (once a month). The different standard solutions used for calibration were prepared just before they were needed by diluting stock solutions with double-deionized water (resistivity $\geqslant$ 18 MΩ). Calculated regression lines, estimated errors, correlation coefficients and detection limits are given in Table 2. With a 5-ml sample volume, ion chromatography allows fluoride, acetate, formate, methanesulphonate and ammonium ions to be measured down to a few tenths ng g^{-1}. A particularly high sensitivity was obtained for fluoride (5×10^{-11} g g^{-1}).

Sample flasks

To store melt-water samples, Legrand et al. [10] used either polyethylene flasks tediously cleaned with double-deionized water or precleaned disposable 30-ml polystyrene vials (Coulter accuvettes). In spite of several washings by

TABLE 2

Parameters of calibration lines and estimation of uncertainty for minor ions present in Antarctic precipitation

Ion	F^-	$HCOO^-$	CH_3COO^-	$CH_3SO_3^-$	NH_4^+
Range ($ng\ g^{-1}$)	0.0–1.0	0.0–5.0	0.0–9.0	0.0–5.0	0.0–2.0
Regression line[a]	$h=6+154c$	$h=-6.5+46.3c$	$h=0.5+20.0c$	$h=0.6+18.4c$	$h=2.5+10.0c$
Error[b] ($ng\ g^{-1}$)	±0.05	±0.3	±0.3	±0.25	±0.2
r[c]	0.998	0.997	0.998	0.999	0.994
Detection limit ($ng\ g^{-1}$)	0.02	0.06	0.15	0.16	0.10

[a]h is the peak height (in mm) as a function of concentration c (in $ng\ g^{-1}$). [b]Estimate at 95% confidence limits. [c]Correlation coefficients.

filling the vials with deionized water and putting them into a microwave oven, such materials continue to release formic and acetic acids in significant quantities. For instance, 3 $ng\ g^{-1}$ acetate and 2 $ng\ g^{-1}$ formate are typical concentrations observed with 20 ml of ultrapure water stored in polystyrene vials. From successive treatments with ultrapure water in a microwave oven, it was concluded that this contamination does not come from the container surface but from inside the material itself (probably from additives used in making the polymers). A similar problem was encountered with other materials such as polycarbonates. Therefore the use of such polymers must be avoided in measurements of carboxylic acids.

Glass apparatus posed no such problems for either formate or acetate. However, because one aim of this work was to measure all ions (organic and inorganic species) in the same melt-water sample, it was necessary to establish whether or not glass affected the other measurements. Special attention was paid to sodium, commonly involved in contamination problems when glass is used. Because such a contamination problem involves ion-exchange phenomena, it depends strongly on the pH value of the liquid phase. A glass vial was filled with a test sodium solution adjusted to pH 5 (i.e., the typical pH value observed in melt-water of Antarctic ice) and sodium was measured at regular intervals. This operation was repeated with an ultrapure water solution. In both cases, no modification of the initial sodium concentration was observed (at least over four hours). On this basis, glass was chosen as the material for the measurement apparatus.

Contamination by atmospheric trace gases

It has been demonstrated elsewhere that measurements of ammonium ion at a few $ng\ g^{-1}$ can be erroneous because of the dissolution of traces of am-

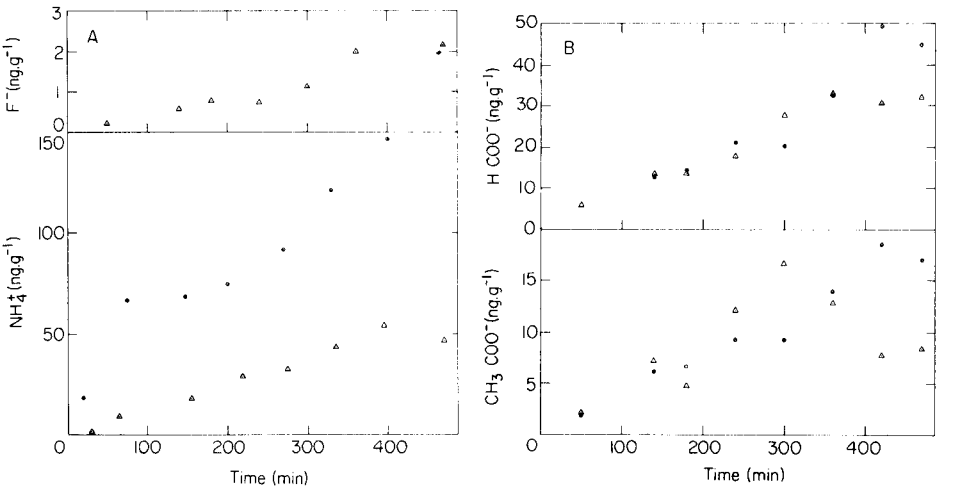

Fig. 3. Concentrations (in ng g^{-1}) of various ions found in vials filled with double-deionized water and left open over increasing time periods within a clean-air bench, both outside (△) and inside (●) the laboratory. (A) Fluoride and ammonium; (B) formate and acetate.

monia present in the atmosphere, if strict precautions are not taken during sample melting [10]. Such difficulties were encountered in this study with fluoride, acetate and formate (no contamination problem was apparent with methanesulphonate). To illustrate the problem, several vials filled with ultrapure water were left open over increasing time periods within two clean-air benches (one left outside and the other inside the laboratory). The results obtained for fluoride, ammonium, formate and methanesulphonate in each vial showed increasing contents of these ions (Fig. 3). This phenomenon was not observed when the vials were closed.

Figure 3A shows that ammonium ion concentrations reach 30 ng g^{-1} in less than 7 h. That confirms previous observations made by Legrand et al. [10], but this increase is even more dramatic (three times higher) when samples are open to the confined atmosphere of the laboratory, even in a clean-air bench. With regard to fluoride, Fig. 3A indicates a slight contamination outside the laboratory whereas this did not seem to occur inside. At first glance, this observation is surprising, but in fact the small portable clean-air bench used during measurements outside the laboratory had previously been stored for several years in a room where hydrofluoric acid was commonly used. This observation clearly demonstrates the long period of time over which plastics previously exposed to high vapor pressures of a pollutant can release significant amounts of this compound.

Both formic and acetic acids are present in the atmosphere as shown in Fig. 3B. Similar contamination levels were detected outside and inside the laboratory: 40 ng g^{-1} and 15 ng g^{-1} for formate and acetate, respectively, over the

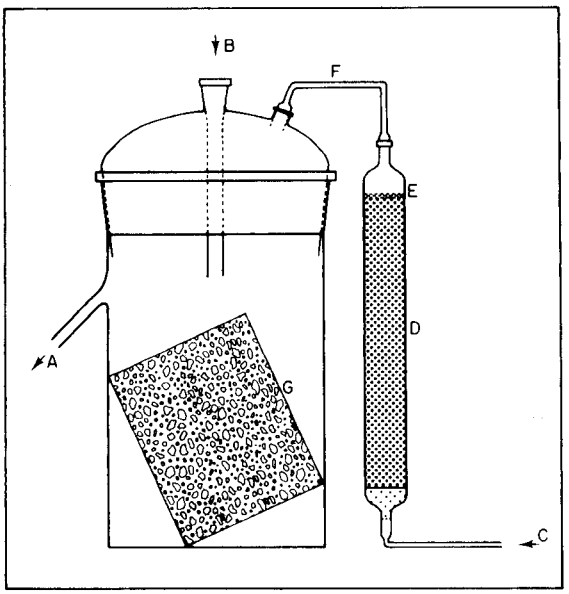

Fig. 4. Air-free melting of samples: (A) small lateral pipe providing an outlet; (B) pipe used to fill with ultrapure water; (C) nitrogen inlet; (D) active carbon particles; (E) fritted glass filter; (F) purified nitrogen inlet; (G) section of the ice core.

same lapse of time (8 h). Comparing these values with the expected amounts of carboxylic acids for Antarctic precipitation (a few ng g^{-1} [6]), it is obvious that this source of contamination must be eliminated.

Air-free melting of ice sample

On the basis of the observation of contamination both by plastic apparatus and by gas dissolution, a special melting device (Fig. 4) was designed. All parts of the set-up are made of glass. Air-tightness is ensured by a water film at the level of the fittings. A pipe (B) is used to fill the receptacle with double-deionized water to wash the ice-core section; liquid waste is then drained through the small lateral outlet (A). This device was stored in a clean-air bench and clean plastic gloves were worn during the experiments.

During sample melting, an inert gas atmosphere must be maintained inside the receptacle. A nitrogen circulation set-up is used for this (C→A). In spite of the high purity of the nitrogen used (type N60), this method still introduces some risk of contamination both from the relief valve of the nitrogen bottle and from degassing along the rubber tubing. Therefore, a glass trap containing activated carbon particles is included on the nitrogen flow line, upstream of the receptacle (D). Activated carbon particles act as an adsorbing filter for many chemical species and especially for organic compounds. Nevertheless, tests on a standard solution (F^-, CH_3COO^-, $HCOO^-$, $CH_3SO_3^-$ and NH_4^+)

TABLE 3

Study of the evolution of a standard solution of the four minor anions with time under sample melting conditions

Time (h)	Fluoride ($ng\,g^{-1}$)	Acetate ($ng\,g^{-1}$)	Formate ($ng\,g^{-1}$)	Methanesulphonate ($ng\,g^{-1}$)
0	0.55	1.7	0.8	3.5
1	0.495	1.5	0.73	3.5

inside the device revealed a retrodiffusion phenomenon for acetate and formate. In fact, chemical compounds rising inside the receptacle against the nitrogen flow were removed by the activated carbon.

The observation of this phenomenon led to the following final experimental procedure. First, the ice-core section is superficially washed with ultrapure water in a clean-air room; it is then placed in the glass receptacle swept by a nitrogen flow, and washed with double-deionized water until 70% of the initial volume of the ice-core section has been melted and drained. Finally, the lateral outlet (A) is closed with a small polyethylene bag, the nitrogen flow is stopped and plugs are fitted in all openings of the main glass vessel. The ice sample melts in a static pure nitrogen atmosphere. The liquid sample is then drawn out through the lateral pipe (first rinsed with ultrapure water) with a syringe which is then used directly to inject the sample into the ion chromatograph.

RESULTS

Analytical tests

Two different experiments were designed to check that sample species were neither contaminated nor degraded in the device used. With regard to liquid samples containing carboxylic acids, biological activity has been reported by Keene et al. [7]: in all aliquots which had not been treated with a biocide, some disappearance of formic and acetic acids was noticed. Similar degradation of the stock solutions used here was also noted after a few weeks. The evolution of a standard solution was therefore studied in the recommended device under sample-melting conditions. Measurements were made after an interval of an hour (approximately the melting time for a sample) and a maximum of 10% degradation was calculated (Table 3). Therefore, because the present samples were analysed immediately after the melting and because the temperature of the liquid phase could not rise significantly above 0°C (thus decreasing the biological activity), the measured levels can be assumed not to underestimate the real values.

In another test, the blank value was determined for the recommended device by analysing a piece of clean ice, i.e., a piece of ice containing none of the

studied ionic species. The best way to avoid all contamination during the preparation of this ice piece was to freeze ultrapure water in the glass device itself. For this purpose, the glass receptacle was placed in a pure nitrogen flow and then was filled with about 500 ml of double-deionized water. While the nitrogen circulation was maintained, the vessel was gradually plunged into a freezing mixture of alcohol and liquid nitrogen ($-30°C$). Once 75% of the water had frozen, two samples were taken and analysed. Melt-water sample 1 came from the clean ice piece once the remaining unfrozen water had been drained. Melt-water sample 2 was taken after washing with ultrapure water inside the glass device. To suppress any effect of retrodiffusion, all the operations except washing were done without nitrogen flow. For the two samples, the concentrations of all the four minor anions and ammonium ion were below the present detection limits. This demonstrates both the purity of the ice piece used in these tests and the contamination-free washing and melting of the ice samples achieved in the recommended device.

Wash melting of an ice-core section

It was necessary to test the effectiveness of washing with ultrapure water inside an airtight glass receptacle. Indeed, ice coring, transport and storage create high contamination levels on the external parts of the cores [1]. The proposed method of decontamination was tested with an ice-core section (from 250-m depth) taken from the 906-m ice core of Dome C (East Antarctica). To measure the steady decrease of ionic species, the ice piece was first sawn to the receptacle dimensions without taking any particular precautions about cleanliness. In fact, it was thought advisable to begin the analysis with a high level of exterior contamination to be sure that during ordinary measurements, the contamination level of the surface of the samples would be much lower (because samples were usually rinsed in a clean-air bench before being placed in the glass receptacle). In this way, the test guarantees reliability of measurements.

Once placed in the pure static nitrogen atmosphere of the device, the sample slowly melted and successive 20-ml melt-water fractions were taken and examined by ion chromatography. Between the first and second fractions, the remaining melt-water was simply drained off. After the second fraction, however, the remaining ice piece was rinsed with ultrapure water under nitrogen circulation. The results of this experiment are given in Fig. 5. Measurements are reported not only for fluoride, acetate, formate, methanesulphonate and ammonium but also for some major ions (Na^+, Cl^-, SO_4^{2-}, NO_3^-, K^+) to provide a reference with respect to well-known decontamination processes [10]. Figure 5 shows that the general diagram is the same for all the compounds; the high values at the surface abruptly decrease during the first two or three fractions and reach a plateau with fluctuations around a mean value, caused by

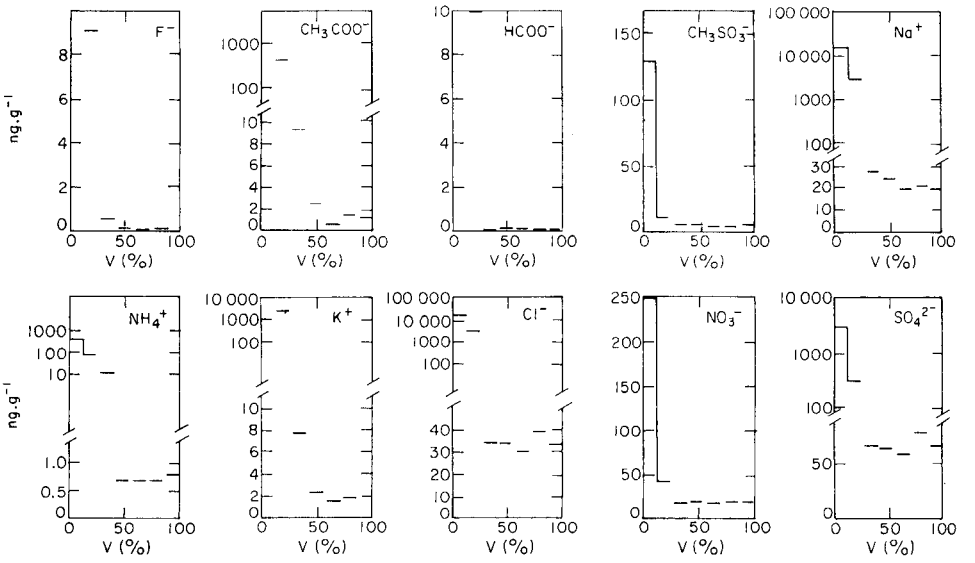

Fig. 5. Decontamination of a piece of ice from 250-m depth at Dome C by "wash-melting" with ultrapure water. Concentrations (ng g^{-1}) are given as a function of the melted fraction of the ice sample (% V).

sample inhomogeneity. This means that, for all species, at the very least 50% of the core is free of contamination.

Some interesting information can be drawn from the plateau values. The low mean concentration observed for ammonium ion in the last four fractions (0.7 ± 0.2 ng g^{-1}) seems to be the real value, which is an order of magnitude lower than previous results [6]. Legrand [6] was never able to avoid gas contamination totally, and defined 1–5 ng g^{-1} as the upper limit. Another analytical method in which gas dissolution was minimized, was also tested. The ice-core section was stored in a supple polyethylene bag with minimum confined air; immediately after melting, a liquid sample was taken through the plastic membrane by using a syringe and a stainless-steel needle. The mean concentration detected with this procedure was 0.5 ng g^{-1}. Both experimental protocols therefore give consistent results, and allow ammonium ion to be quantified at levels below ng g^{-1}.

For the carboxylic acids, it can be contended, as for ammonium ion, that the obtained plateau values corresponds to real concentrations without any contamination. The method gives a general indication of the mean amounts of acetate and formate in precipitation at these high latitudes, respectively, 1.5 ng g^{-1} and 0.06 ng g^{-1}. It may be noted that with the contribution of methanesulphonic acid (5.5 ng g^{-1}), total organic acidity represents 0.083 μeq l^{-1}. Mineral acidity originates from nitric, sulphuric and sometimes hydrochloric acid [2]. Calculations developed in detail elsewhere by Legrand [2], from

nitrate, sulphate, chloride and sodium content, were used to evaluate the corresponding H^+ content of the present 250-m depth ice-core section. The mineral acidity found was equal at 1.4 μeq l^{-1}, thus the organic contribution represents only 6% of the total acidity. Similar results have been obtained by Legrand and Saigne [12], which confirms that in very remote areas organic compounds are only minor contributors to global precipitation acidity.

For fluoride, the present study seems to be the first in which the concentrations in Antarctic precipitation were quantified. The presence of hydrofluoric acid is indicated with a plateau level of 0.12 ng g^{-1}. The only other data for such remote areas are from Herron [3] who reported quite similar background fluoride concentrations in Greenland ice cores (ca. 0.2 ng g^{-1}). Fluoride was not found in Antarctic ice by Ivey and Davies [13] but their detection limit was 5 ng ml^{-1} fluoride.

Conclusion

In spite of the presence of their gaseous precursors in polluted atmospheres, fluoride, acetate, formate, methanesulphonate and ammonium can be measured with good accuracy by ion chromatography. A tedious experimental protocol with stringent sample decontamination procedures is required. The glass equipment used greatly reduces the speed of analysis. Only three or four samples can be analysed per day. However, except for ammonium ion, for which an alternative faster sampling method can be used, this painstaking experimental procedure is the only way to obtain reliable measurements of compounds present in Antarctic precipitation at 10^{-9} ng g^{-1} levels. In addition to providing reliable order-of-magnitude estimates of ammonium levels, the experimental protocol is particularly well suited to the determination of organic acids and fluoride in ice cores for use in geochemical interpretations.

REFERENCES

1 M. Legrand and R.J. Delmas, Atmos. Environ., 18 (1984) 1867.
2 M. Legrand, J. Phys. (Paris), 48 (1987) 77.
3 M.M. Herron, J. Geophys. Res., 87 (1982) 3052.
4 M. Legrand and R.J. Delmas, Ann. Glaciol., 7 (1985) 20.
5 M. Legrand and R.J. Delmas, Tellus, 38 (1986) 236.
6 M. Legrand, Doctoral Thesis, Université Scientifique et Médicale de Grenoble, 1985.
7 W.C. Keene, J.N. Galloway and J.D. Holden, Jr., J. Geophys. Res., 88 (1983) 5122.
8 B.J. Finlayson-Pitts and J.N. Pitts, Atmospheric Chemistry: Fundamental and Experimental Techniques, Wiley-Interscience, New York, 1986.
9 E.S. Saltzman, D.L. Savoie, R.G. Zika and J.M. Prospero, J. Geophys. Res., 88 (1983) 10897.
10 M. Legrand, M. de Angelis and R.J. Delmas, Anal. Chim. Acta, 156 (1984) 181.
11 M. Legrand and R.J. Delmas, Proc. NATO ASI, Les Arcs, France, July 1986, p. 225.
12 M. Legrand and C. Saigne, Atmos. Environ., in press.
13 J.P. Ivey and D.M. Davies, Anal. Chim. Acta, 194 (1987) 281.

Analytica Chimica Acta, 203 (1987) 23–34
Elsevier Science Publishers B.V., Amsterdam — Printed in The Netherlands

ZUR ANALYTIK VON KUPFER/FLAVONOID-KOMPLEXEN ALS ELEMENTSPEZIES IN PFLANZLICHEN LEBENSMITTELN

KRISTIN WEDEPOHL und GEORG SCHWEDT*

Institut für Lebensmittelchemie und Analytische Chemie der Universität Stuttgart, Pfaffenwaldring 55, D-7000 Stuttgart 80 (Federal Republic of Germany)

(Eingegangen den 7 April 1987)

SUMMARY

(*Analysis of copper/flavonoid complexes as element species in vegetables*).

Adsorption on cellulose using a batch procedure seems to be suitable for the separation of an excess of free quercetin from copper-complexed species in synthetic solutions and in an aqueous methanolic onion extract. Liquid/liquid extraction with chloroform is also suitable for separating free flavonoids from metal/flavonoid complexes. With gel-permeation chromatography, it is possible to fractionate the flavonoids in plant extracts without changing the chemical speciation. Determination of copper concentrations in the fractions, and ultraviolet/visible spectrophotometric studies of the flavonoids with shift reagents, provide information on the presence and type of the copper/flavonoid species in vegetables such as onions and tomatoes.

ZUSAMMENFASSUNG

Die Adsorption an Cellulose im Batch-Verfahren erweist sich als geeignete Technik zur Abtrennung eines Überschusses an freiem von Kupfer-komplexiertem Quercetin sowohl in synthetischen Lösungen als auch in einem methanolisch-wäßrigen Zwiebel-Extrakt. Die Flüssig/flüssig-Extraktion mit Chloroform bildet ein zweites Verfahren zur Abtrennung freier Flavonoide von Metall/Flavonoid-Komplexen. Mittels Gel-Chromatographie können die Flavonoide in Pflanzenextrakten fraktioniert werden, ohne daß Änderungen der Element-Bindungsformen eintreten. Bestimmungen der Kupfergehalte in den Fraktionen sowie UV/VIS-spektroskopische Untersuchungen der Flavonoide mit Hilfe von "Shift"-Reagenzien liefern Anhaltspunkte zur Existenz und Art von Kupfer-Flavonoid-Spezies in pflanzenlichen Lebensmitteln wie Zwiebeln und Tomaten.

Die Analytik von Elementspuren beschränkt sich bisher überwiegend auf die Bestimmung von Gesamtgehalten. Da die Bioverfügbarkeit und damit auch die Toxizität von Metallen jedoch wesentlich durch deren Bindungsformen in Komplexen mit organischen Liganden bestimmt sind, ist es notwendig, differenzierende Untersuchungen zu den Elementspezies durchzuführen. Bis heute liegen nur wenige Arbeiten zur Metall bzw. Elementspeziesanalytik in Lebensmitteln vor [1–6]. Diese Untersuchungen sind besonders wichtig bei Ele-

0003-2670/87/$03.50

menten bzw. organischen Verbindungen, die für die menschliche Ernährung entweder wegen ihrer potentiellen Giftigkeit oder wegen ihrer Essentialität und ihres Einflusses auf physiologische Vorgänge von großer Bedeutung sind. Von den Flavonolen bzw. Flavonol-Glykosiden ist bekannt, daß sie "Vitamin P-Aktivität" besitzen [7] und ihre biologische Wirksamkeit in Anwesenheit von Cu^{2+}-Ionen zunimmt [8]. Das Ziel dieser Arbeit war daher, eine Analysenmethodik zu entwickeln, die es ermöglicht, Aussagen über Kupfer-Flavonoid-Bindungen in pflanzlichen Lebensmitteln zu machen.

In Vorversuchen mit synthetischen Lösungen wurde festgestellt, daß Kupfer mit verschiedenen Flavonolen, sowohl Glykosiden als auch Aglykonen, Komplexe bildet, deren Stabilitätskonstanten zwischen 10^{13} und 10^{14} liegen [9]. Zur Untersuchung wurden Lebensmittel eingesetzt, deren Gehalte an Flavonoiden aus der Literatur bekannt sind [10].

EXPERIMENTELLER TEIL

Probenvorbereitung und Aufschußverfahren

Das Pflanzenmaterial wird nach der Gefriertrocknung (Gefriertrocknungsgerät Leybold-Heraeus GT-2) in einer Mühle (Retsch 7M-1; Siebgröße 0,5 mm) zu feinem Pulver vermahlen. Eine ausgewogene Menge (2 g) wird mit 75 ml Methanol/bidestilliertes Wasser (1:1) versetzt und 1 h unter Rückfluß und Rühren extrahiert. Die überstehende Flüssigkeit wird durch ein Faltenfilter und anschließend durch ein Membranfilter (0,45 μm) filtriert. Das Lösungsmittel wird am Rotationsverdampfer (im Vakuum bei 45 °C) abdestilliert, der Rückstand in 20 ml Methanol/bidestilliertes Wasser (1:3) gelöst und mit 0,02% an Natriumazid konserviert.

Zum Druckaufschluß [11]: 100 mg des pulverisierten Materials bzw. 1 ml des Extraktes (siehe oben) entsprechend 100 mg Ausgangsmaterial werden im Teflon-Einsatz des Aufschlußgerätes mit 700 μl konzentriert Salpetersäure (Suprapur) versetzt und nach folgendem Programm erhitzt: 2 h bei 70 °C, 15 min bei 120 °C, 1 h bei 160 °C. Nach dem Abkühlen wird mit bidestilliertem Wasser auf 10 ml aufgefüllt.

Analysenmethoden

Atomabsorptions-Spektrometrie. [Zeeman 3030 AAS mit Printer PR-100 (Perkin-Elmer); GraphitrohrKüvette mit Plattform] Jeweils 20 μl der aufgeschlossenen Probe werden mittels des automatischen Probengebers in das Graphitrohr gebracht und nach folgendem Programm gemessen: Wellenlänge 324,8 nm, Spalt 0,7 nm, Lampenstrom 8 mA. Statistik: 3 Messungen mit je 4 s Meßzeit. Standard-Lösung: 30 μg Cu kg^{-1}. Trocknen: 130 °C/Veraschen 1200 °C/Atomisieren (Gas-stop) 2200 °C/Ausheizen 2600 °C.

Spektrophotometrie des Quercetins [12]. Zirkon(IV)-Lösung (500 µl 0,1 mol l^{-1}, aus $ZrOCl_2$ $8H_2O$ in bidestilliertem Wasser) werden mit 5 ml 0,1 mol l^{-1} HCl und 2 ml Probe versetzt. Mit Methanol wird auf 25 ml aufgefüllt und nach 15 min die Extinktion bei 460 nm gegen Methanol gemessen (1-cm Küvette, Zeiss Spektrophotometer PMQ-II).

Ultraviolett-Spektrophotometrie mit "Shift"-Reagenzien [13]. Die eingedampften Fraktionen (Vakuum-Rotationsverdampfer) aus der Gel-Chromatographie (siehe unten) werden in Methanol (Grundlösung) gelöst. In 1 cm-Küvetten Pye-Unicam SP8-100 Spectrophotometer, werden die Spektren von 550 bis 210 nm aufgezeichnet ("MeOH"-Spektrum). Anschließend werden 3 Tropfen einer 2%igen Natriummethylat-Lösung zugegeben, durchmischt und es wird sofort das "NaOMe"-Spektrum aufgenommen. Die Messung wird nach 5 min wiederholt. Zu einer frischen methanolischen Grundlösung wird eine Spatelspitze wasserfreien Natriumacetats hinzugegeben, gelöst und dann das "NaOAc"-Spektrum registriert. Diese Messungen werden ebenfalls nach 5 min widerholt. Dann wird wasserfreie Borsäure in dieselbe Küvette gegeben (ca. die Hälfte im Vergleich zur NaOAc-Menge) und das "NaOAc/H_3BO_3"-Spektrum registriert. Zur Aufnahme des "$AlCl_3$"-Spektrums werden 6 Tropfen einer 5%igen Aluminiumchlorid-Lösung zu frischer methanolischer Grundlösung gegeben. Anschließend werden 3 Tropfen halbkonzentrierter HCl zur Aufnahme des "$AlCl_3$/HCl"-Spektrums hinzugefügt. Die Interpretation der Spektren erfolgt [14].

Trennmethoden

Adsorption an Cellulose. Die methanolisch-wäßrigen Pflanzenextrakte (5 ml) werden mit 15%iger Essigsäure auf 40 ml aufgefüllt. Diese Lösung versetzt man mit 1,5 g Cellulosepulver (Machery-Nagel MN300), das zuvor mit 2 mol l^{-1} HCl (Suprapur) gewaschen wurde. Nach 30 min Rühren wird durch eine Glasfritte (G3) abfiltriert. Folgende Bestimmungen werden durchgeführt (Lösung bzw. Filtrat): (1) photometrische Bestimmung der Quercetin-Konzentration vor und nach dem Batch-Verfahren; (2) Bestimmung des Kupfergehaltes vor und nach dem Batch-Verfahren; (3) Aufnahme der UV-Spektren des unbehandelten Pflanzenextraktes und des Filtrats.

Flüssig/flüssig-Extraktion. Der wäßrigen Pflanzenextraktes (2 ml; nach Abdestillieren des Methanols und Auffüllen mit bidestillierten Wasser auf 100 ml) werden mit 5 ml Chloroform extrahiert. Die organische Phase wird abgetrennt und analysiert für Kupfer und Quercetin.

Gel-Chromatographie am Sephadex LH-20. [16×400 mm Säule mit Adapter (Pharmacia), 4-Wege-Hahn; Microperpex Peristaltic Pump (LKB 2132); Uvicord S-Detektor mit Filter 254 nm (LKB 2138)] Sephadex LH-20 (10 g in 1:1 Methanol/bidestilliertem Wasser gequollen) wird in die Säule gefüllt und mit den Endstücken zusammengedrückt. Der pH-Wert der Eluenten (Methanol/bidestilliertes Wasser 50:50, 70:30, 80:20, 100:0) wird mit ver-

dünnter Salzsäure auf 2 eingestellt. Die getrennten Fraktionen werden für weitere Analysen für Kupfer, Quercetin und mit Shift-Reagenzien gesammelt. Die Flußrate beträgt 75 ml h^{-1} [9].

ERGEBNISSE UND DISKUSSION

Am Beispiel des Kupfer/Quercetin-Komplexes wurden zwei Verfahren zur Abtrennung des Komplexes von einem Überschuß an Komplexbildner entwickelt. Versuche mit synthetischen Lösungen (0,001 mol l^{-1} Quercetin- und Kupfer-Lösungen) führten zu dem Ergebnis, daß ein Überschuß an Quercetin in 15%iger Essigsäure irreversibel an Cellulose adsorbiert wird, der Kupfer/Quercetin-Komplex jedoch überwiegend in Lösung bleibt. Im Spektrum des Kupfer/Quercetin-Komplexes (Abb. 1) erscheint das Maximum des reinen Quercetins bei 360 nm nach der Adsorption im Batch-Verfahren nicht mehr. Die Intensität des Kupfer-Komplex-Peaks bei 286 nm ist nur unwesentlich verringert. Versuche zur Adsorption von Quercetin an Kieselgel ergaben keine Abtrennung des Quercetin-Überschusses vom Kupfer-Komplex. Die Dünnschicht-Chromatographie an Cellulose bzw. Kieselgel eignet sich zwar zur Trennung von verschiedenen Flavonoiden [13], jedoch gelingt es nicht, freie und metallkomplexierte Flavonoide voneinander zu trennen. Unterschiedliche Gleichgewichtseinstellungen zwischen stationärer Phase und Probe (im Batch-Verfahren erfolgt sie einstufig, bei der Dünnschicht-Chromatographie handelt es sich um ein Vielstufensystem) sind möglicherweise der Grund dafür, daß nur die Adsorption an Cellulose im Batch-Verfahren zu einer Abtrennung des Quercetin-Überschusses führt. Der Vielstufenprozeß in der Dünnschicht-Chromatographie verursacht eine Aufspaltung der Komplexe.

Die Flüssig/flüssig-Extraktion stellt ein zweites Verfahren sowohl zur Abtrennung organischer Metall-Komplexe als auch zur Anreicherung durch Abdestillieren des Extraktionsmittels dar. Von den untersuchten organischen, mit Wasser nicht mischbaren Lösungsmitteln (Essigsäureethylester, Diethylether, Diisopropylether, Methylisobutylketon, Isobutanol, Chloroform) eignet sich Chloroform zur Überführung des Kupfer/Quercetin-Komplexes aus der wäßrigen in die organische Phase. Systematische Untersuchungen mit unterschiedlichen Konzentrationen an Metall bzw. Flavonoid in synthetischen Lösungen geben Aufschluß über die Konzentrationsabhängigkeit der Extraktion (Abb. 2): Je größer die Metallkonzentration in der wäßrigen Phase, desto höher wird die Quercetin-Konzentration in der organischen Phase. Außerdem läßt sich ein Zusammenhang zwischen der Konzentration an extrahiertem Kupfer und dem pH-Wert in der wäßrigen Phase feststellen, wie Abb. 3 zeigt.

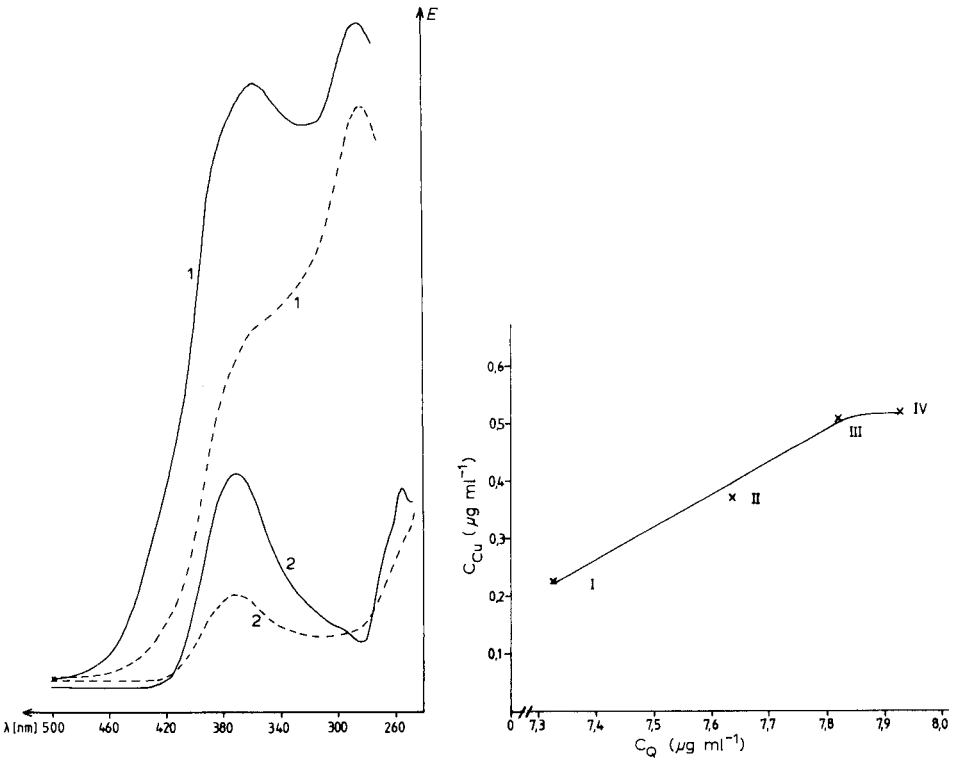

Abb. 1. Spektren: (1) Kupfer/Quercetin-Lösung (molare Verhältnisse 1:4); (2) reinen Quercetin-Lösung. (——) vor Adsorption an Cellulose im Batch-Verfahren; (– – –) nach Adsorption.

Abb. 2. Kupfer/Quercetin-Verteilung bei der Chloroform-Extraktion von Modell-Lösungen für verschiedenen Konzentrationen an Kupfer und Quercetin (Q) in der Chloroform-Phase. Vorgegebene Konzentration an Kupfer in der wäßrigen Phase: (I) 0,32; (II) 0,64; (III) 1,27; (IV) 1,91 μg ml^{-1}. Konzentration an Q: 10,15 μg ml^{-1}.

TABELLE 1

Kupfer- und Quercetin-Gehalte in Zwiebel-Extrakt vor und nach der Adsorption an Cellulose[a]

	Quercetin Konz.		Kupfer Konz.	
	(μg ml^{-1})	(×10^{-5} mol l^{-1})	(ng ml^{-1})	(×10^{-7} mol l^{-1})
Vor dem Batchversuch	16,8	5,0	24,8	3,9
Nach dem Batchversuch	10,4	3,1	26,3	4,1
Adsorption	40%		—	

[a]Gesamtvolumen jeweils 40 ml/1,5 g Cellulosepulver.

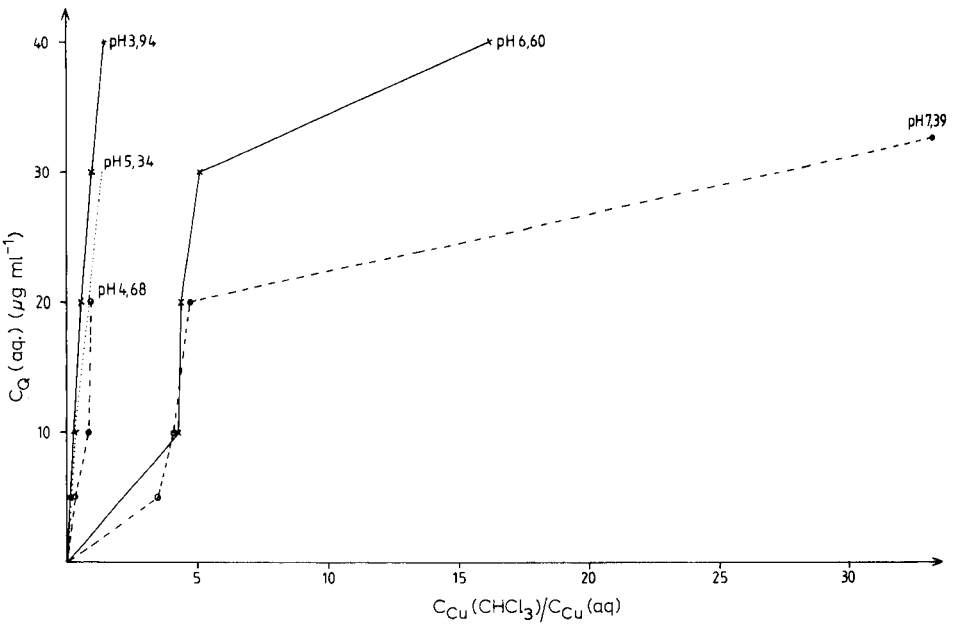

Abb. 3. Chloroform-Extraktion von Kupfer/Quercetin-Lösungen in Abhängigkeit vom pH-Wert in der wäßrigen Phase.

In der Tabelle 1 sind die Ergebnisse zusammengefaßt, die bei der Anwendung des Adsorptionsverfahrens an Cellulose auf einen Zwiebel-Extrakt erhalten wurden. Die Kupfer- und Quercetin-Analysen zeigen, daß an Cellulose auch aus Zwiebel-Extrakten nur Quercetin und kein Kupfer adsorbiert wird. Die unvollständige Adsorption des Quercetins zeigt, daß dieses Flavonoid zum überwiegenden Teil gebunden in Form von Metallkomplexen vorliegt. Kupfer ist dabei nur eines von einer Reihe komplexbildender Metalle. Da nach der Adsorption im Batch-Verfahren die Quercetin-Komplexes (1:1 bzw. auch 1:2) zu erwarten ist, muß angenommen werden, daß auch andere Metalle an der Quercetin-Bindung beteiligt sind.

Das Spektrum des Zwiebel-Extraktes (Abb. 4) weist zwei Absorptionsmaxima bei 360 nm (Bande 1) und bei 290 nm (Bande 2) auf, dessen Verlauf auf überlagerte Absorptionen verschiedener Substanzen schließen läßt. Eine Interpretation des Spektrums unterhalb von 340 nm ist daher nicht sinnvoll. Das Maximum von Bande 1 entspricht der Absorptionsbande des reinen Quercetins. Die Intensität der Bande nimmt nach der Adsorption an Cellulose stark ab, was die Ergebnisse der quantitativen Analysen (Tabelle 2) bestätigt. Versuche mit synthetischen Lösungen haben gezeigt, daß solch niedrige Kupfer-Konzentrationen, wie sie in der Zwiebel vorliegen, keine Verschiebungen der Absorptionsbanden im Quercetin-Spektrum verursachen.

Um festzustellen, ob auch die mit Modell-Lösungen erhaltenen Ergebnisse

Abb. 4. Spektrum des Zwiebel-Extraktes (——) und des Filtrats (– – –) nach Adsorption an Cellulose.

TABELLE 2

Kupfer- und Quercetin-Gehalte in Zwiebeln und Tomatenschalen bzw. deren Extrakten

Lebensmittel	Gesamt-Gehalt Cu ($\mu g\ g^{-1}$)	$MeOH/H_2O$-Extr.		$CHCl_3$-Extr.	
		Cu ($\mu g\ g^{-1}$ Lebensmittel)	Q	Cu	Q
Zwiebel	5,3	2,9 (47%)[a]	2400	1,2 (48%)[b]	204 (9%)
Tomatenschale	7,8	3,0 (39%)	357	1,2 (40%)	46 (13%)

[a]In Klammern: in Prozent des Gesamt-Gehaltes. [b]In Klammern: in Prozent des $MeOH/H_2O$-Extraktes.

TABELLE 3

Kupfer- und Quercetin-Gehalte im Zwiebel-Extrakt nach der Extraktion mit Chloroform und Zugabe steigender Kupfermengen zur wäßrigen Phase[a]

Zugabe an Cu	Gehalte im Extrakt (μmol)	
(μmol)	Cu	Quercetin
0	0,02	0,60
0,50	0,06	0,30
1,00	0,11	0,40
2,00	0,41	1,00
3,00	0,73	1,90

[a]Steigung der Additionsgeraden: 2,5, entsprechend dem Molverhältnis Cu: Quercetin.

der Flüssig/flüssig-Extraktion mit Chloroform auf die Lebensmittel-Extrakte übertragbar sind, wurden entsprechende Untersuchungen mit den Zwiebel- und Tomatenschalen-Extrakten durchgeführt. Nach der Chloroform-Extraktion werden in der organischen Phase die Konzentrationen an Kupfer und Quercetin bestimmt und den im Methanol/Wasser-Extrakt bestimmten Konzentrationen und den Gesamtgehalten gegenübergestellt (Tabelle 2). Es zeigt sich, daß mit Chloroform aus dem Zwiebel-Extrakt ein höherer Metallanteil als aus dem Tomatenschalen-Extrakt in die organische Phase überführt wird: der Kupfer-Gehalt im Zwiebel-Extrakt beträgt 22% des Gesamtgehaltes, derjenige im Tomatenschalen-Extrakt 15%. Der prozentuale extrahierbare Quercetin-Anteil ist im Tomatenschalen-Extrakt größer als im Zwiebel-Extrakt. Wie oben gezeigt wurde, ist die Extrahierbarkeit von Quercetin von der Kupfer-Konzentration abhängig (Abb. 2). Anhand der Zugabe von steigenden Kupfer-Mengen zum Zwiebel-Extrakt (Tabelle 3) kann gezeigt werden, daß Quercetin, welches im Überschuß im Zwiebel-Extrakt vorhanden ist, ausschließlich im Komplex mit Metallen in die Chloroform-Phase überführt wird. Das bestätigt die Ergebnisse aus den Modelluntersuchungen, bei denen keine anderen Inhaltsstoffe Einfluß auf die Extraktion nehmen konnten.

Die Gel-Chromatographie an Sephadex LH-20 eignet sich zur Fraktionierung von Flavonoiden bzw. von deren Metallkomplexen. Dabei wird zum einen die adsorptive Eigenschaft des Gels, zum anderen die Möglichkeit zur Trennung nach Molekülgröße ausgenutzt. Die Faktoren, die das Elutionsvolumen bestimmen, hängen von der Zahl und Position der Hydroxylgruppen der Flavonoide ab. Im Fall der Glykoside spielen sterische Faktoren eine Rolle. Die Elementbindungsform der Metall-Flavonoid-Komplexe wird durch die Fraktionierung an Sephadex LH-20 nicht geändert, was anhand der Spektren der einzelnen Fraktionen von Modell-Lösungen festgestellt werden konnte.

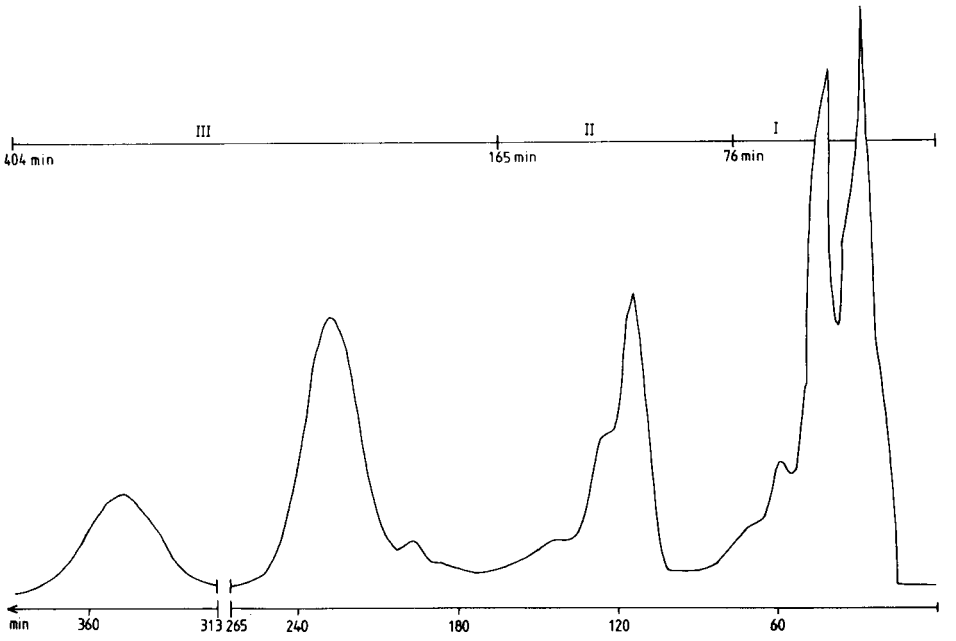

Abb. 5. Fraktionierung des Zwiebel-Extraktes an Sephadex LH-20 mit den verschiedenen Eluenten. Methanol/bidestilliertes Wasser: (I) 50:50; (II) 70:30; (III) 80:20.

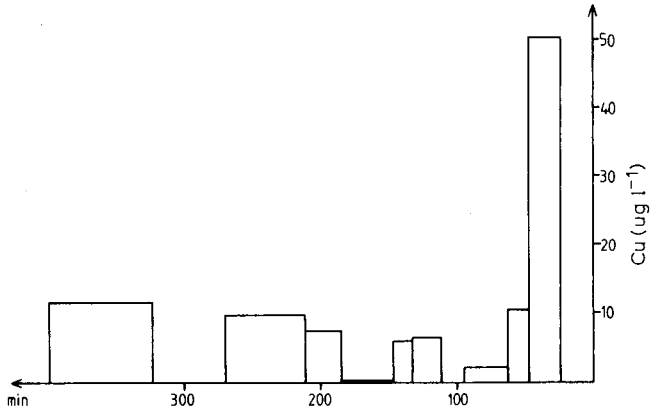

Abb. 6. Kupfer-Verteilung in den Fraktionen des Zwiebel-Extraktes nach gel-chromatographischer Trennung.

Daher ist diese Methode auch zur präparativen Trennung von Flavonoiden in Lebensmittel-Extrakten geeignet. Die Retentionszeiten der freien und komplexierten Flavonoide unterscheiden sich nicht, so daß eine Möglichkeit zur Trennung der beiden Formen nicht gegeben ist. Jedoch erlaubt die Kombination von Chromatographie, Kupfer-Bestimmung (mittels flammenloser AAS) und spektralphotometrischer Methoden (zur Identifizierung von Flavono-

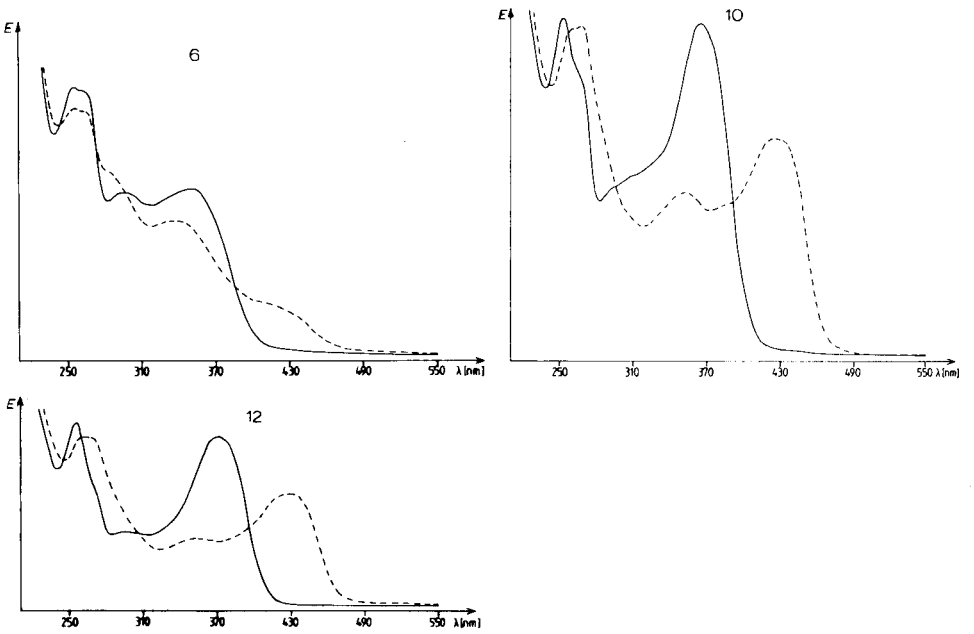

Abb. 7. Spektren der Fraktionen 6, 10 und 12 des Zwiebel-Extraktes vor (——) und nach (– – –) Zugabe einer 10^{-3} mol l^{-1} Cu-Lösung.

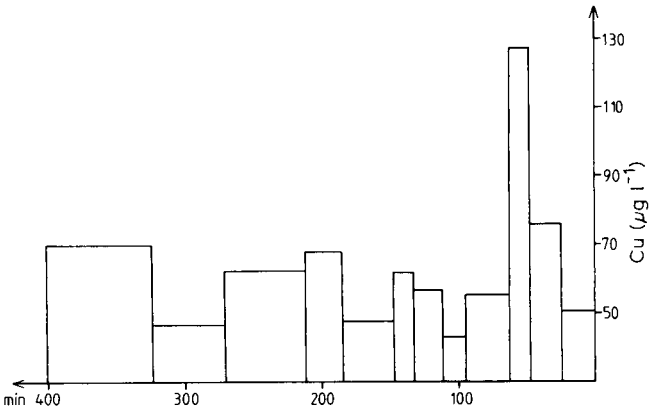

Abb. 8. Kupfer-Verteilung in den Fraktionen des Zwiebel-Extraktes nach gel-chromatographischer Trennung mit Cu-haltigem (50 μg l^{-1} $CuSO_4$ $5H_2O$) Eluenten (siehe auch Abb. 6).

iden) Aussagen über die Existenz einer Beziehung zwischen Flavonoiden und Metallen zu machen. Abbildung 5 zeigt das Chromatogramm eines Zwiebel-Extraktes und in Abb. 6 ist die Kupfer-Verteilung in den einzelnen Fraktionen dargestellt. Der Chemikalien-Blindwert liegt bei 0,1 μg kg^{-1}. Das Maximum der Kupfer-Konzentration ist im Retentionsbereich von 25 bis 50 min zu finden.

Zur Identifizierung der Flavonoide in den einzelnen Fraktionen wurden die

Spektren aufgenommen. Der Verlauf des "Methanol"-Spektrums erlaubt nur eine Zuordnung zu einem bestimmten Flavonoid-Typ. Zusätzliche Informationen werden mittels verschiedener "Shift"-Reagenzien erhalten, die spezifische Reaktionen mit den Flavonoiden bewirken, woraus signifikante Änderungen in den Absorptionsspektren resultieren [14]. In Abb. 7 sind die Spektren derjenigen Fraktionen des Zwiebel-Extraktes abgebildet, die aufgrund der Lage der Absorptionsmaxima die Anwesenheit von Flavonoiden vermuten lassen. Der Verlauf des Fraktion-6 Spektrum läßt auf ein am C-3-Atom substituiertes Flavonol schließen. Die Komplexierung von Kupfer und der Vergleich mit Referenzspektren [15] zeigt, daß es sich wahrscheinlich um Kämpferol-3-O-glucosid handelt. Die Spektren für Fraktionen 10 und 12 zeigen, daß bei einer Kupfer-Zugabe eine für Flavonoide typische Komplexierung stattfindet. In Fraktion 10 (Abb. 7) liegt ein Flavonol mit einer OH-Gruppe am C-3-Atom vor. Die Verschiebung der Absorptionsbande im Kupfer/Komplex-Spektrum gibt einen Hinweis auf ein Quercetin- bzw. Kämpferol-Derivat, das am *b*-Ring in 4-Position anstatt der Hydroxylgruppe andersartig substituiert ist. Aus der Verwendung von "Shift"-Reagenzien und der dünnschicht-chromatographischen Analyse des Zuckerrestes nach saurer Hydrolyse ergibt sich für diese Substanz, daß es sich um Quercetin-4′-glucosid handelt. Der Spektrum für Fraktion 12 läßt sich einwandfrei Flavonolen zuordnen, die am C-3-Atom eine Hydroxylgruppe tragen. Nach der Kupfer-Zugabe und dem Vergleich mit Literaturdaten [15] zeigt sich, daß es sich um Quercetin handelt. Das Ergebnis wird durch die Anwendung von "Shift"-Reagenzien bestätigt [15,16].

Aus den vorgestellten Einzelergebnissen kann folgendes Fazit gezogen werden. Die höchsten Kupfer-Gehalte des Zwiebel-Extraktes sind in einer gelchromatographischen Fraktion konzentriert, die nach kurzer Retentionszeit eluiert wird und keine Flavonoide enthält. In den letzten Fraktionen, die eindeutig Flavonoide enthalten, können ebenfalls relativ hohe Kupfer-Konzentrationen ermittelt werden. Flavonoide spielen also in der Komplexierung von Kupfer in der Pflanze eine Rolle. Wird bei der Gel-Chromatographie mit einem kupferhaltigen Eluenten gearbeitet (Abb. 8), so zeigt sich eine Kupferanreicherung in den Flavonoid-Fraktionen.

LITERATUR

1 M. Fathi und H. Lorenz, Bindungsformen von Quecksilber, Cadmium und Blei in Biotopen, Verhalten in der Nahrungskette und Vorkommen in Nahrungsmitteln, ZEBS-Bericht 1, Reimer-Verlag, Berlin, 1980.

2 G. Schwedt und G. Weber, Dtsch. Lebensm. -Rundsch., 79 (1983) 213.

3 G. Weber und G. Schwedt, Anal. Chim. Acta, 134 (1982) 81.

4 G. Weber und G. Schwedt, Z. Lebensm. -Unters. -Forsch., 178 (1984) 110.

5 H. Dunemann und G. Schwedt, Fresenius' Z. Anal. Chem., 325 (1986) 121.

6 H. Hippe, Dissertation, Göttingen, 1985.

7 H. Böhm, Die Flavonoide: Eine Übersicht über die Physiologie Pharmakodynamik und therapeutische Verwendung, Editio Cantor, Aulendorf, 1967.
8 G. Cetta, G. Pallavicini, R. Tenni und C. Bisi, J. Biochem., 26 (1977) 317.
9 K. Wedepohl, Dissertation, Stuttgart, 1986.
10 K. Herrmann, J. Food Technol., 11 (1976) 433; Arch. Pharm. (Weinheim), 291 (1958) 238.
11 L. Kotz, G. Kaiser, P. Tschöpel und G. Tölg, Fresenius' Z. Anal. Chem., 260 (1972) 207.
12 M. Sakamoto und K. Takamura, Microchem. J., 23 (1978) 374.
13 K.R. Markham, Techniques of Flavonoid Identification, Academic, New York, 1982.
14 E. Wollenweber, in: J.B. Harborne und T.J. Mabry (Eds.), The Flavonoids: Advances in Research, Chapman and Hall, London, 1962.
15 T.J. Mabry, K.R. Markham und B. Thomas, The Systematic Identification of Flavonoids, Springer, Berlin, 1970.
16 T.A. Geissmann, The Chemistry of Flavonoid Compounds, Pergamon, Oxford, 1962.

Analytica Chimica Acta, 203 (1987) 35-42
Elsevier Science Publishers B.V., Amsterdam — Printed in The Netherlands

APPLICATION OF A STOPPED-FLOW TIME-DIFFERENCE TECHNIQUE TO SPECTROPHOTOMETRIC DETERMINATION OF ULTRATRACE LEVELS OF PHOSPHATE

KEN-ICHIRO KANAYA*

Japan Food Research Laboratories, Osaka Branch, Suita, Osaka 564 (Japan)

KEITARO HIROMI

Department of Food Science and Technology, Faculty of Agriculture, Kyoto University, Kyoto 606 (Japan)

(Received 26th March 1987)

SUMMARY

Optimum conditions, interfering substances, and comparisons with other methods are described for a spectrophotometric method for phosphate, which is based on the stopped-flow technique and involves recording the progress curve for formation of the colored complex of 12-molybdophosphate with malachite green. Linear calibration plots were obtained for phosphate in the ranges 5–55 and 100–1000 $\mu g\ l^{-1}$. The sensitivity and the running speed of the method crucially depend on the sulfuric acid concentration. The positive interferences of several anions, especially arsenate, thiosulfate, stannate, tungstate and iodide, are significantly less than in conventional methods. Results for total phosphorus in several foodstuffs agreed with results obtained by a molybdovanadophosphoric acid method.

Numerous methods have been reported for the determination of phosphate. Several spectrophotometric methods based on the heteropoly acid (12-molybdophosphate acid) or "molybdenum blue" are commonly used [1–3]. However, the sensitivities of these methods are not sufficient for the determination of $\mu g\ l^{-1}$ levels of phosphate, unless time-consuming pre-concentration procedures are performed. Itaya and Ui [4] reported a more sensitive spectrophotometric method based on the colored complex formation of 12-molybdophosphate with malachite green. The colored complex was shown by Altmann et al. [5] to be an ion-association complex, $(dye)_3[PO_4(Mo_3O_9)_4]$. This method has been widely used in various fields for the determination of trace amounts of phosphate [6–11].

Recently, stopped-flow methods have widely been used in various fields of analytical chemistry [12, 13]. A fast and sensitive assay procedure based on evaluation of the reaction curve obtained by the stopped-flow method has been reported [14, 15]; the procedure is essentially a fixed-time assay and different from the conventional rate assays [16–19]. The technique, which is termed

0003-2670/87/$03.50

stopped-flow time-difference (SFTD), possesses numerous advantages. Sensitivity and precision are enhanced compared with ordinary spectrophotometry; large backgrounds (up to absorbances of about 1.5) can be eliminated; the effect of side-reactions can be excluded from the main reaction(s); and both the signal amplitude (useful for quantitative work) and a rate parameter (sometimes useful for identification) are simultaneously available from the reaction curve.

Preliminary investigations [15] have shown that a method based on combination of the SFTD technique and the malachite green procedure is superior to conventional methods for the accurate and precise determination of $\mu g\ l^{-1}$ levels of phosphate, without any need for pre-concentration of phosphate or for elimination of interfering substances. A more detailed investigation is described in this paper.

EXPERIMENTAL

Apparatus and reagents

A stopped-flow spectrophotometer (Union Giken SF-70) was used to follow the time course of the reaction. Sometimes, a data processor (Union Giken RA-450) was also used to improve the S/N ratio. The dead time of the flow-system was about 2 ms, as determined by the method of Nakatani and Hiromi [20]. The path length of the cell was 10 mm.

All chemicals, except the dye, were of analytical grade and were used as received. Deionized/distilled water was used.

The stock solution of malachite green (C.I. 42000, Basic green 4) was 0.002 mol l^{-1}. Potassium dihydrogenphosphate was used for preparing the standard solutions of orthophosphate.

For the color-developing reagent, 12.5 ml of concentrated sulfuric acid and 25 ml of the malachite green stock solution were successively added to about 50 ml of water containing 12.35 g of ammonium molybdate. This solution was diluted to 200 ml with water. After standing for 1 h or longer at room temperature, the solution was filtered through a membrane filter. This reagent was stable for only a few days.

For the molybdate/sulfuric acid reagent, 25 ml of concentrated sulfuric acid was added to 75 ml of water containing 24.7 g of ammonium molybdate.

Procedure

Add 2.5 ml of the molybdate/sulfuric acid reagent to 7.5 ml of the sample solution and allow the mixture to stand for about 15 min in order to form 12-molybdophosphate. (The densities of the sample solution treated in this way and the color-developing reagent should be equal, in order to prevent possible artifacts caused by density imbalance in the stopped-flow apparatus [21].)

Put about 10 ml of the pre-treated sample solution and the color-developing reagent, respectively, into the reservoirs of the stopped-flow spectrophotometer. Mix the two solutions rapidly in a 1:1 ratio, and then record the absorbance change at 650 nm for 50 s as a function of time.

RESULTS AND DISCUSSION

Sulfuric acid, molybdate and malachite green concentrations

The molar absorptivity of phosphate at 650 nm crucially depended on the sulfuric acid concentration, as shown in Fig. 1. The reaction rate decreased with increasing sulfuric acid concentration. For example, the rate in 1 mol l^{-1} sulfuric acid was about 3 or 10 times larger than that in 1.5 or 2 mol l^{-1} sulfuric acid, respectively, when 0.05 mol l^{-1} molybdate and 1.25×10^{-4} mol l^{-1} malachite green were used. However, the green pigment was precipitated when <0.8 mol l^{-1} sulfuric acid was present. From these results, a sulfuric acid concentration of 1 mol l^{-1} is most suitable.

The molar absorptivity increased with increasing concentration of either molybdate or malachite green, but the change in each case was less marked than that in the case of sulfuric acid. The concentrations of these reagents had little effect on the reaction rate. Suitable molybdate and malachite green concentrations were 0.05 and 1.25×10^{-4} mol l^{-1}, respectively.

The reaction rates in the following two cases were compared by changing the order of addition: (a) direct mixing of phosphate solution and malachite

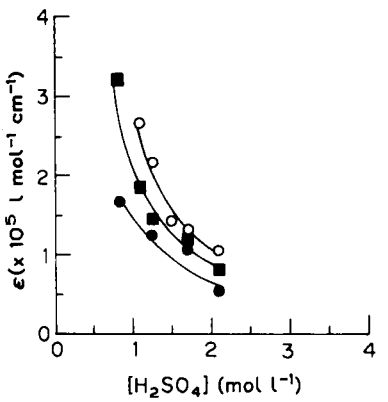

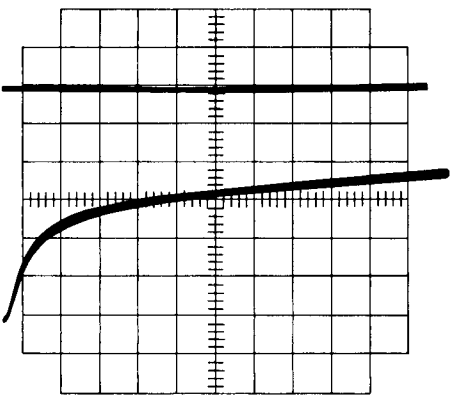

Fig. 1. Effect of sulfuric acid concentration on the molar absorptivity (ϵ) at 650 nm of phosphate. Final concentrations: (●) 0.10 mol l^{-1} molybdate, 2.9×10^{-4} mol l^{-1} malachite green; (■) 0.10 mol l^{-1} molybdate, 1.4×10^{-4} mol l^{-1} malachite green; (○) 0.05 mol l^{-1} molybdate, 2.9×10^{-4} mol l^{-1} malachite green. The sulfuric acid concentration on the horizontal axis is the final concentration.

Fig. 2. Typical progress curve in the present method. The upper trace is the flow velocity trace and the lower trace shows the absorbance change. Phosphate concentration taken, 120 μg l^{-1}. Vertical scale, 0.01 absorbance per major division; horizontal scale, 5 s per major division.

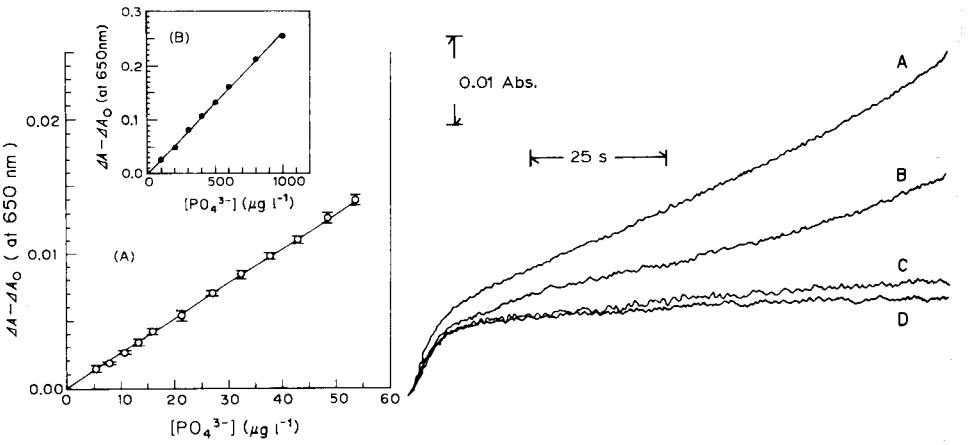

Fig. 3. Typical calibration plots for the proposed method: (A) points and bars represent the mean ± SD for three determinations; (B) each point represents the mean for five determinations.

Fig. 4. Typical progress curves for 30 $\mu g\, l^{-1}$ phosphate in the presence of arsenate. Concentration of $HAsO_4^{2-}$: (A) 5500, (B) 2750, (C) 550, (D) 0 $\mu g\, l^{-1}$.

green/sulfuric acid solution containing molybdate; (b) mixing of malachite green/sulfuric acid solution and 12-molybdophosphate which had been prepared from phosphate and molybdate 15 min or longer before the mixing. It was found that the apparent reaction rate of case (b) was about 10 times larger than that of case (a), and so was much better for SFTD measurements.

Quantitative analysis with progress curves

As previously reported [15], the recommended procedure for determining phosphate was as follows: (1) record the progress curves for 50 s as shown in Fig. 2; (2) measure ΔA (the magnitude of the absorbance change obtained from the progress curve of a sample solution) and ΔA_0 (that obtained from the progress curve of reagent blank) at a certain definite time (30–50 s after the beginning of the reaction); (3) calculate $(\Delta A - \Delta A_0)$, which is proportional to phosphate concentration. The standard deviation (SD) of ΔA as low as 0.002 was less than 0.0003.

Recording for longer than 50 s was unnecessary, because the sigmoidal first phase was terminated within about 20 s of the beginning of the reaction. The value of ΔA_0 was never zero, probably because of contamination in the reagents.

Typical examples of calibration curves are shown in Fig. 3. Proportionality was obtained for phosphate concentrations from zero to 1000 $\mu g\, l^{-1}$, as shown in Fig. 3(B). The detection limit, defined as 3×SD of blank determinations, was 2 $\mu g\, l^{-1}$.

TABLE 1

Effects of co-existing cations on the determination of 250 $\mu g\ l^{-1}$ phosphate[a]

Ion	ΔA at 650 nm		Ion	ΔA at 650 nm	
	Conc. added (M)			Conc. added (M)	
	1×10^{-1}	1×10^{-2}		1×10^{-2}	1×10^{-3}
None	0.064	0.064	None	0.064	0.064
Na^+	0.063	-	Zn^{2+}	0.064	-
NH_4^+	0.064	-	Fe^{3+}	0.084	0.066
K^+	0.064	-	Mn^{2+}	0.063	-
Ca^{2+}	-	0.064	Co^{2+}	0.064	-
Mg^{2+}	-	0.062	Ni^{2+}	0.065	-
Al^{3+}	-	0.064	Cu^{2+}	0.073	0.064

[a]Absorbance change was measured as in the recommended procedure. All metal ions were added as their chloride salts.

Interferences

The interferences of twelve cations on 250 $\mu g\ l^{-1}$ (ca. 2.6×10^{-6} M) phosphate were examined. As shown in Table 1, all cations studied had virtually no effect up to 10^{-3} M. Above 10^{-3} M, however, positive interferences from Fe^{3+} and Cu^{2+} were recognized. Thus, the interferences of all cations studied in the present work were comparable to those in the conventional malachite green method [4].

It was reported that the interferences of arsenate and silicate were similar in the proposed method [15], in contrast to other methods [10, 11]. A more extensive interference study of anions is shown in Table 2. Positive interferences were observed for AsO_2^-, $HAsO_4^{2-}$, $B_4O_7^{2-}$, ClO_4^-, I^-, $H_2PO_2^-$, HPO_3^{2-}, $S_2O_3^{2-}$, SeO_4^{2-}, SiO_3^{2-}, TeO_4^{2-} and WO_4^{2-}, and negative interferences for BrO_3^-, MnO_4^-, $Sb(OH)_6^-$ and VO_3^-. Table 3 shows a comparison of tolerance limits of the positively interfering anions in the present recommended procedure and in one conventional malachite green method [5]. The tolerance limits for AsO_2^-, $HAsO_4^{2-}$, ClO_4^{2-}, I^-, HPO_3^{2-}, $S_2O_3^{2-}$, SnO_3^{2-} and WO_4^{2-} in the present study method are much higher than those in the conventional method. These differences in tolerance limits can be ascribed to the much slower reactions of heteropoly acids such as molybdoarsenate with malachite green compared to the reaction of 12-molybdophosphate. For example, as shown in Fig. 4 (curve C), the side-reactions of up to 550 $\mu g\ l^{-1}$ hydrogenarsenate can be ignored in using the time course up to 50 s; such concentrations would cause large interferences in the conventional method. The proposed method is thus more selective for phosphate, compared with the conventional malachite green method, although there was little difference between the tolerance limits for

TABLE 2

Effects of co-existing anions on the determination of 250 $\mu g\ l^{-1}$ phosphate[a]

Ion	ΔA at 650 nm			Ion	ΔA at 650 nm		
	Conc. added (M)				Conc. added (M)		
	1×10^{-1}	1×10^{-2}	1×10^{-3}		1×10^{-1}	1×10^{-2}	1×10^{-3}
None	0.064	0.064	0.064	SiO_3^{2-}	-	-	0.286
Cl^-	0.063			AsO_2^-	-	0.132	0.071
SO_4^{2-}	0.066			$HAsO_4^{2-}$	-	-	0.638
SO_3^{2-}	0.064			SeO_4^{2-}	0.389	0.101	0.068
$S_2O_3^{2-}$	-	0.728	0.061	SnO_3^{2-}	0.064		
HCO_3^-	0.064			$Sb(OH)_6^-$	-	0.050	0.065
NO_3^-	0.063			TeO_4^{2-}	-	0.112	0.070
ClO_4^-	0.144	0.071	0.065	VO_3^-	-	0.036	0.038
BrO_3^-	0.000	0.039	0.064	MnO_4^-	-	-	0.012
IO_4^-	0.064			WO_4^{2-}	0.109	0.071	0.064
$B_4O_7^{2-}$	0.083	0.065		Br^-	0.064		
HPO_3^{2-}	-	0.176	0.073	I^-	0.103	0.069	0.064
$H_2PO_2^-$	0.099	0.066					

[a]Absorbance change was measured as in the recommended procedure. Anions were added as their sodium or potassium salts.

TABLE 3

Tolerance limits of positively interfering anions

Ion	Tolerance limit (M)[a]		Ratio (A)/(B)	Ion	Tolerance limit (M)		Ratio (A)/(B)
	Present procedure (A)	Reference procedure[b] (B)			Present procedure (A)	Reference procedure (B)	
$S_2O_3^{2-}$	2×10^{-3}	2×10^{-5}	100	$HAsO_4^{2-}$	3×10^{-5}	2×10^{-7}	150
ClO_4^-	4×10^{-3}	2×10^{-4}	20	SeO_4^{2-}	1×10^{-3}	4×10^{-4}	3
$B_4O_7^{2-}$	2×10^{-2}	6×10^{-3}	3	SnO_3^{2-}	$>1\times10^{-1}$	5×10^{-4}	>200
HPO_3^{2-}	3×10^{-4}	3×10^{-5}	10	TeO_4^{2-}	7×10^{-4}	7×10^{-4}	1
$H_2PO_2^-$	9×10^{-3}	4×10^{-3}	2	WO_4^{2-}	7×10^{-3}	2×10^{-5}	350
SiO_3^{2-}	6×10^{-5}	4×10^{-5}	2	I^-	8×10^{-3}	4×10^{-5}	200
AsO_2^-	5×10^{-4}	1×10^{-5}	50				

[a]The tolerance limits are defined as the level at which an error of no more than $\pm5\%$ is caused in determining the absorbance change for 250 $\mu g\ l^{-1}$ phosphate. All anions were added as their sodium salts to the sample solution before addition of molybdate.
[b]The procedure recommended by Altmann et al. [5] was used.

TABLE 4

Determinations of total phosphorus in foodstuffs[a]

Food		Total phosphorus (mg/100 g)	
		Present method	Reference method[b]
Noodle	1	128 ±0.4 (n=4)	128, 127
	2	116 ±0.3 (n=4)	117, 117
Vinegar		3.7±0.01(n=5)	3.7, 3.7
Yoghurt	1	95.0±0.21(n=4)	94.6, 94.9
	2	106 ±0.3 (n=4)	106, 104
Butter		17.1±0.05(n=4)	17.1, 17.0
Honey	1	4.7±0.01(n=5)	4.8, 4.7
	2	3.2±0.01(n=5)	3.1, 3.1
Mayonnaise	1	83.1±0.17(n=4)	83.3, 82.9
	2	79.6±0.20(n=4)	80.1, 79.8
Ketchup		32.4±0.08(n=4)	32.2, 32.4

[a]Perchloric acid digestion was applied. [b]Results obtained by the molybdovanadophosphoric acid method [1, 22, 23].

some anions (see Table 3). There was also little difference for the negatively interfering anions (bromate, permanganate, antimonate and vanadate).

Determination of total phosphorus in food stuffs

In order to confirm the accuracy and precision of the proposed method, total phosphorus was determined in seven kinds of foodstuffs and the results were compared with those obtained by the conventional method (molybdovanadophosphoric acid method [1, 22, 23]), which is known to be almost insusceptible to interferences by arsenate and silicate. Perchloric acid digestion was used as the pre-treatment for all samples. As seen from Table 4, good agreements were obtained between the results of these two methods.

Thus, the present method can be recommended as a sensitive and reliable procedure for the determination of $\mu g\ l^{-1}$ levels of phosphate.

We are grateful to Prof. Tooru Kuwamoto (Faculty of Science, Kyoto University) for his helpful suggestions and thank the staff of the Japan Food Research Laboratories for the determination of total phosphorus in the foodstuffs by the conventional method.

REFERENCES

1 A.P.H.A., A.W.W.A. and W.P.C.F., Standard Methods for the Examination of Water and Wastewater, 16th edn., American Public Health Association, Washington, DC, 1985.
2 W.J. Williams, Handbook of Anion Determination, Butterworths, London, 1979, p. 422.
3 D.F. Boltz and J.A. Howell, Colorimetric Determination of Nonmetals, 2nd edn., Interscience, New York, 1978, p. 337.
4 K. Itaya and M. Ui, Clin. Chim. Acta, 14 (1966) 361.
5 H.J. Altmann, E. Fürstenau, A. Gielewski and L. Scholz, Fresenius' Z. Anal. Chem., 256 (1971) 274.
6 H. van Belle, Anal. Biochem., 33 (1970) 132.
7 C.L. Penney, Anal. Biochem., 75 (1976) 201.
8 A. Kallner, Clin. Chim. Acta, 59 (1975) 35.
9 B. Anner and M. Moosmayer, Anal. Biochem., 65 (1975) 305.
10 S. Motomizu, T. Wakimoto and K. Tôei, Analyst, 108 (1983) 361.
11 S. Motomizu, T. Wakimoto and K. Tôei, Talanta, 30 (1983) 333.
12 K. Hiromi, Trends Biochem. Sci., 3 (1978) 232.
13 K. Hiromi, in D. Glick (Ed.), Methods of Biochemical Analysis, Vol. 26, Interscience, New York, 1980, p. 158.
14 K. Hiromi, C. Kuwamoto and M. Ohnishi, Anal. Biochem., 101 (1980) 421.
15 K. Kanaya and K. Hiromi, Chem. Lett., (1985) 1381.
16 K. Hiromi, H. Nagasawa-Fujimori, J. Yamaguchi-Ito, H. Nakatani, M. Ohnishi and B. Tonomura, Chem. Lett., (1977) 1333.
17 G.M. Ridder and D.W. Margerum, Anal. Chem., 49 (1977) 2090.
18 M.A. Koupparis, E.P. Diamandis and H.V. Malmstadt, J. Assoc. Off. Anal. Chem., 66 (1983) 188.
19 C.C. Kircher and S.R. Crouch, Anal. Chem., 55 (1983) 248.
20 H. Nakatani and K. Hiromi, J. Biochem., 87 (1978) 1805.
21 K. Hiromi, Kinetics of Fast Reactions - Theory and Practice, Kodansha, Tokyo, 1979, p. 107.
22 K.P. Quinlan and M.A. DeSesa, Anal. Chem., 27 (1955) 1626.
23 O.B. Michelsen, Anal. Chem., 29 (1957) 60.

Analytica Chimica Acta, 203 (1987) 43–54
Elsevier Science Publishers B.V., Amsterdam — Printed in The Netherlands

THE METHOD OF MOMENTS FOR MULTIPLET DECONVOLUTION IN GAMMA-RAY SPECTROMETRY

V.V. ATRASHKEVICH*, A.V. GARANIN and V.P. KOLOTOV

V.I. Vernadsky Institute of Geochemistry and Analytical Chemistry, Academy of Sciences, Moscow (U.S.S.R.)

(Received 3rd September 1985)

SUMMARY

The method of moments is described for deconvolution of a mixture of identical distributions; it is not necessary to know the type of the individual peak distribution. The algorithm for computing the positions and contributions of the peaks forming the multiplet is presented. The real shape of the peak is used. The computational stability of the method of moments for the deconvolution of various types of convolved triple peaks is shown to be satisfactory. The algorithm is used for deconvolution of some double peaks obtained in neutron activation analysis of rock standards. The program is fast and suitable for microcomputers.

Application of the method of moments for estimation of the parameters of the individual distributions from the parameters of their mixture is well known. In particular, the method of moments has been described for deconvoluting a mixture of two normal distributions [1]. A bibliography on the use of the method of moments for the estimation of the parameters of some mixed (compound) distributions of the same type (Poisson, exponential, binomial) is available [1].

THEORY

The present paper gives the theoretical basis of the method of moments for estimation of n individual distributions (which are hereinafter termed single peaks) which are mixed to form the multiplet. It is important that it is not necessary to know the type of distribution of the single peaks. This statement is substantiated below.

Mathematical part

Two initial assumptions are introduced. First, the multiplet is considered as the superposition of the single peaks, which is obviously true. Secondly, it is assumed that all peaks forming the multiplet have the same type of distribu-

0003-2670/87/$03.50

tion (shape) with constant parameters. In the case of γ-ray spectrometry with semiconductor detectors, this assumption is close enough to reality. The width of the multiplet is usually not more than a few dozen keV and in this range any modification of the peak shape can be neglected (cf. Fig. 3). For explanation, in the case of Gaussian distribution, the second central moment is σ^2.

It can be assumed that the distribution density of the multiplet can be described by the function

$$F(x) = \sum_{i=1}^{k} a_i f(x-b_i), \tag{1}$$

where $b_i = \bar{\mathbf{x}}_i - \bar{\mathbf{x}}_0$; $\bar{\mathbf{x}}_i$ is the ith peak position (the first non-central moment) and $\bar{\mathbf{x}}_0$ is the same peak position with regard to the multiplet; a_i is the contribution of the ith peak to the integral of the total multiplet; $f(x-b_i)$ is the function of the distribution density representing each peak; $k = 1,2,\ldots$ is the number of peaks forming the multiplet.

It has been proved that the mathematical model of a multiplet (Eqn. 1) as the superposition of the single peaks is the only possible model [2]. To evaluate the coefficients a_i and b_i of Eqn. 1, a system consisting of $2k$ equations is required.

The first equation of this system can be written as the condition for normalizing a_i:

$$\sum_{i=1}^{k} a_i = 1 = \Delta_0^* \tag{2}$$

The remaining $(2k-1)$ equations can be obtained from Eqn. 3 by taking into account Eqn. 1. The lth central moment of the $F(x)$ distribution can be written [3] in the form

$$\mathbf{M}_l = \sum_{j=1}^{n} (x_j - \bar{\mathbf{x}}_0)^l F(x_j) = \sum_{i=1}^{k} a_i \sum_{j=1}^{n} (x_j - \bar{\mathbf{x}}_0)^l f(x_j - b_i) \tag{3}$$

where

$$\bar{\mathbf{x}}_0 = \sum_{j=1}^{n} x_j F(x_j)$$

If it is assumed that the parameters of the $f(x)$ distribution representing the single peak are not variable, then it is possible to write

$$(\mu_l)_i = (\mu_l)_j \text{ for } i,j = 1,2,3\ldots \tag{4}$$

where μ_l is the lth central moment of the $f(x)$ distribution.

From Eqns. 3 and 4, it follows that

$$\mathbf{M}_1 = \sum_{i=1}^{k} a_i \sum_{j=1}^{n} (x_j - \bar{\mathbf{x}}_i + b) f(x_j - b_i) = \sum_{i=1}^{k} a_i \mu_1 + \sum_{i=1}^{k} a_i b_i = \mu_1 + \sum_{i=1}^{k} a_i b_i$$

whence

$$\sum_{i=1}^{k} a_i b_i = \mathbf{M}_1 - \mu_1 = \Delta_1 = \Delta_1^*$$

In a similar way,

$$\mathbf{M}_2 = \mu_2 + 2\mu_1 \sum_{i=1}^{k} a_i b_i + \sum_{i=1}^{k} a_i b_i^2 = \mu_2 + 2\mu_1 \Delta_1^* + \sum_{i=1}^{k} a_i b_i^2$$

or

$$\sum_{i=1}^{k} a_i b_i^2 = \mathbf{M}_2 - \mu_2 - 2\,\mu_1 \Delta_1^* = \Delta_2 - 2\,\mu_1 \Delta_1^* = \Delta_2^*$$

etc. The recurrence formula is

$$\sum_{i=1}^{k} a_i b_i^m = \Delta_m - \sum_{j=1}^{m-1} C_m^j\, \mu_{(m-j)} \Delta_j^* = \Delta_m^*$$

where $\Delta_m = \mathbf{M}_m - \mu_m$

For the determination of the $2k$ unknown parameters of Eqn. 1, the following system of $2k$ equations has been compiled

$$\sum_{i=1}^{k} a_i = 1 = \Delta_0^*;\ \sum_{i=1}^{k} a_i b_i = \Delta_1 = \Delta_1^*;\ \sum_{i=1}^{k} a_i b_i^2 = \Delta_2 - 2\mu_1 \Delta_1^* = \Delta_2^* \qquad (5)$$

$$\vdots$$

and

$$\sum_{i=1}^{k} \mathrm{a}_i \mathrm{b}_i^{k-1} = \Delta_{k-1} - \sum_{j=1}^{k-2} \mathrm{C}_{k-1}^j \mu_{(k-1-j)} \Delta_j^* = \Delta_{k-1}^*$$

$$\sum_{i=1}^{k} a_i b_i^k = \Delta_k - \sum_{j=1}^{k-1} C_k^j \mu_{(k-j)} \Delta_j^* = \Delta_k^*$$

$$\vdots \qquad (6)$$

$$\sum_{i=1}^{k} a_i b_i^{2k-1} = \Delta_{2k-1} - \sum_{j=1}^{2k-2} C_{2k-1}^j \mu_{(2k-1-j)} \Delta_j^* = \Delta_{2k-1}^*$$

The unknown parameters a_i and b_i are evaluated by solution of these two systems of equations. The values a_i are obtained from system 5 by the consecutive elimination method. The general formula for computing a_i (here the calculations are omitted) is

$$a_i = [\Delta_{k-1}^* + (-1)^{k+1} \prod_{\substack{i=1 \\ j \neq i}}^{k} b_j] \Big/ \prod_{\substack{i=1 \\ j \neq i}}^{k} (b_i - b_j) \qquad (7)$$

where k is the number of peaks in the mixture to be separated. From the equation system 6, the values b_i can be obtained. For this purpose, the following symmetric polynomials are introduced:

$$\sigma_1 = \sum_{i=1}^{k} b_i;\ \sigma_2 = \sum_{i=1}^{k-1} \sum_{j=i+1}^{k} b_i b_j;$$

$$\sigma_3 = \sum_{i=1}^{k-2} \sum_{j=i+1}^{k-1} \sum_{l=j+1}^{k} b_i b_j b_l;\ \ldots;\ \sigma_n = b_1 b_2 b_3 \ldots b_n.$$

These are the coefficients of the nth degree polynomial in the Viete formula [4]. By means of the symmetric polynomials, it can be shown that

$$\Delta_m^* = \sum_{i=1}^{k} (-1)^{i+1} \sigma_i \Delta_{m-i}^* \quad (\text{for } m \geqslant 2) \tag{8}$$

Then the system of equations (6) becomes a system of linear equations with respect to the symmetric polynomials:

$$\begin{pmatrix} \Delta_{k-1}^* & -\Delta_{k-2}^* & \cdots & (-1)^{k+1} \\ \vdots & & & \\ \Delta_{2k-2}^* & -\Delta_{2k-3}^* & \cdots & (-1)^{k+1} \Delta_{k-1}^* \end{pmatrix} \begin{pmatrix} \sigma_1 \\ \vdots \\ \sigma_k \end{pmatrix} = \begin{pmatrix} \Delta_k^* \\ \vdots \\ \Delta_{2k-1}^* \end{pmatrix} \tag{9}$$

The solution of system 9 by the methods of linear algebra makes it possible to find the kth degree polynomial for the evaluation of the unknown parameters b_i:

$$b^k - \sigma_1 b^{k-1} + \sigma_2 b^{k-2} \ldots (-1)^k \sigma_k = 0 \tag{10}$$

When Eqn. 10 is solved by the method of iterative isolation of the square binomial with gradual reduction of the polynomial degree, it is possible to obtain all the k roots [5]. By using Eqn. 7, it is then possible to obtain all k values of a_i.

Thus for deconvolution of a multiplet consisting of k peaks, it is necessary to compute $2k-1$ values of the central moments of the multiplet. It is assumed that Eqn. 2 is valid and that $2k-1$ values of the central moments of the single peaks (μ_i) have been calculated in advance. The preparation of the list of central moments is described under Calibration of Peak Shape (see below).

Investigation of the computational stability of the method of moments

From the above description, it is clear that the method of moments can be applied for deconvolution of the total of any number of components. For obvious practical reasons, the computational stability of the method of moments is considered here only for the deconvolution of multiplets consisting of not more than three peaks. On the one hand, multiple peaks with more than three

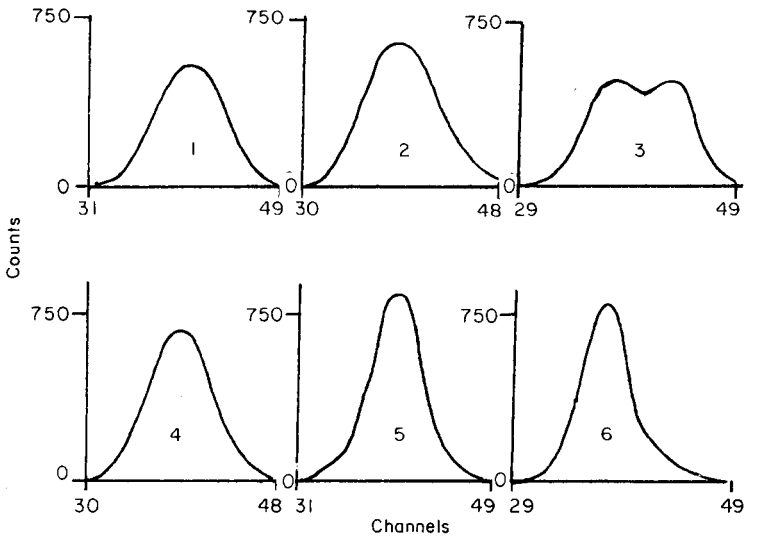

Fig. 1. Composition of the theoretical triple peaks. The distance between the positions of the single peaks is 3 channels. (1) $a_1=a_2=a_3=1/3$; (2) $a_1=0.5, a_2=0.35, a_3=0.15$; (3) $a_1=a_3=0.45; a_2=0.1$; (4) $a_1=a_2=0.45, a_3=0.1$; (5) $a_1=a_3=0.1, a_2=0.8$; (6) $a_1=0.8, a_2=a_3=0.1$.

component peaks are rare in modern γ-ray spectrometry; on the other hand, investigation of the computational stability of the method of moments is very cumbersome in more complicated cases.

For investigation of the computational stability of the method of moments, the correctness of the algorithm and program were first tested. For this purpose, ideal triple peaks were simulated as the sum of normal distributions ($\sigma^2=4$ channels), with the second peak position in the 40th channel. The ratios of the peaks composing the triple peak are shown in Fig. 1. The distances between the maxima of the neighbouring peaks forming the triple peak were the same; ϵ_{12} and ϵ_{23} are the distances between the first and second peaks, and between the second and third peaks, respectively.

The results of deconvolution of some artificial mixtures are marked by asterisks in Table 1 (case $\epsilon_{12}=\epsilon_{23}=3$). These results indicate the absence of computational errors.

In further tests, the influence of the statistical error of the ratioactivity measurements on the deconvolution of the triple peak was studied in the following way. The content of each channel (N_i) of the ideal triple peak (which was simulated above) was distorted so that N_i became equal to the uniformly distributed statistical value in the range $N_i \pm N_i^{1/2}$. The triple peaks distorted in this manner were then deconvoluted. This procedure was repeated thirty times.

TABLE 1

Estimation of the computational stability of the method of moments for triplets deconvolution

Initial ratios of the single peaks $a_1:a_2:a_3$	ϵ^a	a_1	Δa_1 (%)	a_2	Δa_2 (%)	a_3	Δa_3 (%)	b_1	Δb_1 (%)	b_2	Δb_2 (%)	b_3	Δb_3 (%)
0.33:0.33:0.33	3.0*	0.333	-	0.333	-	0.333	-	37.00	-	40.00	-	43.00	-
	5.0	0.332	2.07	0.335	1.78	0.333	2.04	34.99	0.13	39.98	0.31	45.00	0.08
	4.0	0.330	3.69	0.337	3.00	0.333	2.82	35.98	0.18	39.97	0.38	44.00	0.10
	3.5	0.328	5.87	0.339	4.25	0.333	4.05	36.47	0.24	39.96	0.50	43.51	0.13
	3.0	0.325	10.35	0.345	6.39	0.330	7.22	36.96	0.34	39.97	0.75	43.02	0.19
0.50:0.35:0.15	3.0*	0.500	-	0.350	-	0.150	-	37.00	-	40.00	-	43.00	-
	5.0	0.499	1.58	0.351	1.75	0.150	3.83	34.99	0.10	39.99	0.30	45.01	0.14
	4.0	0.497	2.92	0.353	3.15	0.150	5.30	35.99	0.15	39.97	0.37	44.01	0.16
	3.5	0.494	4.73	0.356	4.62	0.150	7.94	36.48	0.19	39.96	0.51	43.51	0.22
	3.0	0.489	8.46	0.362	7.30	0.149	14.64	36.97	0.28	39.95	0.78	43.03	0.36
0.45:0.10:0.45	3.0*	0.450	-	0.100	-	0.450	-	37.00	-	40.00	-	43.00	-
	5.0	0.448	1.92	0.103	5.44	0.449	1.63	34.99	0.11	39.96	1.23	45.00	0.07
	4.0	0.445	3.13	0.107	10.27	0.448	2.87	35.98	0.15	39.90	1.48	44.00	0.09
	3.5	0.441	5.42	0.116	22.40	0.443	6.89	36.47	0.21	39.89	1.90	43.52	0.15
	3.0	0.428	12.06	0.147	57.22	0.425	21.51	36.95	0.35	39.90	2.57	43.10	0.91
0.45:0.45:0.10	3.0*	0.450	-	0.450	-	0.100	-	37.00	-	40.00	-	43.00	-
	5.0	0.449	1.66	0.451	1.34	0.100	5.18	34.99	0.11	39.99	0.21	45.01	0.18
	4.0	0.447	3.12	0.453	2.39	0.100	7.18	35.99	0.16	39.98	0.27	44.01	0.21
	3.5	0.444	5.05	0.455	3.43	0.101	10.75	36.48	0.21	39.97	0.38	43.52	0.29
	3.0	0.440	8.88	0.459	5.33	0.101	19.48	36.97	0.29	39.96	0.58	43.03	0.47
0.10:0.80:0.10	3.0*	0.100	-	0.800	-	0.100	-	37.00	-	40.00	-	43.00	-
	5.0	0.099	3.89	0.801	0.57	0.100	4.16	34.98	0.24	39.99	0.08	45.01	0.15
	4.0	0.098	8.08	0.802	0.93	0.100	5.49	35.96	0.37	39.99	0.10	44.02	0.18
	3.5	0.098	12.78	0.803	1.26	0.099	7.84	36.45	0.49	39.99	0.13	43.53	0.24
	3.0	0.098	21.72	0.804	1.85	0.098	14.21	36.94	0.68	39.99	0.20	43.05	0.36
0.80:0.10:0.10	3.0*	0.800	-	0.100	-	0.100	-	37.00	-	40.00	-	43.00	-
	5.0	0.798	1.23	0.103	5.79	0.099	6.33	34.99	0.08	39.97	1.22	45.02	0.22
	4.0	0.794	2.28	0.107	12.44	0.099	10.58	35.99	0.12	39.91	1.50	44.03	0.30
	3.5	0.787	4.44	0.116	24.64	0.097	20.05	36.48	0.17	39.89	1.98	43.58	0.72
	3.0	0.764	11.65	0.143	54.55	0.093	29.64	36.96	0.31	39.87	2.63	43.32	3.10

[a]The distances in channels between the maxima of adjacent peaks. The undistorted triple peaks are asterisked.

The mean value of the fraction (a_i) and position (b_i) of each peak as well as the standard deviations for these values are given in Table 1. The interval $\pm N_i^{1/2}$ was chosen on the conventional assumption that, in the case of radioactivity measurements, the standard deviation of the counting rate is $S_i = N_i^{1/2}$. Table 1 shows that quite satisfactory results were obtained by deconvolution of all the types of multiplets shown in Fig. 1.

Subtraction of background

So far, the problem of background has been disregarded because only the mathematical aspects of deconvolution have been considered. Obviously, cor-

rect subtraction of background is very important for the accurate deconvolution in practice.

For background subtraction, two interchangeable subroutines were prepared. The algorithm of the first subroutine is fast, simple and suitable for background subtraction if the peak to be deconvoluted is not on the Compton edge. For calculation of the background in the kth channel, the formulae used [6] are

$$F_k = F_m - (F_m - F_n)\left(\sum_{i=m}^{k} N_i\right) \Big/ \sum_{j=m}^{n} N_j, \quad \text{if } m < k \leqslant n$$

$$F_k = N_m, \quad \text{if } k = m$$

where F_k, F_m and F_n are the values of background in the kth, mth and nth channel, respectively; N_i is the content of the ith channel; and m and n are the left and right boundaries of the peak (the determination of these parameters is done by a special subroutine).

The algorithm of the second subroutine for background elimination is more sophisticated and consists in simulation of the background in the form of a fifth-order polynomial. Two models of background are available, one of which is the Compton continuum model. The program selects the model automatically, depending on the behaviour of the background in the neighbourhood of the peak.

Calibration of peak shape

From the theoretical part, it follows that for deconvolution of the multiplet the central moments of the single peaks must be known. It is well known that the shape of a peak depends on the energy of the peak (e.g., with the increasing of the energy peaks become wider). To take this fact into account, a special library of the central moments of single peaks with different energies was created. To compile this library, a special mixture was prepared from long-lived isotopes having single peaks in different parts of the energy scale (ca. 100–1800 keV). The spectrum is presented in Fig. 2.

An automatic program computes the needed central moments of the nine calibration peaks marked in Fig. 2. The data collected together with the information on peak positions are stored in the library. The dependences of the central moments of the same order on the energy can be approximated reasonably well by linear functions with use of the least-squares method (Fig. 3). These linear functions, together with the initial data on the central moments of the peaks, are used further for calculation of the central moments of the single peaks at the preset energy.

This library of peak shapes reflects all the features of the measurement system. In case of any modification of the measurement conditions, e.g., change

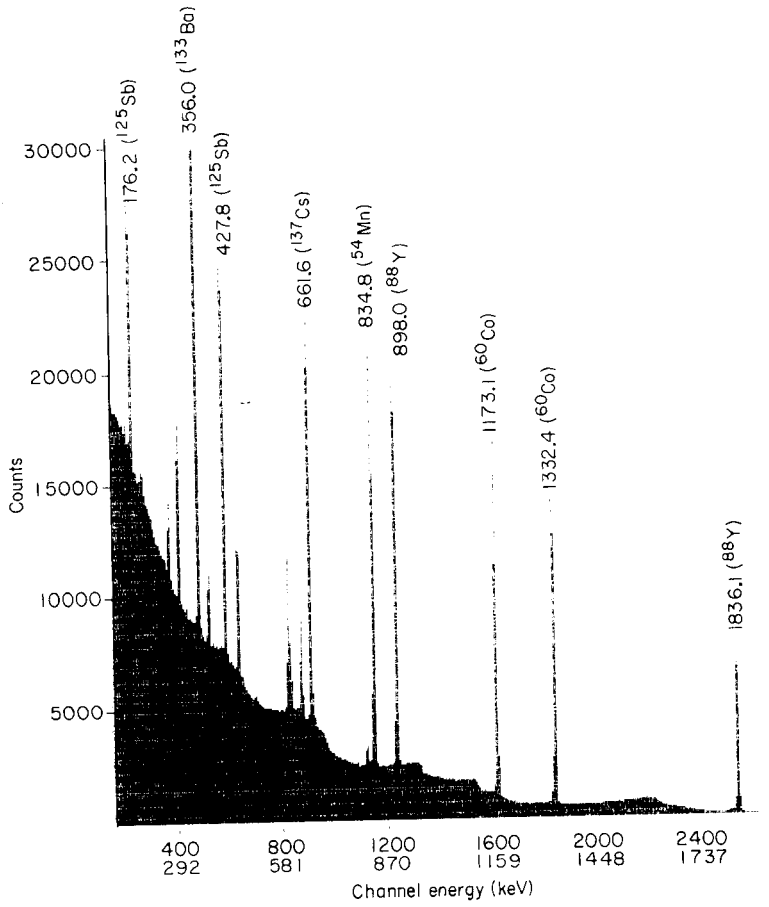

Fig. 2. The spectrum of the special mixture of long-lived isotopes for peak-shape calibration.

of detector, amplification, or any other feature that affects peak shape, the library must be compiled again.

Summary of the algorithm

The algorithm for the multiplet deconvolution can be summarized as follows.

(1) Determination of the centre of gravity of the multiplet to be deconvoluted; (2) computation of all needed central moments of the single peak corresponding to the centre of gravity of the multiplet (with use of the peak-shape library); (3) calculation of the central moments of the multiplet; (4) compilation of the linear equations system (Eqns. 6); (5) insertion of the results of the solution of Eqns. 6 into Eqn. 10, the solution of which gives the positions of the peaks composing the multiplet; (6) use of the values found for these

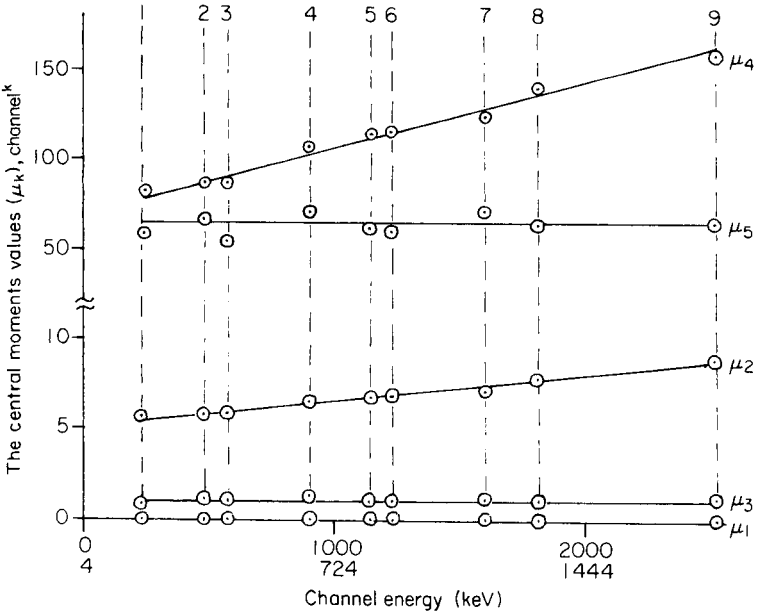

Fig. 3. The dependence of the central moments (μ_k) on the energy of the single peaks ($k=1,2,3,4,5$). (1) ^{125}Sb, 176.2 keV; (2) ^{133}Ba, 356.0 keV; (3) ^{125}Sb, 427.8 keV; (4) ^{137}Cs, 661.6 keV; (5) ^{54}Mn, 834.8 keV; (6) ^{88}Y, 898.0 keV; (7) ^{60}Co, 1173.1 keV; (8) ^{60}Co, 1332.4 keV; (9) ^{88}Y, 1836, 1 keV.

positions in the calculation (Eqn. 7) of the fraction of each peak in the multiplet area.

RESULTS AND DISCUSSION

On the basis of this algorithm, special software was created. The practical application of the program was checked by deconvolution of artificial composites of some isotopes as multiplets in rock standards.

Model mixtures of the isotopes zinc-65 and scandium-46 having different ratios of the components were prepared. The results of deconvolution of these mixtures are presented in Table 2.

Rock standards, ZGI-KH (limestone), ZGI-BM (basalt) and ZGI-TB (slate), were irradiated in a nuclear reactor for 100 h at a neutron flux of 1.2×10^{13} cm^{-2} s^{-1}. After the samples had cooled for one month, the γ-ray spectra were measured (acquisition time 3600 s). The program was used for deconvolution of three multiplets in the areas around 140 keV, 602 keV and 1120 keV (Fig. 4). For quantitative neutron activation analysis based on relative standardization, it is essential that the specific activities of the same isotopes are identical in simultaneously irradiated materials. The problem was

TABLE 2

Results for deconvolution of the model double peaks

Isotope	Composition of model doublet		Result of deconvolution	
	Fraction of single peak in doublet (%)	Peak position (keV)	Fraction of single peak in doublet (%)	Peak position (keV)
^{65}Zn	90.0	1115.5	89.1	1115.6
^{46}Sc	10.0	1120.5	10.9	1119.7
^{65}Zn	70.0	1115.5	71.3	1115.3
^{46}Sc	30.0	1120.5	28.7	1120.5
^{65}Zn	50.0	1115.5	51.9	1115.4
^{46}Sc	50.0	1120.5	48.1	1120.5
^{65}Zn	30.0	1115.5	32.0	1115.2
^{46}Sc	70.0	1120.5	68.0	1120.5

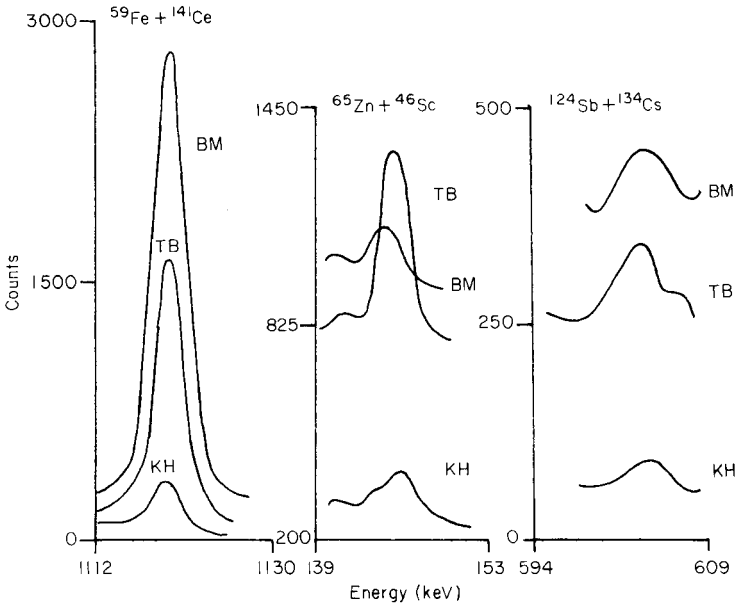

Fig. 4. Portions of the γ-spectra of the rock standards.

therefore to demonstrate this for the rock standards and consequently to confirm the correctness of the deconvolution of the multiplets.

The results are given in Table 3. In all cases, the double peaks obtained were attributed to the isotopes indicated in Table 3. Because the weights and acquisition times for all three standards were the same, Table 3 gives the conditional specific activity; its value was calculated simply by division of the activity of the individual peak in the doublet by the certified content of the correspond-

TABLE 3

Results of deconvolution of some multiplets in spectra of rock standards

Standard rock	Isotope	Multiplet area (counts)	Single peak contribution (%)	Certified content of element (mg kg^{-1})	Conditional specific activity of isotope
ZGI-KH[a]	^{141}Ce	103×10^2	95.12	20	490
	^{59}Fe		4.88	0.93%	537
	^{65}Zn	302×10^2	10.35	22	141
	^{46}Sc		89.64	3	9300
	^{124}Sb	1479	16.71	NC[d]	-
	^{134}Cs		83.29	1.4	880
ZGI-TB[b]	^{141}Ce	442×10^2	94.08	104	339
	^{59}Fe		5.92	6.92%	377
	^{65}Zn	1316×10^2	3.86	94	54
	^{46}Sc		96.14	16	7900
	^{124}Sb	9218	19.00	3.4	515
	^{134}Cs		81.00	9	830
ZGI-BM[c]	^{141}Ce	108×10^2	57.95	22	284
	^{59}Fe		42.05	9.68%	467
	^{65}Zn	250×10^3	7.37	120	155
	^{46}Sc		86.36	34	6800
	^{124}Sb	2362	32.38	2.3	330
	^{134}Cs		67.62	2	800

[a]COMECON standard 2302-80. [b]COMECON standard 2301-80. [c]COMECON standard 2300-80. [d]Not certified.

ing element. From the data obtained, the antimony content (uncertified) in standard ZGI-KH can be estimated as 0.61 mg kg^{-1}. The discrepancy in the specific activity of zinc-65 in the ZGI-TB standard compared to the other standards can be attributed to the low contribution of this isotope in the doublet.

Conclusions

The most widely used methods for the deconvolution of multiplets are various modifications of the least-squares method (LSM). The method of moments is based on quite different principles. The theory of the method of moments has been given above in a general form suitable for the deconvolution of peaks having any number of components.

The algorithm for the method of moments utilizes the real shapes of the peaks, once a library of peak shapes has been set up for a particular measurement system. Within the framework of the theory, it was possible to take into account any distortion of peak shape caused by pile-up effects and spectrum drift during long count times. The resolution ability of the method is similar to that of the LSM, but no iterative procedures are needed, so that the method is very fast in comparison to the LSM. For example, any triplet composite can

be deconvoluted in about 0.8 s by means of the software floating-point arithmetic. Even this duration could be reduced significantly by application of double-precision integer arithmetic for computation of the central moments. When multiple peaks have to be deconvoluted, the advantage in speed of the method of moments becomes more obvious. The algorithm for the method of moments is quite compact. For example, the deconvolution subroutine needs only 1 kword of core memory in the computer.

With use of this algorithm and some original algorithms, the fast ASPRO program was developed expressly for fully automatic spectra processing. Evaluation of a 4096-channel spectrum consisting of 45 peaks including 13 multiplets, requires only 28 s. The progrm runs in the microcomputer of the multichannel analyzers supplied by Nokia (Finland).

REFERENCES

1 A. Clifford Cohen, Technometrics, 9 (1967) 15.
2 H. Teicher, Ann. Math. Stat., 38 (1967) 1300.
3 G. Korn and T. Korn, Mathematical Handbook, Nauka, Moscow, 1977, p. 547.
4 A.G. Kurosh, Course of Higher Algebra, Fizmatgiz, Moscow, 1955, p. 240.
5 I.S. Berezin and N.P. Zhidkov, Computation Methods, Vol. 2, Fizmatgiz, Moscow, 1962, p. 171.
6 J.G. Fieissnev and R. Gunnink, Report of Lawrence Livermore National Laboratory, CA, 1981, Index MLM-2807.

Analytica Chimica Acta, 203 (1987) 55–66
Elsevier Science Publishers B.V., Amsterdam — Printed in The Netherlands

APPLICATION OF EXPERIMENTAL DESIGN FOR INVESTIGATING THE DETERMINATION OF TITANIUM IN GLASS CERAMICS BY FLAME ATOMIC ABSORPTION SPECTROMETRY

OLGA GROSSMANN

Zentralinstitut für Festkörperphysik und Werkstofforschung, Akademie der Wissenschaften der D.D.R., D.D.R.-8027 Dresden (German Democratic Republic)

(Received 14th May 1986)

SUMMARY

Interferences of the matrix elements of glass ceramics (Al, Mg, Na and Si) on the titanium signal obtained by atomic absorption spectrometry with a nitrous oxide/acetylene flame were studied by means of experimental design. Quadratic polynomials were chosen as the model; full factorial designs with two, three and four variables at three levels were applied. As expected, aluminium increased the titanium signal, while magnesium reduced it. All the investigated elements interfered nonadditively with the titanium signal; the standard addition method therefore does not provide accurate results. Graphic evaluation of the empirical response surfaces was used to establish optimum conditions for titanium; these surfaces were compared with the polynomial surfaces to check the models. The results obtained on interactions in the system are used with some thermodynamic data to estimate the nature of the compounds formed in the flame. The strong interferences on the titanium signal requires fairly close matrix matching between the standard and sample solutions. The proposed method allows the determination of 3–6% Ti in glass ceramics with a relative standard deviation of 1%.

The addition of titanium dioxide to a basic $SiO_2/Al_2O_3/MgO/Na_2O$ mixture has a decisive influence on the crystallization behaviour of the final glass, and so on the strength of glass ceramics. Therefore, the concentration of titanium in these ceramics must be controlled carefully. The determination of titanium in aluminosilicates after their decomposition in hydrofluoric/sulphuric acid mixtures is probably best done by atomic absorption spectrometry (AAS) in a nitrous oxide/acetylene flame or by inductively-coupled plasma/atomic emission spectrometry (ICP/AES). Several investigations concerned with the determination of titanium by AAS in different materials have shown that the accuracy of the results is strongly dependent on the composition of the sample

0003-2670/87/$03.50

[1–9]. The presence of Al, Fe, Na, K, Mg and Mn in silicate samples tends to increase the titanium signal; aluminium shows the highest nonadditive interference with the titanium signal [8,9]. The extent of this interference is considerably affected by the presence of other elements, e.g., iron and sodium [8]. In the method for the determination of titanium in silica/alumina-based catalysts by AAS proposed by Fabec and Ruschak [9], the need for matrix matching is avoided by adding a large amount of aluminium and lanthanum to the sample solutions and standards. The addition of lanthanum also decreases fluctuations of the titanium signals caused by fluctuation of the acetylene flow to the flame.

In the present work, experimental design was applied in an attempt to establish conditions for the determination of 2–10% titanium in glass ceramics by AAS, such that the same standard solutions might be applied for different sample compositions with guaranteed accuracy of the analytical results. For better understanding of the complicated interactions of the matrix elements with the titanium, these elements were arranged in several groups: Al and Mg; Al and Na; Mg and Na; Al, Mg and Na; and finally Al, Mg, Na and Si. The full factorial designs were applied at three levels. The forms of the diagonals of the empirical response surfaces were examined [10]. The polynomial coefficients were calculated by a computer program. The empirical response surfaces were compared with the polynomial response surfaces. These features, in addition to the *F*-test, enable conclusions to be drawn about the adequacy of the applied models.

The results obtained were used in an attempt to reduce the effort needed for calibration while maintaining a predefined accuracy of the results obtained for titanium. Consideration of these results in connection with some thermodynamic data made it possible to assess which compounds exist in the flame.

EXPERIMENTAL

Apparatus and reagents

The atomic absorption spectrometer was a Perkin-Elmer Model 422, used with a nitrous oxide/acetylene reducing (fuel-rich) flame. The optimum conditions were as follows: burner head, 50 mm; observation height, 10 mm; slit width, 0.2 nm; wavelength, 363.9 nm.

All the acids used (HCl, HF, H_2SO_4) were distilled. The other chemicals used ($LaCl_3$, Al_2O_3, NaCl, MgO, SiO_2) were of analytical-reagent grade. The standard titanium dioxide, TiO_2, was of stoichiometric composition.

For the preparation of the standard and sample solutions, the salt and oxide mixtures or ceramic powders were placed in platinum dishes and 2 ml of concentrated sulphuric acid and 20 ml of 19 M hydrofluoric acid were added. After dissolution of the samples, the acids were evaporated until the residue was moist. This procedure was repeated twice. The residues were dissolved in 5 ml of 6 M hydrochloric acid on a hot plate; the solutions were cooled and trans-

TABLE 1

The levels of the factors (μg ml^{-1})

Coded level	x_1 c_{Al}	x_2 c_{Mg}	x_3 c_{Na}	x_4 c_{Si}
+1	320	120	240	600
0	210	90	130	480
−1	100	60	20	360

ferred to 100-ml polyethylene volumetric flasks. After the addition of 132 mg of lanthanum chloride, the solutions were diluted to volume with water.

Levels of the factors (independent variables) and optimization parameter (dependent variable)

The three levels of concentrations of Al, Mg, Na and Si used in the investigated solutions are given in Table 1. These concentrations were chosen in accordance with the expected concentrations of these elements in the glass ceramics studied. The coded levels are also given in Table 1. The concentration of titanium in all these solutions was constant (100 μg ml^{-1}).

The normalized titanium signal in AAS was chosen as the optimization parameter. The normalization consisted of making the value of the signal at the centre point of the corresponding design (e.g., point 9, Table 2) equal to unity. The values of the optimization parameter at the other points of the design were calculated relative to this value.

TABLE 2

The design and the results for the relationships $y=f(x_i, x_j)$

No.	x_i	x_j	c_{Al}, c_{Mg} x_1, x_2		c_{Al}, c_{Na} x_1, x_3		c_{Mg}, c_{Na} x_2, x_3	
			$\bar{y}_1$[a]	$\hat{y}_1$[b]	$\bar{y}_2$[a]	$\hat{y}_2$[b]	$\bar{y}_3$[a]	$\hat{y}_3$[b]
1	+	+	0.880	0.871	1.326	1.236	0.972	0.981
2	+	−	1.342	1.306	1.333	1.236	1.076	1.057
3	−	+	0.747	0.744	0.739	0.796	1.000	0.981
4	−	−	0.683	0.654	0.879	0.796	1.052	1.057
5	0	+	0.708	0.720	1.013	1.016	0.970	0.981
6	0	−	0.827	0.892	0.921	1.016	1.042	1.057
7	+	0	1.160	1.206	1.107	1.236	0.947	0.976
8	−	0	0.785	0.817	0.826	0.796	0.980	0.976
9	0	0	1.000	0.923	1.000	1.016	1.000	0.976

[a]Experimental values. [b]Polynomial values.

RESULTS AND DISCUSSION OF THE DESIGNED EXPERIMENTS

The designs and the experimental results are given in Tables 2, 4 and 5. The mean values of the optimization parameters were calculated on the basis of three measurements.

Relationship $y_1 = f(c_{Al}, c_{Mg})$

The calculated polynomial (Table 2) is

$$\hat{y}_1 = 0.923 + 0.195x_1 - 0.086x_2 + 0.088x_1^2 - 0.117x_2^2 - 0.132x_1x_2 \quad (1)$$

with $\hat{S}_s^2 = 1.1 \times 10^{-2}$, $\hat{S}_f^2 = 1.6 \times 10^{-2}$ and $F_{calc} = 8.\smile > F_{tab}$ ($P = 0.99$, $f_1 = 3$, $f_2 = 18$) $= 5.9$. This polynomial does not provide, according to the F-test [11], an adequate description of the empirical relationship.

The corresponding empirical response surface with parallel side lines showing the same shape (Table 3) can, however, be adequately described by a quadratic polynomial like the above Eqn. 1 [10], which describes a surface with a saddle-like shape. Comparison of the empirical response surface ($\bar{y}$-surface, Fig. 1a) and the polynomial surface ($\hat{y}$-surface, Table 2, Fig. 1b) shows that these two surfaces have nearly the same shape with the saddle point. Therefore, in contrast to the verdict of the F-test, the approximation of the investigated empirical relationship by Eqn. 1 can be regarded as good.

In this system, the titanium signal is strongly increased by aluminium and considerably reduced by magnesium. These two elements interfere nonadditively with the titanium signal and show a joint effect (presence of the x_1x_2 term); this means that the interaction of one of these elements depends on the concentration of the other.

TABLE 3

Form of diagonals and of side lines of empirical response surfaces for the relationships $y = f(x_i, x_j)$

Relation	Form of diagonals		Form of lines along the parallel sides of factor space	
	From (+1, +1) to (−1, −1)	From (+1, −1) to (−1, +1)	Along $x_i = +1$ and $x_i = -1$	Along $x_j = +1$ and $x_j = -1$
$y_1 = f(x_1, x_2)$	Convex	Concave	Convex Convex	Concave Concave
$y_2 = f(x_1, x_3)$	Concave	Concave	Concave Straight	Straight Concave
$y_3 = f(x_2, x_3)$	Straight	Concave	Concave Concave	Straight Straight

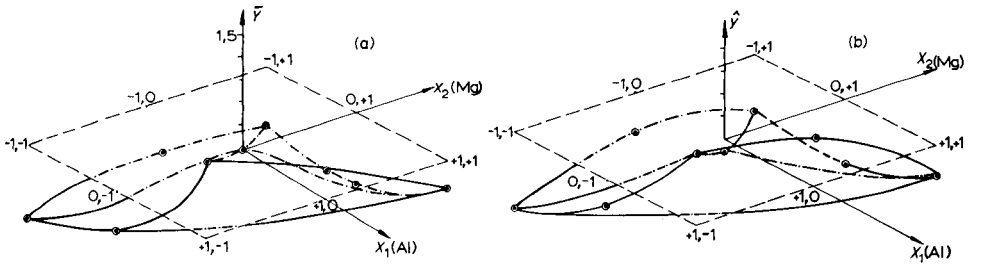

Fig. 1. Response surfaces for the relationship $y=f(c_{Al}, c_{Mg})$: (a) empirical response surface; (b) polynomial surface.

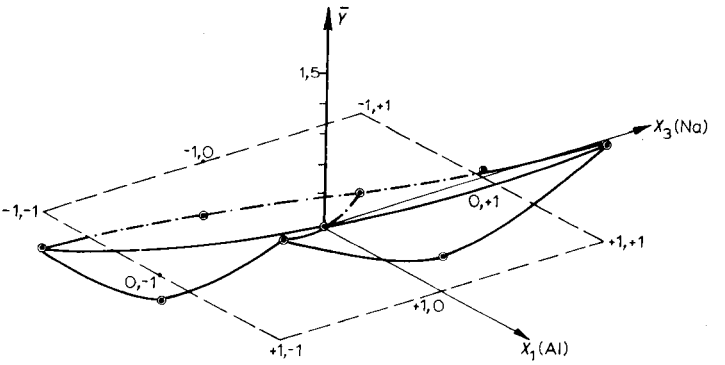

Fig. 2. Empirical response surface for the relationship $y=f(c_{Al}, c_{Na})$.

Relationship $y_2=f(c_{Al}, c_{Na})$

The forms of the parallel side lines of the empirical response surface of this relationship are different (Table 3, Fig. 2). Such a relationship cannot be described adequately by a quadratic polynomial [10]. The calculated equation (Table 2)

$$\hat{y}_2=1.016+0.220x_1 \qquad (2)$$

(with $\hat{S}_s^2=1.4\times10^{-2}$, $\hat{S}_f^2=5.4\times10^{-2}$) describes a plane and cannot be regarded as adequate for the surface in Fig. 2. In this case also, aluminium causes a strong increase of the titanium signal.

Relationship $y_3=f(c_{Mg}, c_{Na})$ *with constant* $c_{Al}=-1$

Because of the strong interference of aluminium with the titanium signal, the relationship $y_3=f(c_{Mg},c_{Na})$ was investigated for 100 μg ml^{-1} Al in each solution. The empirical response surface with two straight and two concave side lines and a concave diagonal (Table 3, Fig. 3) shows the identifying features of a stationary minimum and therefore can be approximated by a quadratic polynomial [10].

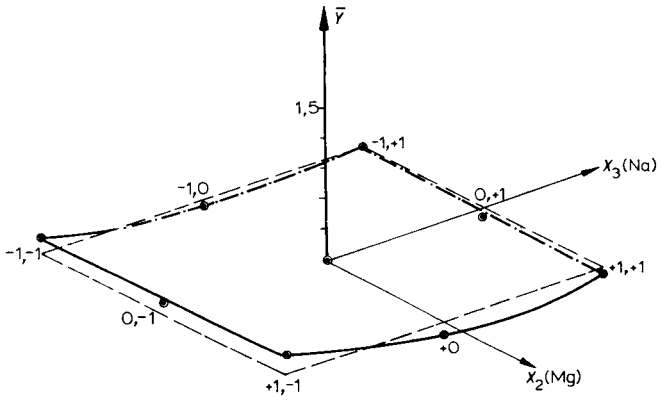

Fig. 3. Empirical response surface for the relationship $y=f(c_{Mg}, c_{Na})$ with $c_{Al}=100\ \mu g\ ml^{-1}$.

The following calculated polynomial (Table 2) adequately describes the empirical relationship:

$$\hat{y}_3=0.976-0.038x_3+0.043x_2^2 \qquad (3)$$

with $\hat{S}_s^2=8.7\times10^{-3}$, $\hat{S}_f^2=1.3\times10^{-3}$, and $F_{calc}=0.45<F_{tab}$ $(P=0.95,\ f_1=6,\ f_2=18)=2.66$.

Relationship $y=f(c_{Al}, c_{Mg}, c_{Na})$

The experimental design and experimental results are shown in Table 4. The following calculated polynomial does not give an adequate description:

$$\hat{y}=1.048+0.096x_1-0.029x_2-0.041x_3+0.059x_1^2$$
$$+0.059x_2^2+0.052x_3^2+0.024x_1x_3 \qquad (4)$$

with $\hat{S}_s^2=1.1\times10^{-2}$, $\hat{S}_f^2=1.3\times10^{-2}$ and $F_{calc}=5.7>F_{tab}$ $(P=0.99,\ f_1=4,\ f_2=19)=4.5$.

The linear interference of Al, Mg and Na with the titanium signal in this system corresponds to the interferences observed in the experiments with two variables. The empirical response surface of the relationship $y=f(x_1, x_2, x_3)$ lying in four-dimensional space can be represented graphically only after reduction of the space dimensionality as described earlier [10], which means that one of the independent variables is kept constant (e.g., $x_1=\pm1$). Each of the conditions $x_1=\pm1$ corresponds to five observations in the design (Table 4). For example, the condition $x_1=+1$ corresponds to observations 1, 2, 3, 4 and 9, condition $x_2=+1$ corresponds to observations 1, 2, 5, 6 and 11, etc. Each of these five observations can be used for a perspective drawing of the response surface. Two corresponding surfaces (e.g., for conditions $x_1=\pm1$) and the four planes including the border lines of the factor space and parallel to the y-axis (border planes) serve to outline a response body in three-dimensional space.

TABLE 4

Full factorial design and results for the relationship $y=f(x_1, x_2, x_3)$

No.	n_j	c_{Al} x_1	c_{Mg} x_2	c_{Na} x_3	$\bar{y}^a$	$\hat{y}^b$
1	2	+	+	+	1.207	1.253
2	2	+	+	−	1.290	1.298
3	2	+	−	+	1.370	1.341
4	2	+	−	−	1.355	1.365
5	2	−	+	+	1.025	1.033
6	2	−	+	−	1.127	1.174
7	2	−	−	+	1.073	1.082
8	2	−	−	−	1.232	1.206
9	2	+	0	0	1.239	1.203
10	2	−	0	0	1.047	1.011
11	2	0	+	0	1.189	1.078
12	2	0	−	0	1.098	1.136
13	2	0	0	+	1.094	1.059
14	2	0	0	−	1.178	1.141
15	6	0	0	0	1.000	1.048

[a]Experimental values. [b]Polynomial values.

Because the empirical response surface of the relationship $y_3=f(c_{Mg}, c_{Na})$ (Fig. 3) has the simplest form, the relationship

$$y=f(x_2, x_3) \text{ with } x_1 = \pm 1 \tag{5}$$

was chosen for the graphic representation of the response body shown in Fig. 4. Each of the two response surfaces forming the response body with concave diagonals has a minimum. Substitution of Eqn. 5 into Eqn. 4 leads to an algebraic approximation of the two response surfaces:

$$x_1 = +1: \hat{y}_{1+} = 1.203 - 0.029x_2 - 0.017x_3 + 0.059x_2^2 + 0.052x_3^2 \tag{6}$$

$$x_1 = -1: \hat{y}_{1-} = 1.011 - 0.029x_2 - 0.065x_3 + 0.059x_2^2 + 0.052x_3^2 \tag{7}$$

These polynomials indeed describe surfaces with minima. Therefore, the approximation of the empirical relationship by Eqns. 6 and 7 can be regarded as good.

The distance between the two response surfaces in Fig. 4 characterizes the interference of aluminium with the titanium signal. If this interference were linear, the surfaces would be parallel to each other. The nonadditive interference of aluminium alters these distances in several parts of the factor space.

The examination of the form of the response body can be useful in solving the analytical problem, namely, to establish conditions under which efforts devoted to calibration can be minimized. It can be seen in Fig. 4 that the upper and lower surfaces between points a $(x_2=+1, x_3=0)$, b $(x_2=+1, x_3=+1)$

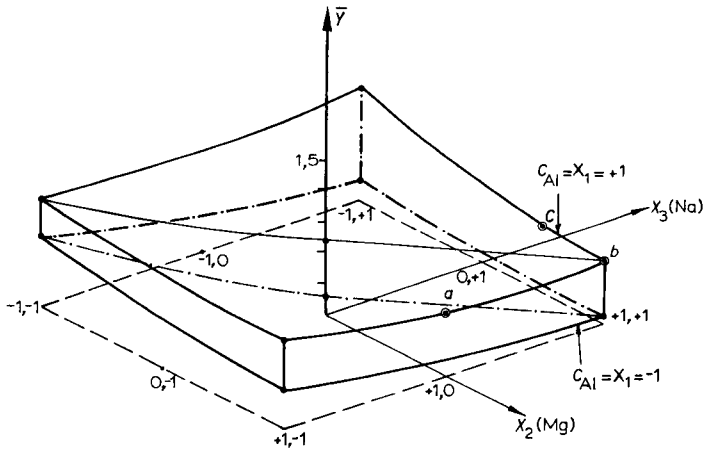

Fig. 4. Empirical response body for the relationship $y=f(c_{Al}, c_{Mg}, c_{Na})$, for the condition $c_{Al}=x_1=\pm 1$.

and c ($x_2=+0.5$, $x_3=+1$) are practically parallel to the factor plane. This means that in this region of the defined aluminium concentration, the titanium signal is independent of the magnesium and sodium concentrations.

Relationship $y=f(c_{Al}, c_{Mg}, c_{Na}, c_{Si})$

This relationship was investigated by means of a full factorial design 2^4 accomplished by the observation at the centre point (Table 5). Two sets of solutions were prepared: (1) by dissolution of a mixture of oxides and salts of all the elements, and (2) by dissolution of the oxides and salts of Al, Mg, Na and Si and the addition of titanium as a solution in hydrochloric acid. In this way, the reliability of the standard addition method should be proved.

The experimental results are presented in Table 5. The empirical relationships are adequately described by the two calculated polynomials:

$$\hat{y}_{mix}=1.000+0.130x_1+0.038x_2+0.018x_3+0.021x_4 + 0.027x_1x_2-0.023x_1x_4+0.047x_i^2 \quad (8)$$

with $\hat{S}_s^2=1.5\times10^{-2}$, $\hat{S}_f^2=7.1\times10^{-3}$ and $F_{calc}=1.1<F_{tab}$ ($P=0.95$, $f_1=9$, $f_2=21$) $=2.4$ and

$$\hat{y}_{add}=1.000+0.102x_1+0.011x_2-0.013x_3-0.012x_1x_2 - 0.020x_1x_4-0.014x_2x_4-0.049x_i^2 \quad (9)$$

with $\hat{S}_s^2=3.6\times10^{-3}$, $\hat{S}_f^2=1.1\times10^{-3}$ and $F_{calc}=0.72<F_{tab}$ ($P=0.95$, $f_1=9$, $f_2=21$) $=2.4$. The big linear interference of aluminium with the titanium signal (x_1 terms) remains after the addition of the fourth variable c_{Si}. Comparison of Eqns. 8 and 9 shows that there are certain differences with respect to

TABLE 5

Full factorial design for the relationship $y=f(x_1, x_2, x_3, x_4)$ and the experimental results

No.	n_j	c_{Si} x_4	c_{Al} x_1	c_{Mg} x_2	c_{Na} x_3	$\bar{y}_{mix}$ [a]	$\bar{y}_{add}$ [b]
1	2	+	+	+	+	1.296	0.995
2	2	+	+	+	−	1.266	1.037
3	2	+	+	−	+	1.068	1.023
4	2	+	+	−	−	1.074	1.059
5	2	+	−	+	+	0.994	0.864
6	2	+	−	+	−	0.893	0.893
7	2	+	−	−	+	0.979	0.847
8	2	+	−	−	−	0.979	0.866
9	2	−	+	+	+	1.189	1.112
10	2	−	+	+	−	1.219	1.067
11	2	−	+	−	+	1.210	1.073
12	2	−	+	−	−	1.098	1.070
13	2	−	−	+	+	0.964	0.842
14	2	−	−	+	−	0.858	0.906
15	2	−	−	−	+	0.826	0.771
16	2	−	−	−	−	0.843	0.820
17	6	0	0	0	0	1.000	1.000

[a]Ti dissolved together with all other elements. [b]Ti added as a hydrochloric acid solution.

the pretreatment of the titanium during the solution preparation. This difference is concerned primarily with the signs on the coefficients of the quadratic members of polynomials.

In the case of $\hat{y}_{mix}$ (Eqn. 8), the response surface lying in a five-dimensional space shows a minimum, but in the case of $\hat{y}_{add}$ it shows a maximum. This fact, and several other differences in the signs and values of the polynomial coefficients, lead to the conclusion that application of a standard addition method cannot guarantee the accuracy of the titanium determination in glass ceramics. It is evident from Eqn. 8, however, that silicon interferes with the titanium signal in two ways: as a linear interference and as a joint effect with aluminium. Therefore, the calibration solutions should contain certain amounts of silicon to compensate for these interferences. Exact matching of the silicon concentrations in the sample and calibration solutions is not necessary because much of the silicon will be eliminated during the evaporation of the sample solutions with the acid mixture containing hydrofluoric acid.

INTERACTIONS IN THE SYSTEMS STUDIED

The dissociation of titanium compounds to form free titanium atoms can take place only at a temperature of 2650–2800 °C in the nitrous oxide/acety-

TABLE 6

Enthalpies of atomization of crystalline salts

Salt	$\Delta' H^0_{298}$ (kJ mol^{-1})	$\Delta' H^0_{298}$ (kJ atom^{-1})[a]
$MgAl_2O_4$	2736	391
$MgTiO_3$	1896	379
$NaAlO_2$	1357	339
Na_2TiO_3	2007	335

[a]Enthalpy relates to each atom in the salt molecule (g-atom).

lene flame [12]. Ionization of titanium atoms at this temperature can be suppressed by addition of lanthanum. When a solution containing the compounds of Ti, Al, Mg, Na and Si is aspirated into a flame, then the salts with high enthalpy of formation are formed first. The enthalpies of atomization of the relevant crystalline salts, which can be formed in the flame, are listed in Table 6. They were calculated according to the equation

$$\Delta' H^0_{298} = -\Delta_B H^0_{298} + \sum^{i} \Delta_{A_i} H^0_{298} \quad (10)$$

where $\Delta_B H^0_{298}$ is the enthalpy of formation of the crystalline salts from their elements [13] and $\Delta_{A_i} H^0_{298}$ is the enthalpy of atomization of the elements [13].

These salts decompose in the flame to give gaseous compounds, mainly oxides: $MgTiO_3 \rightleftarrows MgO + TiO_2$; $TiO_2 \rightleftarrows TiO + O$; $TiO \rightleftarrows Ti + O$. The enthalpies of atomization of gaseous titanium and aluminium oxides are given in Table 7; they were also calculated from Eqn. 10, with $\Delta_B H^0_{298}$ as the enthalpy of formation of gaseous oxides from the elements [13].

From Eqns. 1, 4 and 8, it follows that, regardless of the number of variables, the interaction of aluminium with titanium leads to a considerable increase in the titanium signal. This phenomenon is obviously due to the ability of aluminium to form the stable oxide Al_2O (Table 7). The dissociation energy of Al_2O to form atoms, related to the maximum concentration of aluminium in the solution, is 2.3 times higher than the dissociation energy of TiO_2 and 4.4 times higher than the dissociation energy of TiO (Table 7). Probably, the partial pressure of atomic oxygen in the flame [14] will be so far diminished

TABLE 7

Enthalpies of atomization of some gaseous oxides

Reaction	$\Delta_A H^0_{298}$ (kJ mol^{-1})	c_{Me} (μg ml^{-1})	$\Delta'_A H^0_{198}$ (kJ ml μg^{-1})
$Al_2O \rightleftarrows 2Al + O$	1039	320	6.2×10^{-3}
$TiO_2 \rightleftarrows Ti + 2O$	1304	100	2.7×10^{-3}
$TiO \rightleftarrows Ti + O$	658	100	1.4×10^{-3}

in the presence of aluminium that the atomization of titanium oxides will be considerably increased.

In the system Ti/Al/Mg (Eqn. 1), the magnesium shows a high negative interference with the titanium signal. This can probably be explained by the formation of the stable salts $MgAl_2O_4$ and $MgTiO_3$ (Table 6) in the flame. The existence of a high joint effect between aluminium and magnesium, as well as the nonlinear interference of magnesium with the titanium signal confirms this idea. In the presence of sodium, the interference of magnesium becomes small (Eqns. 4 and 8); this can be explained by the formation of $NaAlO_2$ and Na_2TiO_3 in the flame because these are less stable than $MgAl_2O_4$ and $MgTiO_3$ (Table 6). Other interactions in the systems studied cannot be discussed in this way.

DETERMINATION OF TITANIUM IN GLASS CERAMICS

The above results indicate that the following aspects must be considered in the preparation of solutions for calibration. The concentrations of aluminium in the sample and the standard solutions must be approximately the same. The concentration of magnesium can be varied over a small range (e.g., 105–120 $\mu g\ ml^{-1}$), and the concentration of sodium can be varied over a wider region (e.g., 130–240 $\mu g\ ml^{-1}$). The presence of some silicon in the standard solutions is necessary.

The method of standard additions is not recommended. The same standard solutions can be applied for several sample compositions only if the concentrations of matrix elements in all sample solutions will be nearly the same. The accurate determination of titanium is possible only if the composition of glass samples has been estimated by a preliminary analysis.

The precision and accuracy of the titanium determination were tested for three glass samples, in which the titanium was also determined spectrophotometrically. The compositions of the samples are given in Table 8. The sample

TABLE 8

Comparison of reference values and AAS results for titanium in three samples of glass ceramics

Sample	Reference values (%)			Weight of sample (mg)	Additions to samples (mg)			Ti by AAS (%)
	Ti	Al	Mg		NaCl	Al_2O_3	MgO	
1	3.9	10.5	9.4	256	69	-	-	3.94
2	6.0	12.6	6.1	167	69	9.5	26.5	5.97
3	4.2	10.9	11.4	238	69	-	-	3.80

weights were chosen so as to provide 100-ml sample solutions with expected titanium concentrations of ca. 100 μg ml^{-1}. The additions to the samples for equalization of the concentrations of matrix elements are also given in Table 8. Three calibration solutions were prepared with 80, 100 and 120 μg ml^{-1} titanium as well as 280 μg ml^{-1} Al, 260 μg ml^{-1} Mg, 240 μg ml^{-1} Na, 750 μg ml^{-1} La and some silicon. In this range, the calibration graph is linear.

The results obtained for titanium are listed in Table 8. According to the *t*-test ($P=0.90, f=9$), the titanium values for samples 1 and 2 determined by AAS are not significantly different from the spectrophotometric values. In contrast, the titanium content of sample 3 is significantly lower. The relative standard deviation was found to be 0.01 ($n=11$).

Conclusion

The designed experiments have shown that the interferences of matrix elements of glass ceramics on the titanium signal by AAS are very complicated. For this reason, it was not possible to establish conditions under which the same standard solutions could be applied for different sample compositions. The problem outlined at the start of this paper seems to have no simple solution.

The author is indebted to Dr. W. Kluge for support in computer calculations, to Ek. Müller for assistance in experimental work, and to Mrs. Erxleben for preparation of the glass ceramics.

REFERENCES

1 J.A. Bowman and J.B. Willis, Anal. Chem., 39 (1967) 1210.
2 L. Capacho-Delgado and D.C. Manning, Analyst, 92 (1967) 553.
3 R.A. Mostyn and A.F. Cunningham, At. Absorpt. Newsl., 6 (1967) 86.
4 B. Bernas, Anal. Chem., 40 (1968) 1682.
5 G.G. Welcher and H. Kriege, At. Absorpt. Newsl., 8 (1969) 97.
6 W.D. Cobb, W.W. Foster and T.S. Harrison, Anal. Chim. Acta, 78 (1975) 293.
7 M. Damiani, M.G. Del Monte Tamba and F. Bianchi, Analyst, 100 (1975) 643.
8 J.N. Walsh, Analyst, 102 (1977) 972.
9 J.L. Fabec and M.L. Ruschak, At. Spectrosc., 5 (1984) 142.
10 O. Grossmann, Anal. Chim. Acta, 186 (1986) 185.
11 B. Pegel, Empirische Modellbildung und Versuchsplanung, Akademie-Verlag, Berlin, 1980, p. 26.
12 B. Welz, Atom-Absorptions-Spektroskopie, Verlag Chemie, Weinheim, 1975, p. 31.
13 M.Kh. Karapetyanc and M.L. Karapetyanc, Osnovnye Termodinamicheskie Konstanty Neorganicheskikh i Organicheskikh veshchestv, Khimiya, Moscow, 1968.
14 B.V. L'vov, L.P. Kruglikova, L.K. Polzik and D.A. Katskov, Zh. Anal. Khim., 30 (1975) 846.

Analytica Chimica Acta, 203 (1987) 67–77
Elsevier Science Publishers B.V., Amsterdam — Printed in The Netherlands

APPLICATION OF EXPERIMENTAL DESIGN FOR INVESTIGATING THE DIFFERENTIAL SPECTROPHOTOMETRIC DETERMINATION OF LARGE AMOUNTS OF NIOBIUM WITH 4-(2-PYRIDYLAZO)-RESORCINOL

OLGA GROSSMANN

Zentralinstitut für Festkörperphysik und Werkstofforschung, Akademie der Wissenschaften der D.D.R., D.D.R.-8027 Dresden (German Democratic Republic)

(Received 6th August 1986)

SUMMARY

Differential spectrophotometry is used to determine large amounts of niobium in the alkali metal/niobium/fluoride mixes involved in the electrolytic separation of pure niobium. In tartrate medium, niobium forms a purple mixed-ligand complex with 4-(2-pyridylazo)resorcinol (PAR). The pH range for constant absorbance found, for two tartrate concentrations, is 6.1 ± 0.05; outside this pH range, the absorbance is strongly affected by small changes of pH. The optimum concentrations of tartrate and PAR for the differential method were found by means of experimental design. A quadratic polynomial model was applied; the results obtained were also used to calculate the stability constants of the coloured complexes. Comparison of the variation of these constants with changes in the absorption spectra of the solutions and with changes in the empirical response surfaces provided an explanation of the inadequacy of the calculated polynomial; several tartrate complexes and mixed ligand complexes of niobium appeared in some parts of the investigated factor space. The differential spectrophotometric procedure developed allows determination of 10–30% niobium with a relative standard deviation of 0.0025; its accuracy is proved by the determination of niobium in the stoichiometric compound K_2NbF_7.

The differential spectrophotometric determination of large amounts of niobium has been described by several workers [1–7]. Thiocyanate, picramine, pyrogallol and other reagents have been used to develop the colour. The results of the applied procedures show a fairly high relative standard deviation (S_r) of about 0.01.

Spectrophotometric determinations of small amounts of niobium have been applied in the analysis of steels and alloys [8–10]. The most sensitive reagent, sulphochlorophenol S, gives poorly reproducible results. The most suitable reagent seems to be 4-(2-pyridylazo)resorcinol (PAR) which provides a selective and accurate determination of niobium under optimum conditions [9, 11].

0003-2670/87/$03.50

The complexation of niobium with metallochromic reagents is affected by hydrolysis of niobium ions. To overcome this interaction, hydrogen peroxide, oxalate or tartrate are used [8–18]. With tartrate, niobium forms the complexes $[NbO(tart)_2]^-$ [13–15], $[NbO(OH)_2(tart)]^-$ [15] or $[NbO_2(tart)]^-$ [12]. The niobium tartrate complexes form mixed ligand complexes of the composition Nb: tart: PAR = 1:1:1 [11,14,15,17] or 1:1:2 [17]. The complexes have maximum absorption at 550 nm with a molar absorptivity ($l\ mol^{-1}\ cm^{-1}$) of 39 000 [15] or 37 800 [11]. Belcher et al. [11] found that at pH 6.0 the colour system is less likely to be affected by small fluctuations of pH.

The aim of the work presented here was to develop an accurate differential spectrophotometric method for the determination of 10–30% niobium in niobium potassium oxyfluorides and similar materials, with a relative standard deviation of ca. 0.003. These materials are applied in the preparation of high-purity niobium by electrolysis [19]. Accurate monitoring of residual niobium in the melts after electrolysis is of importance.

The optimum conditions for accurate niobium determination were investigated by designed experiments. The problem was to establish conditions for complex formation which would provide a molar absorptivity of around 10 000 $l\ mol^{-1}\ cm^{-1}$. It is then possible to provide an accurate differential spectrophotometric determination of niobium in complex samples [20]. For this purpose, the absorbance of the niobium complex was investigated in relation to the concentrations of PAR and tartrate.

EXPERIMENTAL

Apparatus and reagents

Absorbances were measured in a double-beam spectrophotometer (Specord M40; Carl Zeiss Jena); the accuracy of the wavelength setting was ± 0.05 nm. The pH values were measured (± 0.002) with a MV 85 meter (Präcitronic Dresden) and a glass electrode (GB-50-N; Forschungsinstitut Meinsberg).

All chemicals used were of analytical grade; PAR was Reanal grade.

Niobium stock solution. Fuse 0.07153 g of stoichiometric high-purity Nb_2O_5 with 1.5 g of potassium pyrosulphate and 1 ml of concentrated sulphuric acid in a platinum dish for 10 min and then evaporate the sulphuric acid to fumes. Extract the melt with 25 ml of 0.45 M ammonium tartrate on a hot plate, and transfer this solution with 75 ml of hot water into a 500-ml beaker. Adjust to pH 6.10 (pH meter) with ammonia solution. Transfer the solution to a 1-l volumetric flask with 0.1 M ammonium tartrate at pH 6.10 and dilute with this solution to the mark. The stock solution contains 50 $\mu g\ ml^{-1}$ niobium and is stable for about 10 days in a refrigerator.

Study of the effect of pH

The range of existence of each type of mixed ligand complexes of metal ions is generally small [11,13,21] and depends on the ligand concentration in the solution. Therefore the possible pH range for the Nb/tartrate/PAR complexes was studied at two concentrations of tartrate ions (0.0226 and 0.226 M). The niobium concentration was 1.076×10^{-4} M (500 μg Nb in 50 ml) and the PAR concentration was 5×10^{-4} M. The procedure was as follows.

Niobium stock solution (10 ml) was placed in 100-ml beakers, and 0.13 or 10.3 ml of 1 M ammonium tartrate was added. The pH was adjusted to different values in the range 3–7 with tartaric acid or ammonia solution. With the high ammonium tartrate concentration at pH 3–5, potassium hydrogentartrate precipitated; these solutions were rejected. The remaining solutions were left for 24 h to attain equilibrium of complex formation. The pH was then checked and the solutions were transferred to 50-ml volumetric flasks; 2 ml of 1.25×10^{-2} M of PAR solution in methanol was added and the solutions were diluted to volume with tartaric acid or ammonia solution of corresponding pH. After 1 h, the excess of PAR was extracted into 50 ml of chloroform. The PAR was re-extracted from the chloroform phase by 50 ml of 0.0226 or 0.226 M of tartrate, as appropriate. These re-extracts were applied as the blanks for the absorbance measurements.

The results are shown in Fig. 1. The shape of the pH curve with 0.0226 M tartrate solution (curve 1) is the same as the shapes reported earlier [11,17]. With the 0.226 M tartrate, curve 2 was obtained. The pH range within which

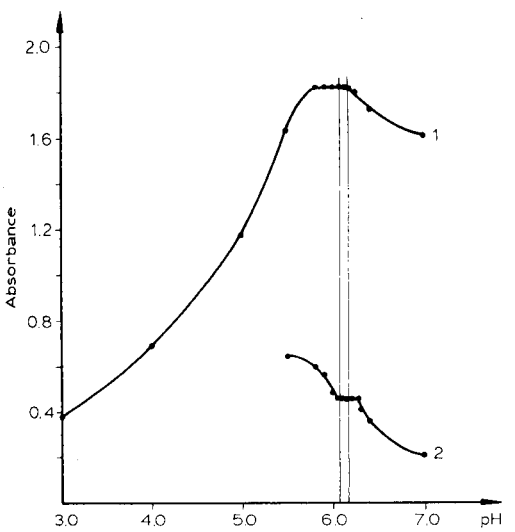

Fig. 1. Relation between the absorbance of the niobium complex and the pH value (1) 0.0226 M tartrate; (2) 0.226 M tartrate. Conditions: 1.076×10^{-4} M Nb, 5.0×10^{-4} M PAR, 0.5-cm cuvettes.

TABLE 1

Preparation of a set of solutions for the differential photometric measurements

Solution	Niobium solution (ml)	Tartrate solution (ml)	Absorbance
Blank, C_{10}	11.50	10.15	$A_{10} \approx 1.0$
Standard **I**, C_I	15.00	9.8	$A_{21,I} \approx 0.3$
Sample, C_p	18.00	9.5	$A_{21,p} \approx 0.57$
Standard **II**, C_{II}	20.00	9.3	$A_{21,II} \approx 0.7$

the colour system is independent of pH value, common for both tartrate concentrations, lies between 6.05 and 6.15; therefore a pH of 6.10 ± 0.01 was maintained exactly in all experiments.

Recommended method for the determination of niobium

Preparation of standard and sample solutions. Weigh the sample containing about 25 mg Nb, and a standard from 0.07153 g of pure Nb_2O_5, on a microbalance in platinum crucibles. Prepare the solutions as described above for the preparation of the niobium stock solution. Transfer the sample solution to a 500-ml volumetric flask and the standard solution to a 1-l flask. Dilute the solutions to volume with 0.1 M ammonium tartrate at pH 6.10 ± 0.1.

Spectrophotometric procedure. Transfer aliquots of the sample and the standard solution, as well as the volumes of 1 M ammonium tartrate at pH 6.10, to 50-ml beakers, as shown in Table 1. Add to these beakers 10 ml of 0.02 M EDTA adjusted to pH 6.10. Check the pH after 24 h, and if necessary adjust it to 6.10. Transfer the solutions to 50-ml volumetric flasks with water adjusted to pH 6.10, add 2 ml of 7×10^{-3} M PAR, and dilute the solutions to volume with water at pH 6.10. After 1 h, measure the absorbance of the standard and sample solutions at 550 nm in 1-cm cuvettes against the blank solution containing 575 μg of niobium (Table 1). The niobium concentration in the sample aliquots is calculated from the equation

$$C_p = [A_{21,p}(C_{II} - C_I) - C_{II} A_{21,I} + C_I A_{21,II}]/A_{21,II} - A_{21,I}$$

DESIGNED EXPERIMENTS

Experimental design was used to establish the conditions providing minimum error in the niobium determination. For differential spectrophotometry, this means that the molar absorptivity of the complex must be between 6000 and 18 000 l mol^{-1} cm^{-1} [20].

TABLE 2

Levels of factors

Coded levels	Levels of factors		
	x_1 C_{tart} (M)	x_2 C_{PAR} (M)	$x_3 V_{CHCl_3}$ (ml)
+1	0.226	2.13×10^{-3}	50
0	0.124	1.27×10^{-3}	30
−1	0.0226	4.1×10^{-4}	10

TABLE 3

Full factorial design and results for the relationship $y=f(C_{tart}, C_{PAR}, V_{CHCl_3})$

N	n_j[a]	Levels of factors			$\bar{y}$	$\hat{y}$
		x_1	x_2	x_3		
1	2	+1	+1	+1	0.1715	0.1791
2	2	+1	+1	−1	0.2535	0.2459
3	2	+1	−1	+1	0.0865	0.0789
4	2	+1	−1	−1	0.1290	0.1366
5	2	−1	+1	+1	0.3860	0.3784
6	2	−1	+1	−1	0.3985	0.4061
7	2	−1	−1	+1	0.3490	0.3566
8	2	−1	−1	−1	0.3830	0.3754
9	4	0	0	0	0.2668	0.2668

[a] n_j is the number of test repetitions.

The absorbance at 550 nm in a 0.1-cm cuvette was chosen as the parameter for optimization (dependent variable). The factors (independent variables) chosen were the concentration of tartrate (x_1), the concentration of PAR (x_2) and the volume of chloroform (x_3). The levels of the factors are given in Table 2.

In the system studied, the signal is produced by niobium complex formation during several chemical reactions. In such cases, the empirical relationship between the dependent and independent variables can be approximated by a quadratic polynomial [22]. The full factorial design at three levels [23] and the results obtained are given in Table 3. The following calculated polynomial did not describe the empirical relationship adequately (F-test):

$$\hat{y}=0.2668-0.1092x_1+0.0328x_2-0.0214x_3+0.0196x_1x_2 -0.0098x_1x_3-0.0023x_2x_3+0.0029x_{ii}^2 \quad (1)$$

with $\hat{S}_s^2 = 5.9 \times 10^{-5}$, $\hat{S}_f^2 = 4.6 \times 10^{-4}$ and $F_{calc} = 86 > F_{tab}$ ($P = 0.99$, $f_1 = 1$, $f_2 = 11$) $= 9.7$.

Elimination of the two smallest terms of the polynomial enhanced the calculated Fisher criterion ($F_{calc} = 106$).

According to earlier work [22], the adequacy of model 1 can also be estimated by graphic representation of the response surface. In the case of three independent variables, the response surface of model 1 lying in a four-dimensional space must be converted to a response body lying in a three-dimensional space by setting one of the independent variables to ± 1, for example $x_1 = \pm 1$. The shape of the response surfaces $y = f(x_2, x_3)$, $x_1 = \pm 1$ can only be recognized if the $\bar{y}$ values in the centres of these surfaces are known. They were found to be $\bar{y}_{1+}$ ($x_1 = +1, x_2 = 0, x_3 = 0$) $= 0.161$ and $\bar{y}_{1-}$ ($x_1 = -1, x_2 = 0, x_3 = 0$) $= 0.376$.

The corresponding response body is shown in Fig. 2. The lower response surface ($x_1 = +1$) is diagnosed as a saddle-shape surface, because one of its diagonals is concave and the other is convex. Meanwhile the upper response surface ($x_1 = -1$) is a plane. This state of affairs can be caused by a change in the empirical relationship within the factor space and can explain the inadequacy of model 1 [22]. The two polynomials describing the two response surfaces in Fig. 2 are calculated from eqn. 1 under the conditions $x_1 = \pm 1$:

$$\hat{y}_{1+} = 0.1576 + 0.0524x_2 - 0.0312x_3 - 0.0023x_2x_3 + 0.0029x_{ii}^2 \quad (2)$$

$$\hat{y}_{1-} = 0.3760 + 0.0132x_2 - 0.0116x_3 - 0.0023x_2x_3 + 0.0029x_{ii}^2 \quad (3)$$

The coefficients of the free polynomial members ($\hat{y}$ values at $x_2 = x_3 = 0$) correspond very well with the experimental values of $\bar{y}_{1+}$ and $\bar{y}_{1-}$. The same is true for $\hat{y}$ and $\bar{y}$ for all the observations of the design (Table 3). Accordingly, model 1 can be used for interpretation of the effects in the system studied.

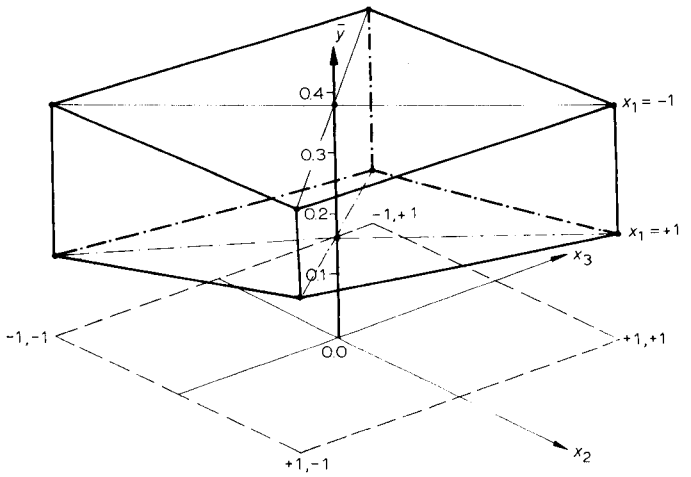

Fig. 2. Empirical response body for the relationship $y = f(x_2, x_3)$ under the conditions $x_1 = \pm 1$.

In the solutions studied, the absorbance of the coloured complex depends strongly on the tartrate concentration; large concentrations destroy the coloured complexes. This is reflected in the large distance between the two response surfaces in Fig. 2.

The joint effect $x_1 \times x_2 = C_{tart} \times C_{PAR}$, which is responsible for the different distances between the two response surfaces in several parts of the factor space (Fig. 2), increases the concentration of the coloured complex. This means that the mixed ligand complex will be formed even in the presence of only small amounts of PAR, as has been pointed out previously [15]. The weak joint effect $x_1 \times x_3$ can be considered analogously to the joint effect $x_1 \times x_2$.

The results obtained make it possible to establish the conditions under which the molar absorptivity (ϵ) required for optimization can be achieved. The best conditions relate to observation 3, (Tables 3 and 4) with $\epsilon = 8040\ l\ mol^{-1}\ cm^{-1}$. Because the concentration of the coloured complex depends heavily on the concentrations of tartrate and PAR, it is necessary to take this into account in the analytical procedure.

COMPLEX FORMATION IN THE Nb/TARTRATE/PAR SOLUTIONS

The above results enable additional information to be obtained about complex formation. The conditional stability constant of the mixed ligand complex of niobium was calculated for each observation point in the design (Table 4). For this purpose, the dissociation and formation constants of the starting and intermediate compounds available in the literature were applied.

In the pH range 4–12, PAR exists as $HPAR^-$ with $\lambda_{max} = 415$ nm [14,15].

TABLE 4

Calculated conditional stability constants for the niobium complex

N	C_{tart}/C_{Nb}	C_{tart}/C_{PAR}	C_{PAR}[a]$/C_{Nb}$	ϵ_{exp}	pH_{eq}	K	$\bar{K}$
1	2100	265	7.9	15 940	6.75	2.60×10^{15}	
2	2100	121	17.4	23 560	6.64	1.19×10^{15}	
3	2100	1378	1.5	8 040	6.58	1.72×10^{15}	$(1.7 \pm 0.7) \times 10^{15}$
4	2100	626	3.4	11 990	6.57	1.21×10^{15}	
5	200	26	7.9	35 875	7.80	6.96×10^{20}	
6	200	12	17.4	37 035	7.70	3.25×10^{20}	$\approx 5 \times 10^{20}$
7	200	134	1.5	32 435	7.00	1.17×10^{19}	
8	200	61	3.4	35 595	6.91	4.09×10^{18}	
9	1150	202	5.7	24 795	6.93	5.10×10^{16}	

[a]Concentration of PAR in the aqueous phase.

At pH $\geqslant 6$, tartaric acid is completely dissociated ($pK_{a1}=2.80$, $pK_{a2}=3.96$ [24]). It was shown that the formation of the mixed ligand complex did not lead to a change of pH in the system.

If it can be assumed in accordance with earlier work that both $[NbO(tart)_2]^-$ [13–15] and [NbO(tart) (HPAR)] [11,14–17] exist, then the equation

$$K=[NbO(tart)\ (HPAR)]\ [tart^{2-}]/[NbO(tart)_2^-]\ [HPAR^-] \qquad (4)$$

can be used for the calculation of the conditional stability constant of the mixed ligand complex. The equilibrium concentration of the complex [NbO (tart) (HPAR)] was calculated for each observation point from the following equation:

$$[NbO(tart)\ (HPAR)]=C_{Nb}\ \epsilon_{exp}/\epsilon_{max} \qquad (5)$$

where $C_{Nb}=1.076\times10^{-4}$ mol l^{-1} (the starting concentration of niobium); $\epsilon_{max}=38\ 500$ l mol^{-1} cm^{-1}, the molar absorptivity of the coloured complex calculated from the present results by extrapolation of the complex absorbance to the point where $C_{Nb}\approx C_{tart}$; and ϵ_{exp} is the conditional molar absorptivity calculated at each observation point (Table 4).

The equilibrium concentrations of the ions $NbO(tart)_2^-$, $HPAR^-$ and $tart^{2-}$ were calculated by means of the stability constants of the following equations:

H_3PAR^+	$\rightleftharpoons$	$H^+ + H_2PAR$	$K_1=7\times10^{-4}$ [15]
H_2PAR	$\rightleftharpoons$	$H^+ + HPAR^-$	$K_2=2.5\times10^{-6}$ [15]
H_2PAR_{aq}	$\overset{CHCl_3}{\rightleftharpoons}$	H_2PAR_{org}	$K_3=1.5$ (this work)
$HPAR^-$	$\rightleftharpoons$	$H^+ + PAR^{2-}$	$K_4=1.25\times10^{-12}$ [15]
H_2tart	$\rightleftharpoons$	$H^+ + Htart^-$	$K_5=1.6\times10^{-3}$ [24]
$Htart^-$	$\rightleftharpoons$	$H^+ + tart^{2-}$	$K_6=1.1\times10^{-4}$ [24]
$NbO(tart)_2^-$	$\rightleftharpoons$	$NbO(tart)^+ + tart^{2-}$	$K_7=1.4\times10^{-8}$ [15,18]
$NbO(tart)^+$	$\rightleftharpoons$	$NbO^{3+} + tart^{2-}$	$K_8=7\times10^{-26}$ [15,18]
$NbO(OH)_3$	$\rightleftharpoons$	$NbO(OH)_2^+ + OH^-$	$K_9=2.5\times10^{-15}$ [25]
$NbO(OH)_2^+$	$\rightleftharpoons$	$NbO(OH)^{2+} + OH^-$	$K_{10}=1.3\times10^{-20}$ [25]
$NbO(OH)^{2+}$	$\rightleftharpoons$	$NbO^{3+} + OH^-$	$K_{11}=6.3\times10^{-26}$ [25]

The pH values obtained in the solutions after extraction of the excess of PAR are given in Table 4, as are the calculated constants.

Elinson and Mal'tseva [15] used a solution with 2×10^{-5} M niobium, 2×10^{-2} M tartrate, 2×10^{-5} M PAR and pH 4, and calculated a stability constant of

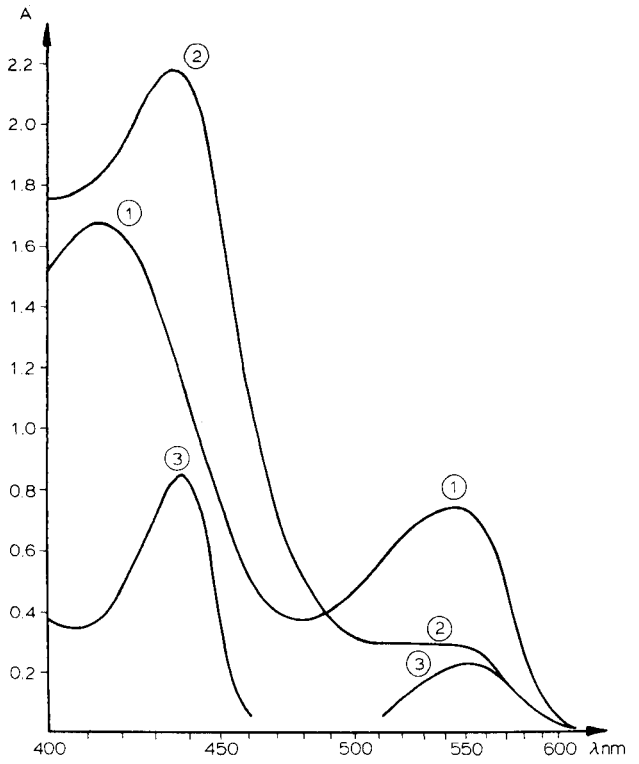

Fig. 3. Absorption spectra of the mixed-ligand niobium complexes measured against the re-extracted tartrate/PAR solution in 0.2-cm cuvettes: (1) 4.1×10^{-4} M PAR; (2) 2.13×10^{-3} M PAR; (3) blank solution as (2) but with 1-cm cuvettes.

$K = 1.7 \times 10^{21}$, which is similar to the value of $K \approx 5 \times 10^{20}$ calculated for observation points 5 and 6 (Table 4). The differences between the stability constants calculated at several points of the factor space indicates that, with different concentrations of the ligands, several species take part in the complex formation or that several complexes are formed. To investigate this further, the absorption spectra of the complexes were recorded. At a low concentration of PAR (observation points 3, 4, 7 and 8), the spectrum showed maximum wavelengths at 414 nm for $HPAR^-$ and at 547.6 nm for the niobium complex (spectrum 1, Fig. 3). With a 5-fold higher concentration of PAR (observation points 1, 2, 5 and 6), the spectrum (2, Fig. 3) had an absorbance maximum at 437.4 nm for $HPAR^-$ and a broad shoulder at 500–560 nm. Compensation of the $HPAR^-$ absorption in this wavelength range by variation of the optical path length of the cuvettes allows selection of an absorption peak at 552.5 nm (spectrum 3).

The form of PAR with $\lambda_{max} = 437.4$ nm is probably the dimeric form $(HPAR^-)_2$; this suggestion is compatible with the bathochromic shift of the

maximum absorption by 23 nm compared to the monomeric $HPAR^-$ form. This dimeric form apparently takes part in the formation of mixed ligand complexes and causes the bathochromic shift of 5 nm compared with spectrum 1. This last observation agrees with earlier results [17], where the Nb/PAR ratio at higher PAR concentrations was found by the method of equilibrium shift to be 1:2.

Table 4 shows that there are correlations between the C_{tart}/C_{Nb} ratio and the value of the stability constant. This means that, besides the dimerization of PAR, the composition of the niobium tartrate complexes in the starting solutions influences the value of the stability constant. From the literature, the Nb/tartrate ratio can be 1:1 or 1:2 [12,13,15].

The change of the stoichiometry of the complexation reaction responsible for the differences in the stability constants is reflected by the different shapes of the two response surfaces, $y=f(x_2, x_3)$, $x_1=\pm 1$, and is finally the reason for the inadequacy of model 1. These conclusions conjoin to indicate a change in the empirical relationship in the investigated factor space. A better approximation by using several models in a larger factor space was not attempted because it was not necessary for the optimization problem.

The above results make it reasonable to assume the existence of mixed ligand complexes of niobium with the compositions Nb/tart/PAR = 1:1:1 and 1:1:2.

DIFFERENTIAL SPECTROPHOTOMETRIC DETERMINATION OF LARGE AMOUNTS OF NIOBIUM IN NIOBIUM/FLUORIDE MATERIALS

For the determination of the 10–30% niobium in mixtures of KF, NaF, LiF and K_2NbF_7, the conditions of observation point 3 (Tables 3 and 4) were chosen, except that extraction was not included. Interferences from possible impurities producing an absorbance with PAR were eliminated by adding EDTA [11]. Fluoride interferes seriously with the niobium determination but was removed during the fusion with potassium pyrosulphate.

When the procedure recommended in the Experimental section was followed, the relative standard deviation for the determination of 900 μg of niobium in a solution was 0.0025 ($n=8$). To estimate the accuracy of the results, the stoichiometric compound K_2NbF_7 with an expected niobium content (μ_0) of 30.55% was prepared four times and analysed. The mean value found was $30.48 \pm 0.08\%$ niobium ($P=0.95$, $f=3$). According to the t-test, $t_{calc} = [\,|\bar{x}-\mu_0|/S\,]\, n_j^{\frac{1}{2}} = 1.87 < t_{tab}(P=0.90, f=3) = 2.35$, thus the values of $\bar{x}$ and μ_0 belong to the same population.

The author is indebted to Dr. W. Kluge for useful discussion of some aspects of designed experiments and to Mrs. Ch. Kuentscher for assistance in experimental work.

REFERENCES

1 I.P. Alimarin, I.M. Gibalo and Tshin Guan-Zhun, Zh. Anal. Khim., 17 (1962) 60.
2 C.V. Banks, K.E. Burke, J.W. O'Laughlin and J.A. Thompson, Anal. Chem., 29 (1957) 995.
3 S.V. Elinson, S.B. Savvin, Yu.M. Dedkov and V.T. Tsvetkova, Zavod. Lab., 32 (1966) 654.
4 T.M. Malyutina, E.L. Futoryanskaja and F.A. Vinokurova, Zavod. Lab., 28 (1962) 540.
5 D.F. Wood and I.R. Scholes, Anal. Chim. Acta, 21 (1959) 121.
6 S.V. Elinson, Yu.M. Dedkov and V.T. Tsvetkova, Zh. Anal. Khim., 31 (1976) 1372.
7 N.T. Sizonenko, L.A. Egorova and A.K. Timchenko, Zh. Anal. Khim., 34 (1979) 2182.
8 G. Ackermann and S. Koch, Talanta, 9 (1962) 1015.
9 V.I. Kurbatova, G.N. Emashova and N.V. Zobnina, Standartnye Obrazcy v Chernoi Metallurgii, Metallurgiya, Moscow, 3 (1974) 92.
10 E.N. Pashchenko, L.A. Vasil'eva, V.F. Mal'tsev and N.P. Volkova, Zavod. Lab., 39 (1973) 1297.
11 R. Belcher, T.V. Ramakrishna and T.S. West, Talanta, 10 (1963) 1013.
12 G. Ackermann and S. Koch, Z. Chem., 9 (1969) 345.
13 I.P. Alimarin and O.M. Petrukhin, Zh. Anal. Khim., 7 (1962) 401.
14 S.V. Elinson, Spektrofotometriya Niobiya i Tantala, Atomizdat, Moscow, 1973.
15 S.V. Elinson and L.S. Mal'tseva, Zh. Anal. Khim., 24 (1969) 1524.
16 S.V. Elinson, L.I. Pobedina and A.T. Rezova, Zavod. Lab., 31 (1965) 1434.
17 F.I. Lobanov, G.K. Nurtaeva and I.M. Gibalo, Zh. Neorg. Khim., 23 (1978) 982.
18 B.I. Nabivanec, Zh. Neorg. Khim., 11 (1966) 2732.
19 J.I. Mönch, K. Fischer, G. Enderlein, O. Grossmann, M. Kubsch, C. Rodig, and U. Stahlberg, 6th Int. Symp. High-Purity Materials in Science and Technology, Dresden, 1985, Poster Abstracts, Part I, p. 54.
20 O. Grossmann, Fresenius' Z. Anal. Chem., 320 (1985) 229; 321 (1985) 422.
21 S. Koch, Z. Chem., 22 (1982) 317.
22 O. Grossmann, Anal. Chim. Acta, 186 (1986) 185.
23 R.M. De Baun, Technometrics, 1 (1959) 1.
24 J. Kragten, Atlas of Metal-Ligand Equilibria in Aqueous Solution, Horwood, Chichester, 1978, p. 779.
25 A.K. Babko, V.V. Lukachina and B.I. Nabivanec, Zh. Neorg. Khim., 8 (1963) 1839.

Analytica Chimica Acta, 203 (1987) 79-83
Elsevier Science Publishers B.V., Amsterdam — Printed in The Netherlands

Short Communication

A CONCENTRATION CELL WITH AN ION-SELECTIVE MEMBRANE AS JUNCTION AND ITS APPLICATION TO COPPER DETERMINATION

RYSZARD STĘPAK

Jagiellonian University, Faculty of Chemistry, Karasia 3, 30-060 Kraków (Poland)

(Received 23rd March 1987)

Summary. A concentration cell with a copper selenide ion-selective membrane as the junction between the solutions is described. Copper (8×10^{-4}-4×10^{-5} M) is determined by direct potentiometry, a standard addition method or differential potentiometry. The procedure is very simple, as is preparation of the cell. Relative standard deviations are around 1%.

Copper ion-selective electrodes are widely used for the determination of copper by direct potentiometry and potentiometric titrations [1,2]. In this communication, a concentration cell with an ion-selective membrane of the copper selenide type between the solutions is described for copper determinations.

Theory

The cell consists of two open polyethylene compartments separated by a wall in which the ion-selective membrane is sealed. Compartment 1 contains a standard copper solution, with concentration C_0; compartment 2 contains an unknown copper solution, C_x. Two saturated calomel electrodes (SCE) immersed in these solutions complete the electrochemical cell:

$$\text{SCE 1} \;\|\; \begin{matrix}\text{standard}\\ \text{solution } C_0\end{matrix} \;|\; \begin{matrix}\text{CuSe-type}\\ \text{membrane}\end{matrix} \;|\; \begin{matrix}\text{unknown}\\ \text{solution } C_x\end{matrix} \;\|\; \text{SCE 2}$$

Of course, if one compartment of the cell is sealed, the assembly is identical with a conventional ion-selective electrode. However, little attention has been paid to the advantages of this kind of open concentration cell and its application in chemical analysis. The following discussion and equations will refer to copper specifically, but the assembly is general and should be applicable for other determinations.

It is assumed that the two SCE's (or other reference electrodes) used have nearly identical characteristics so that there is only a small or zero (asymmetry) potential, ΔE_{SCE}, across the SCE pair when the solutions in both com-

0003-2670/87/$03.50

partments are of the same concentration. The ionic strength of the solutions in both compartments is assumed to be the same. Under these conditions, the e.m.f. of the cell is given [1–3] by

$$E = S \log C_x/C_0 \tag{1}$$

where S is the slope factor (theoretically $2.303RT/2F$).

Direct potentiometry. When one compartment of the cell contains a standard copper solution and the second compartment the unknown solution, the sought concentration of copper is calculated from Eqn. 1. The slope can be calculated theoretically or found experimentally.

Standard addition method. If compartment 1 contains V_0 ml of the standard solution C_0 and compartment 2 contains V_0 ml of the unknown solution C_x, then the e.m.f. of the cell is

$$E = S \log [(V_0C_x/V_0)/(V_0C_0/V_0)] \tag{2}$$

When V_x ml of another standard copper solution with concentration C is added to the solution in compartment 2 and the same volume V_x ml of inert solution (e.g., potassium nitrate) containing no copper but at the same ionic strength is added to the solution in compartment 1, then the e.m.f. of the cell is given by

$$E = S \log \{[(V_0C_x + V_xC)/(V_0 + V_x)]/[V_0C_0/(V_0 + V_x)]\} \tag{3}$$

Rearrangement and linearization by Gran's method [4] gives

$$10^{E/S} = (C_x/C_0) + (V_xC/V_0C_0) \tag{4}$$

This equation is linear in one unknown because S can be evaluated separately. A plot of $10^{E/S}$ vs. V_x ml is a straight line with slope C/V_0C_0 and intercept C_x/C_0. The C_x/C_0 value can also be found from the intercept of a linear least-squares fit of the data.

Differential potentiometry. Differential potentiometry (also known as null-point potentiometry) [5] with conventional concentration cells has been used successfully for determinations of silver [6], chloride [7–11] and fluoride [12,13]. The method seems especially suitable for copper determination in the nonlinear region of the cell response (i.e., when the slope factor S is not constant) so that the above methods cannot be applied. Differential potentiometry consists simply of adding an inert solution containing no analyte (here, 0.1 M potassium nitrate) to compartment 1 containing V_0 ml of standard copper solution (C_0) and the other standard copper solution (C) to compartment 2 containing V_0 ml of unknown solution C_x ($C_0 > C_x$) until ΔE_{SCE} is reached. At

this point, the copper concentration in both compartments is the same. If V_e is the volume of standard copper solution C added, then C_x is given by

$$C_x = C_0 - V_e C / V_0 \quad (5)$$

Experimental

Apparatus. The cell assembly was made of two 30-ml polyethylene containers. In the middle of their common wall, a CuSe-type membrane, taken from a broken copper ion-selective electrode (type 29-17, Crytur, Czechoslovakia) was sealed. Two SCE's (Druopta, Czechoslovakia) were used to measure the membrane potential with a Meratronik V-540 (Poland) digital voltmeter reading to 0.01 mV. When both compartments contained the same copper solution, the asymmetry potential ΔE_{SCE} (about 1 mV) was stable during experiments but often changed overnight, and had to be measured daily. All the potentials given below have been corrected for ΔE_{SCE}.

Microliter quantities of standard and potassium nitrate solutions were added from Plastomed (Poland) micropipets.

The membrane manufacturer suggests the limit of linear response for the CuSe-type membrane as 10^{-4} M. The S value found experimentally was 29.00 mV/decade at 20°C in the concentration range 10^{-1}–8×10^{-4} M, which is in good agreement with the theoretical value, and 28.5 mV/decade for the range 8×10^{-4}–10^{-4} M. These values were used in the C_x calculations.

Reagents. All chemicals were of analytical grade. Copper(II) nitrate trihydrate was used to prepare the standard 0.1 M copper solution. More dilute solutions were prepared by serial dilution. All solutions were prepared with deionized water. Constant 0.1 M ionic strength was maintained in all solutions with 1 M potassium nitrate.

Determination of copper by direct potentiometry. The standard copper solution C_0 was placed in compartment 1 and unknown solution C_x in compartment 2. The e.m.f. of the cell was measured and C_x calculated from Eqn. 1.

Determination of copper by the standard addition method. A portion (V_0 ml) of the unknown solution was placed in compartment 2 and V_0 ml of the standard copper solution C_0 in compartment 1. Small portions (0.07 ml) of standard copper solution C (with ionic strength 0.1 M) were added to compartment 2 and 0.1 M potassium nitrate to compartment 1. After each addition, the e.m.f. was recorded. This procedure kept the ionic strength of the solutions the same. Usually, 5–7 points were used to obtain a linear plot of $10^{E/S}$ vs. V_x ml of standard solution C added. A linear least-squares fit was used to calculate the intercept from which C_x was obtained.

Differential potentiometry. The procedure was the same as above, but the additions of standard copper and potassium nitrate solutions were continued until the potential reached the ΔE_{SCE} value. The unknown copper concentration C_x was calculated from Eqn. 5.

TABLE 1

Results obtained for the determination of different copper solutions

Cu^{2+} concentration taken (M)	Cu^{2+} found[a] (M)		
	Direct potentiometry	Standard addition	Differential potentiometry
8×10^{-4} [b]	8.021×10^{-4} (4.93×10^{-6})	8.012×10^{-4} (1.85×10^{-6})	8.023×10^{-4} (5.78×10^{-6})
4×10^{-4} [c]	4.009×10^{-4} (2.70×10^{-6})	3.998×10^{-4} (1.89×10^{-6})	4.090×10^{-4} (4.30×10^{-6})
4×10^{-5} [d]	—	—	4.03×10^{-5} (1.3×10^{-6})

[a]Each result is the mean of 6 or 7 determinations; standard deviations are in parentheses. [b]$V_0=20$ ml, $C_0=10^{-3}$ M, $C=10^{-2}$ M, $S=29.00$ mV/decade. [c]$V_0=20$ ml, $C_0=8\times10^{-4}$ M, $C=10^{-2}$ M, $S=28.50$ mV/decade. [d]$V_0=20$ ml, $C_0=10^{-5}$ M, $C=10^{-4}$ M.

Results and discussion

Copper was successfully determined with the concentration cell with the CuSe-type membrane as the junction between standard and unknown copper solutions, as shown in Table 1. The results obtained show good accuracy and precision. The cell assembly is cheap and easy to build in the laboratory. Both surfaces of the membrane can be polished when necessary. The measurements are simple, and the concentration can be measured precisely without reference to a calibration curve.

The concentration cell described has the advantages of both ion-selective electrodes and conventional concentration cells. Concentration cells with other ion-selective membranes are being examined.

REFERENCES

1 P.L. Bailey, Analysis with Ion-Selective Electrodes, Heyden, London, 1978.
2 K. Cammann, Working with Ion-Selective Electrodes, Springer, Berlin, 1979.
3 J. Koryta, J. Dvořák and V. Boháčková, Lehrbuch der Elektrochemie, Springer, Berlin, 1975.
4 G. Gran, Analyst, 77 (1952) 661.
5 IUPAC Classification and Nomenclature of Electroanalytical Techniques, Pure Appl. Chem., 45 (1976) 81.
6 R.A. Durst and J.K. Taylor, Anal. Chem., 39 (1967) 1374.
7 N.H. Furman and G.H. Low, J. Am. Chem. Soc., 57 (1935) 1585, 1588.

8 W.J. Blaedel, W.B. Lewis and J.W. Thomas, Anal. Chem., 24 (1952) 509.
9 H.V. Malmstad, E.R. Fet and J.D. Winefordner, Anal. Chem., 28 (1956) 1878.
10 H.V. Malmstad and J.D. Winefordner, Anal. Chim. Acta, 20 (1959) 283.
11 M.I.D. Brand and G.A. Rechnitz, Anal. Chem., 42 (1970) 1172.
12 R.A. Durst and J.K. Taylor, Anal. Chem., 39 (1967) 1483.
13 R.A. Durst, Anal. Chem., 39 (1967) 937.

Analytica Chimica Acta, 203 (1987) 85–89
Elsevier Science Publishers B.V., Amsterdam — Printed in The Netherlands

Short Communication

SYNTHESIS OF A FLUORESCENT 14-CROWN-4 DERIVATIVE BEARING A PROTON-DISSOCIABLE MOIETY AND ITS USE FOR SELECTIVE LITHIUM-ION EXTRACTION

KEIICHI KIMURA, SHIN-ICHI IKETANI and TOSHIYUKI SHONO

Department of Applied Chemistry, Faculty of Engineering, Osaka University, Yamada-oka, Suita, Osaka 565 (Japan)

(Received 20th March 1987)

Summary. The fluorescent 14-crown-4 derivative possesses a *p*-(1,8-naphthalenedicarboximido)phenol moiety as the proton-dissociable fluorophore; its synthesis is described. Highly selective extraction of lithium is achieved with the crown ether, based on a proton/metal ion-exchange mechanism. Extraction is accompanied by significant changes in the absorption and fluorescence spectra of the organic phase. Extraction equilibrium constants for the lithium and sodium ions are evaluated, the Li^+/Na^+ selectivity ratio being 200; other alkali metal ions were not extracted. The Li^+ extraction quenched the fluorescence intensity of the crown ether, in correlation with the initial cation concentration in the aqueous phase.

Chromogenic crown ethers that have easily ionizable moieties on the chromophore are useful reagents for extraction-spectrophotometric determination of alkali and alkaline-earth metal ions [1]. The crown ethers, when proton-dissociated, are able to form complexes with particular cations in which positive charges of the crown-complexed cations are compensated intramolecularly by the anionic sites produced on the chromophore and can thus extract the cations selectively from an alkaline aqueous phase to an organic phase. Because the absorption spectra of proton-dissociable chromogenic crown ethers are generally changed drastically by the proton dissociation followed by the cation complex formation, the crown ethers also serve as spectrophotometric reagents after the selective cation extraction. Also, when proton-dissociable fluorophores are incorporated into the crown ether rings, the resulting fluorescent crown ethers are candidates for extraction-fluorimetric reagents for particular cations [2,3].

Chromogenic 14-crown-4 (1,4,8,11-tetraoxacyclotetradecane) derivatives incorporating nitrophenol- and azophenol-type chromophores are quite promising as extraction-spectrophotometric reagents for lithium [4,5]. In this com-

0003-2670/87/$03.50

munication, the synthesis of a new 14-crown-4 derivative containing a *p*-(1,8-naphthalenedicarboximido)phenol moiety is described and its applicability to the extraction, spectrophotometry and fluorimetry of lithium is assessed.

Experimental

Synthesis of the fluorescent crown ether. The fluorescent 14-crown-4 (**3**), 6-dodecyl-6-[2-hydroxy-5-(1,8-naphthalenedicarboximido)benzyl]-1,4,8,11-tetraoxacyclotetradecane, was synthesized by the following reaction scheme:

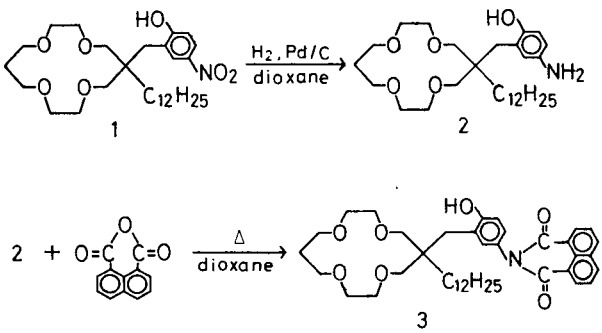

Crown *p*-nitrophenol **1** was prepared as described elsewhere [5]. A dioxane solution (150 ml) of **1** (0.2 mmol) and 5% palladized carbon (1 g) were placed in a glass autoclave. Hydrogenation to the corresponding crown *p*-aminophenol **2** was achieved under a hydrogen pressure of 4 kg cm^{-2} at room temperature for 9 h with mechanical stirring. The catalyst was filtered off and washed with dioxane. The filtrate was concentrated to about 50 ml. Compound **2** was subjected to the subsequent reaction without isolation because of its instability in air. To the dioxane solution (50 ml) of **2** (ca. 0.2 mmol) was added a dioxane solution (50 ml) of 1,8-naphthalic anhydride (0.2 mmol) dropwise under a nitrogen atmosphere. The mixture was then refluxed for 4 h. The dioxane was evaporated off under a nitrogen atmosphere and thereafter the residue was heated for the conversion to the imide at 120°C for 4 h. Chloroform and water were added to the residue and the chloroform phase was separated. Evaporation of the chloroform afforded a crude product, which was purified by preparative reversed-phase liquid chromatography to yield a colorless solid of **3**. [Yield 34%; m.p. 91–92°C. I.r. (KBr) 3225, 1670, 1240, 1130, 1110 cm^{-1}. ^{1}H-N.m.r. (CCl_4): δ 0.84 (t, 3H, CH_3), 0.9–1.5 (m, 22H, $(CH_2)_{11}$), 1.5–1.9 (m, 2H, $(OCH_2)_2CH_2$), 2.42 (s, 2H, $PhCH_2$), 3.1–3.8 (m, 16H, OCH_2), 6.7–8.6 (m, 9H, aromatic H), 9.02 (s, 1H, OH). M.s. (M^+): 673. Found: 72.8% C, 8.35% H, 2.05% N; calcd. for $C_{41}H_{55}NO_7$: 73.1% C, 8.2% H, 2.1% N.]

Extraction and spectral measurements. For qualitative comparison of cation extractability, the extraction was tested at room temperature as follows. Equal

volumes (5 ml) of a crown ether solution in 1,2-dichloroethane and a metal chloride solution containing 2.2×10^{-2} M tetramethylammonium hydroxide (TMAOH) in water were placed in a stoppered centrifuge tube (1.5-cm diameter$\times$10-cm height). The concentrations were 7×10^{-5} M for the crown ether and 1 M for the metal salts, unless otherwise specified. The tube was vigorously shaken for 30 s. After centrifugation, 4 ml of the organic phase solution was transferred to a 1-cm quartz cell for spectral measurements. The absorption and fluorescence spectra were measured by using a Hitachi 340 spectrophotometer and a Hitachi M850 fluorescence spectrophotometer, respectively.

For the determination of extraction equilibrium constants, the extractions were done at 25°C, by varying the metal ion concentration (7×10^{-2}–7×10^{-1} M for Li^+ and 7×10^{-1}–1.5 M for Na^+); the crown ether concentration was kept constant (7×10^{-5} M for the Li^+ extraction and 1.75×10^{-3} M for the Na^+ one). The aqueous phase also contained 1.1×10^{-2} M TMAOH. A stoppered tube connected to a 1-cm quartz cell containing the dichloroethane and aqueous solutions (3 ml each) was shaken and then allowed to stand for 12 h in a water bath thermostated at 25°C. The absorption spectrum of the organic phase (the lower phase) was measured in situ in a cell holder held at 25°C. If the assumption is made that the crown ether (HL) forms only 1:1 cation (M^+)/crown (L^-) complexes (ML), the extraction equilibrium constant (K_{ex}) is defined as follows:

$$K_{ex} = ([ML]_o[H^+]_a)/([HL]_o[M^+]_a)$$

where subscripts "a" and "o" stand for the species of the aqueous and organic phase, respectively. The constants were evaluated graphically according to a previously reported procedure by absorption spectra [6].

Results and discussion

Cation extractions were examined for the crown ether bearing the ionizable fluorophore **3**, from an alkaline aqueous solution of the alkali metal ion into a 1,2-dichloroethane solution. Relatively high pH conditions in the aqueous phase were required for the cation extraction based on the H^+–M^+ exchange mechanism, because of the small acidity constant which was found to be $pK_a = 10.79$ in water/dioxane (50/50). Typical changes in the absorption spectra of the organic phase on cation extraction are shown in Fig. 1. Obviously, the appearance of the new peak around 412 nm is attributable to the cation extraction from the aqueous phase caused by complex formation between metal ions and the proton-dissociated species of **3**. The Figure shows that the crown ether can extract lithium ion selectively. Sodium ion was extracted only slightly and no significant extraction was attained for the other alkali metal ions. The excellent lithium selectivity of **3** is ascribed primarily to that of the 14-crown-4 ring itself [6,7]. Attempts were made to evaluate spectrophotometrically the extraction equilibrium constants of **3** for alkali metal ions on the assumption of

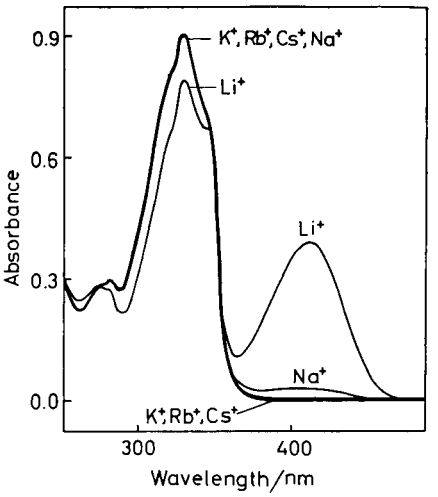

Fig. 1. Changes in the absorption spectra of the organic phase on extraction of alkali metal ions with ionizable 14-crown-4 derivative **3**. For conditions, see the experimental section.

the formation of 1:1 crown ether/cation complexes. The K_{ex} values for Li^+ and Na^+ are listed in Table 1, together with the absorption-spectral data. Values for the other alkali metal ions could not be obtained because of the poor extraction properties for these ions. The Li^+/Na^+ ratio in the K_{ex} value again indicates the extremely high lithium selectivity of the crown ether.

It is of much interest to see how the fluorescence spectrum of **3** varies on the cation extraction (Fig. 2). Definitely, the complex formation of **3** on extraction of lithium decreases the intensity of fluorescence derived from the naphthalenedicarboximido group. Very little change in the fluorescence spectra was observed for K^+, Rb^+, and Cs^+, which are not extractable with **3**. The fluorescence quenching produced by the cation extraction depends on the initial cation concentration in the aqueous phase, as demonstrated in Fig. 3.

Thus, the 14-crown-4 derivative possessing the proton-dissociable fluoro-

TABLE 1

Extraction equilibrium constants, ion-selectivity ratio and absorption-spectral data for fluorescent 14-crown-4 **3**

pK_{ex}[a]		Li^+/Na^+ selectivity	ϵ_{ML} (at λ_{max}, nm)[b]	
Li^+	Na^+		LiL	NaL
11.13	13.43	200	5330 (412)	5240 (413)

[a]In $ClCH_2CH_2Cl/H_2O$ system, at 25 °C. [b]In the organic phase.

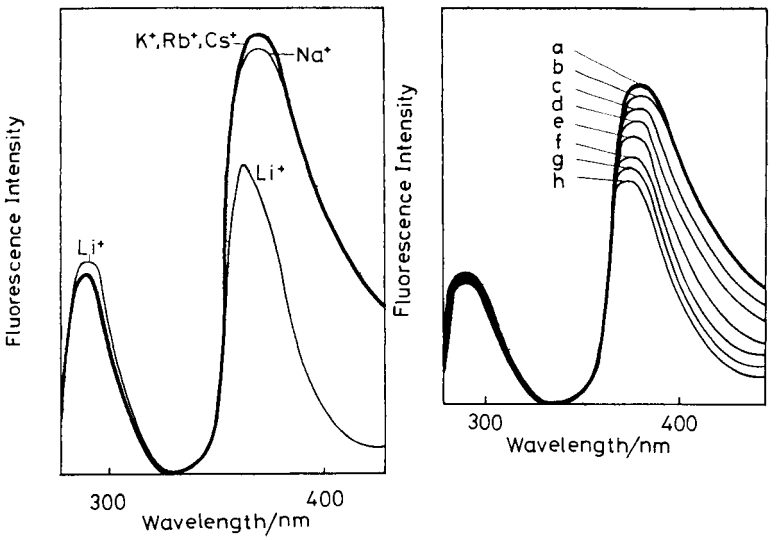

Fig. 2. Changes in the fluorescence spectra of the organic phase on cation extraction with fluorescent 14-crown-4 **3**. Conditions: $\lambda_{ex}=261$ nm; [crown ether] $=2.1\times10^{-4}$ M in 1,2-dichloroethane; other conditions as for Fig. 1.

Fig. 3. Dependence of fluorescence on initial cation concentration for aqueous phase on Li^+ extraction with **3**. [Li^+]: (a) none; (b) 2×10^{-3} M; (c) 4×10^{-3} M; (d) 7×10^{-3} M; (e) 2×10^{-2} M; (f) 4×10^{-2} M; (g) 7×10^{-2} M; (h) 1×10^{-1} M. Other conditions as for Fig. 2.

phore seems applicable to selective determinations of lithium by extraction spectrophotometry and fluorimetry.

REFERENCES

1 M. Takagi and K. Ueno, Top. Curr. Chem., 121 (1984) 39 (and references cited therein).
2 H. Nishida, Y. Katayama, H. Katsuki, H. Nakamura, M. Takagi and K. Ueno, Chem. Lett., (1982) 1853.
3 K. Nakashima, S. Nakatsuji, S. Akiyama, I. Tanigawa, T. Kaneda and S. Misumi, Talanta, 31 (1984) 749.
4 K. Kimura, M. Tanaka, S. Kitazawa and T. Shono, Chem. Lett., (1985) 1239.
5 K. Kimura, M. Tanaka, S. Iketani and T. Shono, J. Org. Chem., 52 (1987) 836.
6 S. Kitazawa, K. Kimura, H. Yano and T. Shono, J. Am. Chem. Soc., 106 (1984) 6978.
7 B.P. Czech, D.A. Babb, B. Son and R.A. Bartsch, J. Org. Chem., 49 (1984) 4805.

Analytica Chimica Acta, 203 (1987) 91-92
Elsevier Science Publishers B.V., Amsterdam — Printed in The Netherlands

Short Communication

COMPLEXIMETRIC TITRATION OF CHROMIUM(III) WITH CATALYTIC END-POINT DETECTION

SIEGBERT PANTEL

Institut für Anorganische und Analytische Chemie der Universität, D-7800 Freiburg i.Br. (Federal Republic of Germany)

(Received 1st May 1987)

Summary. Chromium(III) (2-20 mg) is determined by reaction with excess of EDTA and back-titration with a standard copper(II) solution to a catalytic end-point. The indicator reaction is the copper(II)-catalyzed autodecomposition of hydrogen peroxide, which is observed biamperometrically. For 10 mg of chromium(III), the relative standard deviation was $<0.5\%$ ($n=10$).

Small amounts of chromium(III) are usually determined by physical methods of analysis (e.g., atomic absorption or fluorescence spectrometry, pulse polarography or voltammetry) or kinetic methods, as has been outlined in recent reviews [1-6]. For more concentrated solutions, titrimetric determinations mostly involve chromium(VI), which necessitates an additional chemical step in the determination of chromium(III); in one case, chromium(III) has been determined in the millimolar range with hexacyanoferrate(II) and amperometric indication [7].

The complexiметric determination of chromium(III) presents considerable difficulties, because the CrEDTA complex is formed very slowly at room temperature, thus making it impossible to titrate chromium(III) directly with EDTA. Moreover, the CrEDTA complex is intensely coloured (red-violet at pH 5, intense blue in ammoniacal solution), so that metallochromic indicators cannot be applied for end-point detection in titrations of higher concentrations of chromium(III). In one suggested procedure [8], Cr(III) is determined by addition of EDTA in excess, heating to 60-90°C and back-titrating with a standard lead(II) solution in the presence of chromate; at the titration end-point, lead chromate is precipitated, but the turbidity is difficult to see in titrations of concentrated solutions.

Catalytic end-point detection has been used for the back-titration of EDTA with hydroquinone or resorcinol/hydrogen peroxide as the indicator reaction; The titrant, copper(II) or iron(III), catalyzes this reaction, which is applied

0003-2670/87/$03.50

with thermometric observation [9]. In this communication, it will be shown that the complexiметric titration of chromium(III) with catalytic end-point detection can also be done by using the copper(II)-catalyzed autodecomposition of hydrogen peroxide as indicator reaction with biamperometric observation of the end-point. Because most commercially available mV-pH meters now offer a facility for dead-stop titrations without additional equipment, this is a simple method for the titrimetric determination of higher amounts of chromium(III) without preceding oxidation. There are no problems in dealing with intensely coloured or turbid solutions.

Experimental

To the neutral sample solution containing 2–20 mg of chromium(III), add 5 ml of standard 0.1 M EDTA and just dissolve the precipitate formed by adding 1 M hydrochloric acid (pH 5); heat to boiling for a minute, thus getting a deep red-violet solution. Add 2 M ammonia solution until the colour changes to blue and then 5 ml more to give a pH of about 10; heat again to boiling for a minute and cool to room temperature. Dilute with water to 50 ml and add 1 drop of 30% hydrogen peroxide (equivalent to 10 mg of H_2O_2; more will oxidize the EDTA) and back-titrate the excess of EDTA with standard 0.1 M copper(II) using biamperometric end-point indication (polarization voltage 100 mV). Near the end-point, the current rises to a maximum and then falls to zero within 1–2 min after addition of a further drop of copper(II) solution.

Results

The reproducibility of the titration described was tested for 10 mg of chromium(III) in 50 ml of solution. The relative standard deviation ($n=10$) was found to be 0.49% under the conditions described. The back-titration can also be done with a 0.02 M copper(II) standard solution; semi-automatic determinations are possible.

The method described was used to standardize chromium(III) chloride stock solutions for the preparation of calibration solutions for atomic absorption spectrometry. The results agreed well with those from established methods.

REFERENCES

1 H. König, Staub-Reinhalt. Luft, 42 (1982) 134.
2 Y.K. Agrawal and G.D. Mehd, Rev. Anal. Chem., 6 (1982) 185.
3 V.M. Rao and M.N. Sastri, J. Sci. Ind. Res., 41 (1982) 607.
4 K. Bansho and A. Miyazaki, Bunseki Kagaku, (1983) 862.
5 L. Fishbein, Ind. J. Environ. Anal. Chem., 17 (1984) 113.
6 International Union of Pure and Applied Chemistry, Pure Appl. Chem., 56 (1984) 1477.
7 I.B. Bulycheva, Zavod. Lab., 51 (1985) 20.
8 L. Szekeres, Microchem. J., 17 (1972) 360.
9 T. Kiss, Mikrochim. Acta, (1973) 847.

ANALYTICA CHIMICA ACTA, VOL. 203 (1987)

AUTHOR INDEX

INFORMATION FOR AUTHORS

Detailed "Information for Authors" was published in Vol. 190, No. 2, pp. 375–378. A free reprint is available from the Editors or from:
Elsevier Editorial Services Ltd., Mayfield House, 256 Banbury Road, Oxford OX2 7DH (Great Britain)
Types of contribution. The journal welcomes original research papers, short communications and reviews. Reviews are written by invitation of the editors, who welcome suggestions for subjects. Short communications are usually complete descriptions of limited investigations, and should generally not exceed six printed pages. Preliminary communications of important urgent work can be printed within four months of submission, if the authors are prepared to forgo proofs.
Manuscripts. The preferred language of the journal is English, but French and German manuscripts are also acceptable. For authors whose first language is not English, French or German, linguistic improvement is provided as part of the normal editorial processing. Authors should submit three copies of the manuscript in double-spaced typing on one side of the paper only, with a margin of 4 cm, on pages of uniform size. If any variety of machine copying is used (e.g. xerox), authors should ensure that all copies are easily legible and that the paper used can be written on with both ink and pencil. Authors are advised to retain at least one copy of the manuscript. Manuscripts should be preceded by a sheet of paper carrying (a) the title of the paper, (b) the name and full postal address of the person to whom proofs are to be sent, (c) the number of pages, tables and figures.
Information on the *submission of papers* is given on the inside front cover.
Summary. Research papers and reviews begin with a Summary (50–250 words) which should comprise a brief factual account of the contents of the paper, with emphasis on new information. Short communications and preliminary communications require summaries, which should not exceed 50 words. Uncommon abbreviations, jargon and reference numbers must not be used. The Summary should be suitable for use by abstracting services without rewriting. Papers in French or German require a Résumé or Zusammenfassung preceded by a Title and Summary in English; authors are encouraged to provide translations where necessary.
Introduction. The first paragraphs of the paper should contain an account of the reasons for the work, any essential historical background (as briefly as possible and with key references only) and preliminary experimental work.
Figures. Figures should be prepared in black waterproof drawing ink on drawing or tracing paper of the same size as that on which the manuscript is typed. One original (or sharp glossy print) and two photostat (or other) copies are required. Attention should be given to line thickness, lettering (which should be kept to a minimum) and spacing on axes of graphs, to ensure suitability for reduction during printing. Axes of a graph should be clearly labelled, along the axes, and outside the graph itself.
All figures should be numbered with Arabic numerals, and require descriptive legends. Explanatory information should be placed not in the figure, but in the legend, which should be typed on a separate sheet of paper. Simple straight-line graphs are not acceptable, because they can readily be described in the text by means of an equation or a sentence. Claims of linearity should be supported by regression data that include slope, intercept, standard deviations of the slope and intercept, standard error, and the number of data points; correlation coefficients are optional.
Photographs should be glossy prints and be as rich in contrast as possible; colour photographs cannot be accepted. In general, line diagrams are more informative and less liable to dating than photographs of equipment, which are therefore not usually acceptable.
Computer outputs for reproduction as figures must be good quality on blank paper, and should preferably be submitted as glossy prints.
Nomenclature, abbreviations and symbols. In general, the recommendations of the International Union of Pure and Applied Chemistry (IUPAC) should be followed, and attention should be given to the recommendations of the Analytical Chemistry Division in the journal *Pure and Applied Chemistry* (see also IUPAC *Compendium of Analytical Nomenclature,* 1978).
References. The references should be collected at the end of the paper, numbered in the order of their appearance in the text (*not* arranged alphabetically), and typed on a separate sheet.
In the list of references the following forms should be adopted.
Journals
1 W. Lund and M. Salberg, Anal. Chim. Acta, 76 (1975) 131.
2 M. McDaniel, A.D. Shendrikar, K.D. Reizneir and P. W. West, Anal. Chem., 48 (1976) 2240.
The title of the journal must be abbreviated as in the Bibliographic Guide for Editors and Authors.
Books
1 D.D. Perrin, Masking and Demasking of Chemical Reactions, Interscience-Wiley, New York, 1970, p. 188.
2 S. Hofmann, in G. Svehla (Ed.), Wilson and Wilson's Comprehensive Analytical Chemistry, Vol. 9, Elsevier, Amsterdam, 1979, p. 89.
Titles of papers are unnecessary. Citations of reports which are not widely available (e.g., reports from government research centres) should be avoided if possible. Authors' initials should not be used in the text, unless real confusion could be caused by their omission. If the reference cited contains three or more names, only the first author's name followed by et al. (e.g., McDaniel et al.) should be used in the text; but the reference list must contain the initials and names of *all* authors.

NEW! ELSEVIER'S PERIODIC TABLE OF THE ELEMENTS

Compiled by **P. Lof**

A Full Color Wall Chart 85 x 136 cm – 33″ x 54″

With this new full color wall chart, Elsevier introduces an informative and decorative reference medium for students and professionals in the exact and applied sciences.

This educational wall chart features the periodic table of the elements supported by a wealth of chemical, physical, thermodynamical, geochemical and radiochemical data laid down in numerous colorful graphs, plots, figures and tables.

Here is a wall chart that will help you to find the most important chemical and physical properties of the elements – without turning pages.

All properties are presented in the form of tables or graphs. More than 40 properties are given, ranging from melting point and heat capacity to atomic radius, nuclear spin, electrical resistivity and abundance in the solar system. Sixteen of the most important properties are color coded, so that they may be followed through the periodic system at a glance. Twelve properties have been selected to illustrate periodicity, while separate plots illustrate the relation between properties. In addition, there are special sections dealing with units, fundamental constants and particles, radioisotopes, the Aufbau principle, etc. All data on the chart are fully referenced, and S.I. units are used throughout.

Designed specifically for university and college undergraduates and high school students, ELSEVIER'S PERIODIC TABLE OF THE ELEMENTS will also be of practical value to professionals in the fields of funda mental and applied physical sciences and technology.

- **all chemical elements at a glance**
- **data on more than 40 properties**
- **quick comparison of properties**
- **visual presentation of the periodicity of properties**

The wall chart is ideally suited for self-study and may b used by students as a complementary reference for textbook study and exam preparation. Lecturers may record sections on slides for projection during classes.

Elsevier's Periodic Table of the Elements is available from the publisher in the foll wing quantities only:

1 copy	Dfl. 45.00 / US $ 17.50	ISBN 0-444-4265 (including postage)
10 copies	Dfl. 235.00 / US $ 122.50	ISBN 0-444-4265 (postage will be added unless order is prep

Orders for single copies must be prepaid. Customers The Netherlands should add 6% B.T.W. The charts ar mailed in a sturdy cardboard tube. Quantities of ten an single copies may be available from your regular Elsevie supplier.

Be the first in your lab to have this marvellous Periodic Table on your wall!

Order now and pay by check or credit card (give number, expiry date and signature) or ask for the colo brochure giving full details.

ELSEVIER THE SCIENCE PUBLISHER
P.O. BOX 211 • 1000 AE AMSTERDAM • THE NETHERLANDS
P.O. BOX 1663 • GRAND CENTRAL STATION • NEW YORK • NY 10163